UNIVERSIDAD NACIONAL DE COLOMBIA
SEDE BOGOTÁ
FACULTAD DE INGENIERÍA

Modelado del cambio de propiedades indicativas de calidad en el almacenamiento de feijoa (*Acca Sellowiana Berg*) utilizando atmósferas modificadas

Diego Alberto Castellanos Espinosa

Universidad Nacional de Colombia
Facultad de Ingeniería
Doctorado en Ingeniería – Ingeniería Química
Bogotá D. C., Colombia
2016

Los derechos de este tesis de investigación son propiedad del autor y de las editoriales y medios en donde parte de este se ha publicado. Se permite la descarga de copias individuales con propósitos de estudio e investigación únicamente. Este trabajo no puede ser reproducido en cualquier otro medio sin el permiso expreso del autor.

Modelado del cambio de propiedades indicativas de calidad en el almacenamiento de feijoa (*Acca Sellowiana Berg*) utilizando atmósferas modificadas

Diego Alberto Castellanos Espinosa

Tesis presentada como requisito parcial para optar al título de **Doctor en Ingeniería, Área de Ingeniería Química**

Director:
Prof. Aníbal Orlando Herrera Arévalo

Línea de Investigación:
Envases y empaques en alimentos

Grupo de Investigación:
Horticultura

Universidad Nacional de Colombia
Facultad de Ingeniería
Doctorado en Ingeniería – Ingeniería Química
Bogotá D. C., Colombia
2016

Modelling change of quality-indicative properties of feijoa (*Acca sellowiana* Berg) in modified atmosphere packaging

Diego Alberto Castellanos Espinosa

A thesis presented in partial fulfilment of the requirements for the Degree of Doctor of Engineering – Field of Chemical Engineering

Advisor:
Prof. Aníbal Orlando Herrera Arévalo

Research field:
Food Packaging

Research group:
Horticultura

Universidad Nacional de Colombia
Facultad de Ingeniería
Doctorado en Ingeniería – Ingeniería Química
Bogotá D. C., Colombia
2016

Dedicatoria

Bendito eres tu Señor mi Dios, Rey del universo, que me has mantenido vivo, me has preservado y me has permitido llegar a ver este día.

A mis padres, abuelos y hermanos por su amor y por su apoyo incondicional

A mis queridos Nancy Paola, Luis Alejandro y Nelcy Rocío que ahora me alientan desde arriba

Agradecimientos

Muchas personas e instituciones han hecho esta tesis posible con su apoyo económico, sus equipos, su conocimiento y su aliento. En primer lugar agradezco enormemente a aquellas personas que me dieron parte de su tiempo para la mejor construcción de este trabajo; sin toda esa valiosa ayuda no habría llegado tan lejos.

Agradezco muy especialmente:
Al profesor **Aníbal**, mi director y mi consejero en estos años, por sus aportes, su paciencia y su gran apoyo.
A mis compañeros de investigación y laboratorio, **Rolando, Wilson, Deissy Rocío, Juan Camilo, Helber, Carlos, Juan Carlos, Liz**, por toda su colaboración, su conocimiento y su amistad.
A la profesora **Bárbara Teruel Mederos** de la Universidade Estadual de Campinas por su ayuda en la construcción de la propuesta de esta tesis.
Al profesor **Henry Alexander Váquiro** de la Universidad del Tolima por su ayuda en la revisión del primer capítulo y las correcciones finales del trabajo.
Al profesor investigador **Rafael Gavara Clemente** del Instituto de Agroquímica y Tecnología de Alimentos de Valencia, España, por su acertada dirección en mi pasantía de investigación y por su ayuda y gran colaboración en la construcción del segundo y el tercer capítulo de este trabajo. A todo su grupo de trabajo por su apoyo y colaboración.
Al Doctor **Mauricio Espinal Ruiz** por su apoyo en la revisión y corrección del tercer capítulo de este trabajo.
Al profesor **Luis Felipe Gutiérrez** del Instituto de Ciencia y Tecnología de Alimentos por su tiempo y gran ayuda en la preparación de la defensa de la propuesta de este trabajo y la exposición de parte de los resultados obtenidos en el *10th European Congress of Chemical Engineering* en 2015.
A los profesores **Rodrigo Jiménez Pizarro** y **Álvaro Orjuela Londoño** por su dirección y sus contribuciones a este trabajo en los seminarios de investigación del Doctorado.
A los profesores **Juan Carlos Serrato**, **Claudia Patricia Pérez** del Departamento de Ingeniería Civil y Agrícola y **Andrés Gonzáles Barrios** de la Universidad de los Andes,

jurados en la presentación de la propuesta de este trabajo por sus valiosos aportes y comentarios.

A mis colegas y compañeros de los posgrados en Ingeniería Química y Ambiental por sus valiosos conocimientos y aportes.

A todo el personal de los diferentes laboratorios en los que realicé mis experimentos por su amable colaboración.

En cuanto a las entidades e instituciones, debo agradecer:

Al Departamento Administrativo de Ciencia, Tecnología e Innovación – **Colciencias**, por su apoyo económico con la *Convocatoria Nacional para Estudios de Doctorado en Colombia* de 2012, beca-crédito condonable de la cual he sido beneficiario desde 2013.

A la **Vicerrectoría Académica** de la Universidad Nacional de Colombia por su apoyo con la beca de Estudiantes Sobresalientes de Posgrado de la cual fui beneficiario entre 2012 y 2013.

A la **Vicerrectoría de Investigación y Extensión** de la Universidad Nacional de Colombia por su financiación del proyecto de investigación "Modelado de la cinética de respiración y de generación de etileno en frutos de feijoa (*Acca sellowiana* Berg) y Aguacate (*Persea americana* Mill)" a través de la *Convocatoria del Programa Nacional de Proyectos para el Fortalecimiento de la Investigación, la Creación y la Innovación en Posgrados de la Universidad Nacional de Colombia 2013-2015*, y por su apoyo económico en la traducción y corrección de estilo de varios de los artículos que constituyen los capítulos de este trabajo a través de la *Convocatoria del Programa Nacional para la Visibilidad Internacional de la Producción Académica Mediante el Apoyo para la Traducción o Corrección de Estilo de Artículos de Investigación 2013-2015*.

Al **Instituto de Agroquímica y Tecnología de Alimentos** del Consejo Superior de Investigaciones Científicas del Gobierno de España y especialmente al **Grupo de Envases** por su apoyo técnico, científico y de infraestructura en el desarrollo de mi pasantía de Investigación en el año 2014.

Al **Instituto de Ciencia y Tecnología de Alimentos**, al **Laboratorio de Fisiología Vegetal** y al **Laboratorio de Calidad Poscosecha** de la Facultad de Ciencias Agrarias y al **Laboratorio de Ingeniería Química** por su apoyo y disponibilidad en el desarrollo de los experimentos para este trabajo.

Acknowledgements

Many people and institutions have made this thesis possible with their financial support, equipment, knowledge and encouragement. First, I am very grateful to the many people who gave me part of their time to the better construction of this work. Without all that valuable support, I would not have gotten this far.

I am particularly grateful to:

Professor **Aníbal**, my boss and advisor during these years for his contributions, patience and strong support.

My research and laboratory partners **Rolando, Wilson, Deissy Rocío, Juan Camilo, Helber, Carlos, Juan Carlos, Liz**, for their collaboration, knowledge and friendship.

Professor **Bárbara Teruel-Mederos** of the Universidade Estadual de Campinas for her assistance in the construction of the proposal for this dissertation.

Professor **Héctor Alexander Váquiro** of the Universidad del Tolima for his help in revising the first chapter and the final proofreading of the dissertation.

Research Professor **Rafael Gavara-Clemente** of the Institute of Agro-chemistry and Food Technology in Valencia, Spain, for his guidance in my research internship and for his support and great collaboration in the construction of the second and third chapters of this dissertation and his entire research group for their support and collaboration.

Dr. **Mauricio Espinal-Ruiz** for their support in the review and correction of the third chapter of this study.

Professor **Luis Felipe Gutierrez** of the Institute of Food Science and Technology (Universidad Nacional de Colombia) for his time and great assistance in preparing the public defense of the proposal of this work and the oral presentation in the 10th European Congress of Chemical Engineering in 2015.

Professors **Rodrigo Jiménez-Pizarro** and **Alvaro Orjuela-Londoño** for their guidance and contributions to this dissertation in the doctoral research seminars.

Professors **Juan Carlos Serrato**, **Claudia Patricia Pérez** of the Department of Civil and Agricultural Engineering (Universidad Nacional de Colombia) and **Andres González-Barrios** of the Universidad de los Andes, which were reviewers in the presentation of the proposal of this study for their valuable contributions and comments.

My colleagues of the postgraduate programs in Chemical and Environmental Engineering for their valuable insights and contributions.
All personnel of the different laboratories in which I made the different experiments for their kind collaboration.

As to the entities and institutions, I must thank to:
The Administrative Department of Science, Technology and Innovation - **Colciencias** for its financial support with the national convocation for PhD in Colombia year 2012, forgivable loan-scholarship of which I have been a beneficiary since 2013.
The **Academic Vice-presidency** of the Universidad Nacional de Colombia for its support with the Outstanding Students Graduate Scholarship of which I was a beneficiary between 2012 and 2013.
The **Research and Extension Vice-presidency** of the Universidad Nacional de Colombia for its funding in the research project "Modeling of the kinetics of respiration and ethylene generation of feijoa (*Acca sellowiana* Berg) and avocado (*Persea americana* Mill) fruits" through the 'Convocation of the National Program of Projects to Strengthen Research, Creation and Innovation in Graduate Studies at the National University of Colombia 2013-2015'. Also for their financial support in the translation and proofreading of several of the articles that constitute the chapters of this work through the 'Convocation of the National Program for International Visibility of the Academic Production Through Support for the Translation or Proofreading of Research Articles 2013-2015'.
The **Institute of Agricultural Chemistry and Food Technology** of the Higher Council for Scientific Research, Government of Spain and especially the Group of packaging for its technical, scientific and infrastructure in developing my research internship in 2014.
The **Institute of Food Science and Technology**, **Laboratory of Plant Physiology** and **Laboratory of Postharvest Quality** of the Faculty of Agricultural Sciences and the **Laboratory of Chemical Engineering** (Universidad Nacional de Colombia) for their support and availability in the developing of the experiments for this work.

Resumen

El uso de sistemas de empaque con atmósferas modificadas (AM) puede contribuir a extender la vida útil de productos frescos retrasando la maduración y disminuyendo el deterioro por acción fisiológica o microbiana. Esto ocurre cuando se produce un equilibrio entre la respiración y transpiración del producto empacado y la permeación de gases a través del empaque llevando a una atmósfera interna favorable para su preservación. En esta tesis se presenta en primer lugar un modelo matemático para describir la evolución en los niveles de O_2, CO_2 y vapor de agua en el espacio de cabeza del sistema de empaque y la pérdida de peso del producto almacenado para un sistema de AM con perforaciones y de volumen variable. En segundo lugar se aplica el modelo desarrollado para determinar configuraciones de empaque en AM favorables para la conservación del producto y se desarrolla otro modelo para representar la evolución en la firmeza y color de este producto durante el almacenamiento. En el modelo de AM, la respiración en el producto fue representada usando una cinética enzimática de Michaelis-Menten, mientras que se consideró la transpiración y pérdida de peso como la suma del agua evaporada debido al calor de respiración y a la diferencia de actividad de agua entre el producto y la atmósfera que lo rodea. La transferencia de los gases a través del empaque fue descrita empleando ecuaciones de Fick de difusión, mientras se consideró que la influencia de la temperatura en todos los procesos anteriores sigue un comportamiento de Arrhenius. El modelo fue validado satisfactoriamente (R^2 mayores a 0.9) empacando frutos de feijoa (*Acca sellowiana* Berg) en diferentes condiciones de almacenamiento: tipo de empaque, numero de perforaciones, temperatura y humedad relativa. Empleando el modelo de AM, se evaluó el efecto de diferentes configuraciones de empaque sobre el índice de deterioro, pérdida de peso, contenido de ácidos orgánicos, firmeza y color de los frutos. De acuerdo a la evolución de estas propiedades, los frutos empacados a 6 °C y con concentraciones de 8.2 kPa de O_2 – 5.8 kPa de CO_2 se preservaron hasta 38 días, significativamente más que los 17 días obtenidos para frutos almacenados sin empaque a 17 °C. Con los datos obtenidos para las diferentes configuraciones de AM se desarrolló un segundo modelo para representar el cambio en la firmeza y el color de los frutos en función de la concentración de O_2 y CO_2, la temperatura y el tiempo de almacenamiento. El modelo

representa adecuadamente el comportamiento experimental de las propiedades evaluadas con coeficientes de regresión mayores a 0.93.

Palabras clave: almacenamiento poscosecha, sistemas de empaque, modelado y simulación, peso, color, firmeza

Abstract

By using modified atmosphere packaging (MAP) systems, it is possible to extend the shelf-life of fresh produce, delaying the ripening process and reducing the deterioration due to physiological or microbial action. This occurs when an equilibrium between the respiration and transpiration of the packed produce and gas permeation through the packaging system is obtained, leading to an internal atmosphere that is favorable for preservation. This thesis first presents a mathematical model that describes the evolution in the water vapor, O_2 and CO_2 concentrations in the packaging headspace and the weight loss of produce packed in a MAP system with perforations and variable volume. Secondly, the developed model was used to determine a packaging configuration that is favorable for the preservation of the packed produce and to develop other models to represent the evolution in firmness and color of this produce during storage. In the MAP model, the respiration was represented using Michaelis-Menten enzyme kinetics. Transpiration was considered as the sum of the water evaporated due to the respiratory heat and the difference in water activities between the fresh produce and the surrounding atmosphere. The gas transfer through the packaging and the perforations was described with Fick equations. The temperature influence on all of these processes was considered following Arrhenius' law. The model was successfully validated (R^2 greater than 0.9) by packing feijoa fruits (*Acca sellowiana* Berg) in different storage conditions: packaging, perforations, relative humidity and temperature. Using the MAP system, the effect of the different packaging combinations on the storage-life of the fruits was determined by evaluating the change in the deterioration index, weight, firmness, color and organic acids. According to the evolution of these properties, the fruits packed at 6 °C and with 8.2 kPa of O_2 and 5.8 kPa of CO_2 were preserved for up to 38 days, significantly more than the 17 days obtained for fruits stored without packing at 17 °C. With the data obtained for the different MAP configurations, a second model to describe the evolution in firmness and flesh color of the stored fruits, depending on O_2 and CO_2 levels, temperature and storage time was also developed. This model adequately represented the behavior of the evaluated properties, obtaining R^2 values greater than 0.94.

Keywords: postharvest storage, packaging systems, modelling and simulation, weight loss, firmness, color.

Contents

Resumen/Abstract XIII
Introduction 23
Modified Atmosphere Packaging 24
Feijoa fruits 26
Research aim 27
Thesis structure 28
References 29
Chapter 1. Mathematical models for the representation of some physiological and quality changes during fruit storage 35
1.1 Introduction 35
1.2 The effect of environmental conditions on quality properties 36
1.2.1 Temperature 36
1.2.2 Oxygen 37
1.2.3 CO_2 37
1.2.4 Ethylene 38
1.3 Use of models to represent physiological and quality changes in harvested fruits according to storage conditions 38
1.3.1 Respiratory intensity (RI) 39
1.3.2 Transpiration rate (TR) and moisture loss 43
1.3.3 Firmness change 47
1.3.4 Color change 50
1.4 Conclusions 54
1.5 References 55
Chapter 2. Modelling the evolution of O_2 and CO_2 concentrations in MAP of a fresh product. An first example with tomato 69
2.1 Introduction 71
2.2 Mathematical approach 73
2.2.1 Respiration rates 74
2.2.2 Gas exchange in the packaging system 74
2.2.3 Gas balance equations 77
2.2.4 Consistency of the system of differential equations 77
2.3 Materials and methods 78
2.3.1 Fresh produce 78

2.3.2 Packages 78
2.3.3 Respiration rates 78
2.3.4 Gas transfer through the package 79
2.3.5 Modelling 81
2.3.6 Packaging and validation 81
2.4 Results and discussion 82
2.4.1 Respiration rates 82
2.4.2 Gas transfer through the package 83
2.4.3 Modelling and Validation 87
2.4.4 Setting a specific concentration in the headspace 91
2.5 Conclusions 95
2.6 References 96
Chapter 3. Modelling respiration of feijoa fruits and application in modified atmosphere packaging 101
3.1 Introduction 102
3.2 Materials and Methods 104
3.2.1 Fruit samples 104
3.2.2 Determination of the respiration rates 104
3.2.3 Application in MAP and validation 107
3.3 Results and discussion 109
3.3.1 Respiration rates 109
3.3.2 Validation in MAP 113
3.4 Conclusions 116
3.5 References 117
Chapter 4. Representing water vapor transport, transpiration and weight loss in a perforated MAP system for feijoa fruits 121
4.1 Introduction 123
4.2 Materials and Methods 125
4.2.1 Fresh fruits 125
4.2.2 Packages 125
4.2.3 Packages permeability 126
4.2.4 Gas transmission through perforations in the packaging 127
4.2.5 Fruit respiration 127
4.2.6 Determination of the fruit transpiration in the MAP 128
4.2.7 Mathematical Approach 129
4.2.8 MAP modelling 132
4.2.9 Validation test 135
4.3 Results and discussion 136

4.3.1 Gas permeation through the packages....136
4.3.2 Permeation parameters to water vapor....137
4.3.3 Respiration and O_2 and CO_2 evolution....138
4.3.4 Determination of the fruit transpiration in the MAP....139
4.3.5 Validation packaging test with PP and PLA....144
4.4 Conclusions....146
4.5 References....146
Chapter 5. Development of an suitable EMAP system for feijoa fruits and modelling firmness and color evolution....151
5.1 Introduction....153
5.2 Materials and Methods....155
5.2.1 Fresh samples....155
5.2.2 Packaging material....155
5.2.3 Making the EMAP systems and storage....156
5.2.4 Simulation of gas evolution in the EMAP systems....156
5.2.5 Fruit quality properties....158
5.2.6 Modelling firmness and color....160
5.2.7 Parameter estimation for the color and firmness models....162
5.3 Results and discussion....162
5.3.1 EMAP simulation....163
5.3.2 Packaging tests....165
5.3.3 Deterioration Index....165
5.3.4 Weight loss....166
5.3.5 Firmness....168
5.3.6 Color....169
5.3.7 Organic acids....171
5.3.8 Most suitable EMAP system....172
5.3.9 Modelling firmness and color....173
5.4 Conclusions....181
5.5 References....181
General conclusions and future research....187
Conclusions....189
Future developments....190
Rigid packaging and temperature variations....190
Active packaging....191
Predicting storage life....191
Annex A. Publications of the Thesis....193
Annex B. Participation in academic and scientific events....195

Annex C. Funded projects..... 197

Introduction

In recent decades, demand for fresh fruits has been growing steadily worldwide. New habits, awareness of the nutritional importance of these foods and population increases have been the major reasons for this growth. Currently, there is a greater preference for fresh fruits with respect to these same products when frozen, canned or processed, since preservation of their full sensory and nutritional properties is desired.

In the case of Colombia, the production and exportation of fresh fruits are becoming more relevant to the agricultural sector, with an increase in production from 2,577,935 to 3,556,888 metric tons between 2002 and 2012 (Agronet, 2014). This market is very promising due to the low availability of these products in North America and Europe and the increasing demand due their nutritional and sensory characteristics (Fischer, et al., 2005). The free trade agreements that are in the implementation phase or close to be implemented with Europe, Canada, South Korea and United States provide even greater momentum to the sector and new export opportunities that should be seized. However, most fruits have a very limited postharvest shelf-life that is affected greatly by storage conditions, such as relative humidity, temperature and availability of oxygen in the atmosphere surrounding the product; these conditions can contribute to deterioration. This has resulted in significant losses in the distribution chain, as high as 30% (CCI, 2006).

Considering the need to develop a supply chain, growing demand and rapid deterioration for fresh fruits, it is necessary to ensure efficient production, handling and distribution of these products and, hence, reduce postharvest losses. The selection of suitable conditions during storage and distribution is of great importance since a failure at these stages will directly result in increasing the rate of deterioration and in a shorter shelf-life.

Following harvest, fruits undergo a ripening phase, leading to the development of characteristic color, aroma and flavor, acidity reduction and tissue softening, to values that make them acceptable for consumption, which is known as eating ripeness (Kader, et al., 1989; Herianus, et al., 2003; Lee & Kader, 2000). In the ripening stage, different biochemical reactions take place, leading to an increase of the respiration process, ethylene

production, degradation of chlorophylls and carotenoid biosynthesis, change in the concentration of organic acids, lipids and phenolic compounds, generation of volatiles, structural polysaccharides breakdown, starch conversion into sugars and loss water retention capacity (El-Ramady, et al., 2015; Prasanna, et al., 2007).

Once the ripening substrates are consumed, other catabolic processes take place, leading to undesired alterations in the quality properties, which is a consequence of the progressive deterioration of the cell structures and the degradation of compounds responsible for the sensory characteristics (Lee, et al., 1995). In this period, known as senescence, the product ceases to be consumable, ending its useful life.

The development of the biochemical processes that lead to ripening and subsequently to senescence and other undesirable processes that can occur due to the presence of microorganisms is influenced greatly by the conditions under which the product is maintained, such as temperature and gas composition of the surrounding atmosphere, mainly the concentration of O_2, CO_2 and water vapor (Sandhya, 2010). A conservation system for fresh fruits must then set those conditions at appropriate levels to meet the goals of maintaining quality and extending the shelf-life.

Modified Atmosphere Packaging

Modified atmosphere packaging (MAP) systems have been recognized as an effective method of preserving fresh fruits and vegetables during the storage and distribution stage because they slow degradation of the quality properties and delay senescence (Li, et al., 2010; Sandhya, 2010). MAP entail the modification of the composition of gases in the atmosphere surrounding a packed product, to levels that are favorable for preservation. This modification is a consequence of the dynamic interaction of two processes: on the one hand, the product metabolism that through respiration and transpiration consumes O_2 and generates CO_2 and water vapor, and, on the other hand, the exchange of these gases through the package walls, between the headspace atmosphere surrounding the product and the external atmosphere (Yam & Lee, 1995; Del-Nobile, et al., 2007). This leads to the depletion of O_2 and a rise in CO_2 and water vapor concentrations in the package headspace (Floros & Maxos, 2005; Heydari, et al., 2012; Mahajan, et al., 2007). The goal of the MAP system is to regulate gas concentrations at appropriate levels, establishing a balance between the product respiration and transpiration and the gas exchange through the package, reaching an equilibrium modified atmosphere packaging (EMAP).

At low O_2 and moderate CO_2 levels, the MAP system, in general, delays the ripening process, reduces the consumption rate of substrates (carbohydrates, organic acids and other cellular structures), ethylene sensitivity and production, and physiological decay and increases the postharvest shelf-life of the fresh product, as compared to ambient conditions (Saltveit, 2004; Santos, et al., 2006).

Understanding the dynamics of the interactions established between the product, the atmosphere surrounding it and the package is required to achieve an effective MAP system (Yam & Lee, 1995). It is necessary to have knowledge of the fruit physiological processes and gas exchange through the package so a number of variables should be associated. These variables are the product respiration and transpiration rates as a function of temperature, the optimum gas levels and the tolerance limits for the product, and the permeation rate of gases through the package film, which is also dependent on the temperature, the area of gas exchange, the free package volume (packaging headspace), and the product weight, among others (Jayas & Jeyamkondan, 2002).

Given the large number of variables and conditions that must be determined when designing a suitable MAP system, past studies have sought to describe changes in the modified atmosphere inside packages, using mathematical models. From these models, it has been sought to define the conditions that the system should fulfill in order to maintain the product at the appropriate levels of gases and to predict the evolution of these gases during the storage time.

A number of models have been developed to describe changes in gas concentrations in MAP systems (Del-Nobile, et al., 2007; González-Buesa, et al., 2009; Mahajan, et al., 2007). In these models, the respiration process has been generally described using Michaelis-Menten enzyme kinetic equations and the gas exchange through the package using Fick diffusion equations, while the effect of temperature on both processes has been represented through Arrhenius equations. Otherwise, the change in the free package volume, which is a result of the difference in respiration and transpiration rates and gas permeation through the package walls, and the change in product weight due to the transpiration process have scarcely been taken into account.

As mentioned above, the storage shelf-life of a packed food, and in general any food, is related to certain properties that may be indicative of quality. These properties are

influenced by the conditions in which that product is preserved. Many models have been developed to describe changes in quality properties of stored fruits as a function of some storage conditions (Caleb, et al., 2012; Hertog, et al., 2004; Hertog, et al., 2003; Lukasse & Polderdijk, 2003; Schouten, et al., 2007). However, few consider the influence of the storage conditions (temperature, atmosphere O_2 and CO_2 concentrations, and relative humidity) on the quality properties of the product. Each particular product has properties that reflect quality and ripening changes; in general, properties that are easy to measure, representative throughout the shelf-life, non-destructive if possible, and affected by storage conditions should be investigated to build prediction models. For many products, color, texture and weight loss have been successfully used to represent evolution in the shelf-life (Hertog, et al., 2001; Jha, 2010; Mangaraj & Goswami, 2011; Tijskens & Schouten, 2009).

Feijoa fruits

The feijoa (*Acca sellowiana* Berg) has been chosen as a case study in this thesis due to its wide potential in the horticultural sector in Colombia in the short and medium term. This tropical fruit is also called pineapple guava and is an evergreen shrub of the Myrtaceae family, native to southern Brazil and northern Uruguay (Dos Santos, et al., 2009; East, et al., 2009). The commercial production of feijoa is centered in New Zealand, Georgia, Azerbaijan, Colombia and the United States (California), with Brazil and Uruguay as emergent countries (Dos Santos, et al., 2009). It is widely recognized for its excellent nutritional qualities, with a high content of iodine and vitamin C, antioxidant compounds such as flavonoids and polyphenols, and anticancer and antimicrobial activity (Bontempo, et al., 2007; Manabe & Inobe, 2005; Parra & Fischer, 2013; Vuotto, et al., 2000).

This fruit was introduced to Colombia in the eighties (Quintero & Ovalle, 1992) and has since been cultivated for economic purposes due to the excellent organoleptic characteristics that it possesses. It was placed among 10 promising fruits for cultivation in Colombia (DANE, 2004; Parra & Fischer, 2013) given its great adaptability and the availability of large regions for its production, mainly in the departments of Boyacá, Cundinamarca, Caldas, Antioquia and Nariño (Benavides & Mora, 2003; Parra & Fischer, 2013). As a fresh fruit, it is highly coveted, both domestically and in foreign markets, given the large number of derivative products that can be obtained (Quintero, 2012). However, its rapid deterioration make it difficult for the fruit to be produced and marketed more widely (Gálvis, 2003; Valderrama, et al., 2005). At 23 °C, its shelf-life is less than one week and, at 17 °C, it is between 8 and 14 days (Rodríguez, et al., 2006).

There have been some studies that evaluated the use of MAP and refrigeration temperatures as a method to extend the shelf-life of feijoa fruits (East, et al., 2009; Gálvis, 2003); however, information about how the packing system affects the evolution of the quality properties and storage shelf-life of this fruit is scarce. The conditions that have been considered more favorable in previous studies include fruits stored at temperatures between 4 and 6 °C and the use of MAP with low O_2 and CO_2 concentrations (1-5 kPa of O_2 and 0.2-5 kPa of CO_2), achieving a shelf-life of 25 to 30 days (East, et al., 2009; Gálvis, 2003; Ramírez, et al., 2005).

In this study was expected to confirm that storage in MAP systems is an effective method for preserving fresh feijoa fruits and to determine the more suitable packaging conditions for its preservation. Furthermore, it was expected to describe the changes in the fruit quality properties and the gas evolution inside the package by using the appropriate mathematical models and thus be able to pre-select the most favorable conditions for fruit preservation given a particular requirement.

Research aim

The aim of this thesis was to develop mathematical models, supported by experimental results, to describe changes in O_2, CO_2 and water vapor in the headspace of a MAP system for feijoa fruits, to represent the evolution in the weight, firmness and color considering the influence of the packaging configuration and temperature and to determine favorable packaging conditions.

To achieve the research aim the following specific objectives were set:

- Experimental determination of the respiration and transpiration rates for the packed fruit and gas permeation rates through the package in the MAP system, considering variations in temperature and type of packaging.
- Mathematical representation of the evolution in O_2, CO_2 and water vapor concentrations in the internal atmosphere of a MAP system, considering the respiration and transpiration of the packed fruits, the gas exchange through the package and the dependence on temperature.
- Experimental evaluation of changes in weight, firmness and flesh color of the packed fruits in the MAP system, considering variations in the package permeability and

storage temperature and determination of favorable MAP conditions to preserve the fruit.

- Development of mathematical expressions to describe the behavior of firmness, color and weight for the fruits packed in a MAP system, considering the influence of gas concentrations inside the package and storage temperature.
- Validation of the developed model by assessing its ability to predict the evolution in the gas concentration of the MAP system and in the quality properties of the packed fruits.

Thesis structure

This research study is divided into five chapters in addition to the introduction and the general conclusions. All five chapters were written in the form of articles and submitted with the appropriate modifications to different research journals according to each topic. In these chapter-articles, a response was given for the research objectives.

In Chapter 1, a review of relevant mathematical models to describe respiration, transpiration and changes in quality properties (weight, firmness and color), depending on the storage conditions during the postharvest handling is presented.

In Chapter 2, the mathematical approach of a MAP system is developed, a methodology to determine the evolution in O_2 and CO_2 concentrations in a package of variable volume with a respiring fruit inside is discussed, and the experimental determination of the required respiration parameters and permeability coefficients of three types of packaging materials with perforations is shown. As a fruit example for the development of the model, a variety of tomato with a low respiration rate was used.

In Chapter 3, equations to describe the respiration process for feijoa fruits depending on O_2 and CO_2 concentrations and temperature are presented where the respective parameters were established experimentally. Then, the feijoa respiration kinetics is included in the MAP model in a validation test to determine their usefulness to predict the O_2 and CO_2 evolution in the packaging headspace.

In Chapter 4, a model to describe the transpiration process and weight loss for feijoa fruits in a MAP system is developed and the respective experiment parameters are estimated.

In Chapter 5, the mathematical models used to describe the change in firmness and color of feijoa fruits packed in a MAP system and depending on the gas concentration and temperature are presented and the more suitable conditions for its storage in MAP are determined.

Finally, the main conclusions are stated and recommendations for future developments are suggested.

Additional information related to publications, presentations at scientific events and funded projects in the development of this thesis is found in the annexes.

References

Agronet, 2014. Sistema de estadísticas agropecuarias. [Online] Available at: http://www.agronet.gov.co/agronetweb1/ [Accessed august 2014].

Benavides, M. & Mora, H. 2003. Problemática del complejo moscas de la fruta (Diptera: Tepritidae) y otras plagas de importancia económica en el cultivo de la feijoa. In: G. Fischer, D. Miranda, G. Cayón & M. Mazorra (Eds.). *Cultivo, poscosecha y exportación de la feijoa (Acca sellowiana Berg)*. Bogotá: Produmedios, pp. 73-85.

Bontempo, P., Mita, L., Miceli, M., Doto, A. & Nebbioso, A. 2007. Feijoa sellowiana derived natural Flavone exerts anti-cancer action displaying HDAC inhibitory activities. *The International Journal of Biochemistry & Cell Biology*, 39: 1902-1914.

Caleb, O.J., Mahajan, P.V., Opara, U.L. & Witthuhn, C. 2012. Modelling the respiration rates of pomegranate fruit and arils. *Postharvest Biology and Technology*, 64: 49-54.

CCI-Ministerio de Agricultura y Desarrollo Rural. 2006. *Plan Hortícola Nacional (2006-2010)*. [Online] Available at: http://www.cci.org.co/publicaciones/1_PHNfinal.pdf [Accessed august 2014].

DANE. 2004. Resultados del censo del cultivo de feijoa. In: *I Censo nacional de 10 frutas agroindustriales promisorias*. Bogotá: DANE, pp. 277-295.

Del-Nobile, M.E., Licciardello, F., Scrocco, C., Muratore, G. & Zappa, M. 2007. Design of plastic packages for minimally processed fruits. *Journal of Food Engineering*, 79: 217-224.

Dos Santos, K.L., Peroni, N., Guries, R.P. & Nodari, R.O., 2009. Traditional knowledge and management of feijoa (*Acca sellowiana*) in Southern Brazil. *Economic Botany*, 63(2): 204-214.

East, A.R., Trejo-Araya, X.I., Hertog, M.L. A.T.M., Nicholson, S.E. & Mawson, A.J. 2009. The effect of controlled atmospheres on respiration and rate of quality change in 'Unique' feijoa fruit. *Postharvest Biology and Technology*, 53: 66-71.

El-Ramady, H. R., Domokos-Szabolcsy, E., Abdalla, N.A., Taha, H.S. & Fári, M. 2015. Postharvest Management of Fruits and Vegetables Storage. *Sustainable Agriculture Reviews*, 15: 65-152.

Fischer, G., Miranda, D., Piedrahita, W. & Romero, J., 2005. *Avances en cultivo, poscosecha y exportación de la uchuva (Physalis peruviana L.)*. Bogotá: Unibiblos, Universidad Nacional de Colombia.

Floros, J.D. & Maxos, K.I. 2005. Introduction to modified atmosphere packaging. In: J. Han (Ed.), *Innovations in Food Packaging*. New York: Elsevier Academic Press, pp. 159-172.

Gálvis, J. A., 2003. Manejo de la cosecha y poscosecha de la feijoa. In: G. Fischer, D. Miranda, G. Cayón & M. Mazorra, eds. Cultivo, poscosecha y exportación de la feijoa (Acca sellowiana Berg). Bogotá: Produmedios, pp. 111-123.

González-Buesa, J., Ferrer-Mairal, A., Oria, R. & Salvador, M. L., 2009. A mathematical model for packaging with microperforated films of fresh-cut fruits and vegetables. Journal of Food Engineering, Volume 95, pp. 158-165.

Herianus, J. D., Singh, L. Z. & Tan, S., 2003. Aroma volatiles production during fruit ripening of ‘Kensington Pride’ mango. Postharvest Biology and Technology, Volume 27, pp. 323-336.

Hertog, M.L.A.T.M., Nicholson, S.E. & Banks, N.H., 2001. The effect of modified atmospheres on the rate of firmness change in ‘Braeburn’ apples. *Postharvest Biology and Technology*, 23(3): 175-184.

Hertog, M.L.A.T.M., Nicholson, S.E. & Jeffery, P.B. 2004. The effect of modified atmospheres on the rate of firmness change of ‘Hayward’ kiwifruit. *Postharvest Biology and Technology*, 31: 251–261.

Hertog, M.L.A.T.M., Nicholson, S.E. & Whitmore, K. 2003. The effect of modified atmospheres on the rate of quality change in Hass avocado. *Postharvest Biology and Technology*, 29: 41-53.

Heydari, A., Alemzadeh, I. & Vossoughi. M. 2012. Study and Mathematical Modeling of Transient Gas Compositions for Modified Atmosphere Packaging. In: A. Öchsner, L.F.

M. Da Silva & H. Altenbach (Eds.). Analysis and Design of Biological Materials and Structures. Berlin Heidelberg: Springer-Verlag, pp. 163-174.

Jayas, D.S. & Jeyamkondan, S. 2002. Modified Atmosphere Storage of Grains, Meats, Fruits and Vegetables. *Biosystems Engineering*, 82(3): 235-251.

Jha, S.N. 2010. Color measurements and modeling. In: S.N. Jha (Ed.), *Nondestructive Evaluation of Food Quality*. Theory and practice. Berlin Heidelberg: Springer-Verlag, pp. 17-40.

Kader, A.A., Zagory, D. & Kerbel, E.L. 1989. Modified atmosphere packaging of fruits and vegetables. *Critical Reviews in Food Science and Nutrition*, 28: 1-30.

Lee, L., Arul, J., Lencki, R. & Castaigne, R. 1995. A review on modified atmosphere packaging and preservation of fresh fruits and vegetables: physiological basis and practical aspects. Part I. *Packaging Technology and Science*, 8(6): 315-331.

Lee, S.K. & Kader, A.A. 2000. Preharvest and Postharvest factors influencing Vitamin C content of horticultural crops. *Postharvest Biology and Technology*, 20(3): 207-220.

Li, L., Xi-Hong, L. & Zhao-Jun, B. 2010. A Mathematical Model of the Modified Atmosphere Packaging (MAP) System for the Gas Transmission Rate of Fruit Produce. *Food Technology and Biotechnology*, 48(1): 71-78.

Lukasse, L. J.S. & Polderdijk, J.J. 2003. Predictive modelling of post-harvest quality evolution in perishables, applied to mushrooms. *Journal of Food Engineering*, 59: 191-198.

Mahajan, P.V., Oliveira, F.A.R., Montanez, J.C. & Frias, J. 2007. Development of user-friendly software for design of modified atmosphere packaging for fresh and fresh-cut produce. *Innovative Food Science and Emerging Technologies*, 8: 84-92.

Manabe, M. & Inobe, Y. 2005. Suppressing effects of Feijoa sellowiana Berg (Feijoa) on cytokine secretion by intestinal epithelium. *Food Science and Technology Research*, 11: 71-76.

Mangaraj, S. & Goswami, T.K. 2011. Modeling of respiration rate of litchi fruit under aerobic conditions. *Food Bioprocess Technology*, 4: 272–281.

Parra, A. & Fischer, G. 2013. Maduración y comportamiento poscosecha de la feijoa (*Acca sellowiana* (O. Berg) Burret). Una revisión. *Revista Colombiana de Ciencias Hortícolas*, 7(1): 98-110.

Pranamornkith, T. 2009. Effects of postharvest treatments on storage quality of lime (Citrus 1014 latifolia Tanaka) fruit. PhD Thesis. Auckland: Massey University.

Prasanna, V., Prabha, T.N. & Tharanathan, R.N. 2007. Fruit ripening phenomenon – An overview. *Critical Reviews in Food Science and Nutrition*, 47: 1-19.

Quintero, O.C. 2012. Feijoa (*Acca sellowiana* Berg). In: G. Fischer, (Ed.9, *Manual para el cultivo de frutales en el trópico*. Bogotá: Produmedios, 443-473.

Quintero, O. & Ovalle, G. 1992. La feijoa (*Feijoa sellowiana* Berg), fruta promisoria para Colombia. *Acta Horticulturae*, 310: 239-248.

Ramírez, J.M., Galvis, J.A. & Fischer, G. 2005. Maduración poscosecha de la feijoa (*Acca sellowiana* Berg) tratada con $CaCl_2$ en tres temperaturas de almacenamiento. *Agronomía Colombiana*, 23(1): 117-127.

Rodríguez, M., Arjona, A.E. & Galvis, J.A. 2006. Maduración del fruto de feijoa (*Acca sellowiana* Berg) en los clones 41 (Quimba) y 8-4 a temperatura ambiente en condiciones de la Sabana de Bogotá. *Agronomía Colombiana*, 24(1): 68-76.

Saltveit, M.E., 2004. Cucumber. In: K. C. Gross, C. Y. Wang & M. E. Saltveit (Eds.), *The commercial storage of fruits, vegetables, and florist and nursery stocks*. Beltsville: USDA/ARS. Agricultural handbook, 66.

Santos, C.M.S., de Barros Vilas Roas, E.V., Botrel, N. & Marques, A.C. 2006. Influência da atmósfera controlada sobre a vida pos-colheita e qualidad de banana 'Prata Ana'. *Ciencia e Agrotecnologia*, 30(2): 317-322.

Schouten, R.E., Huijben, T.P.M., Tijskens, L.M.M. & van Kooten, O. 2007. Modeling quality attributes of truss tomatoes: Linking color and firmness maturity. *Postharvest Biology and Technology*, 45(3): 298–306.

Tijskens, L.M.M. & Schouten, E. 2009. Modeling Quality Attributes and Quality-related Product Properties. In: W. Florkowski & B. Bruckner (Eds.), *Postharvest Handling: A Systems Approach*. San Diego: Academic Press, pp. 483-512.

Valderrama, J.K., Fischer, G. & Serrano, M.S. 2005. Fisiología poscosecha en frutos de dos cultivares de feijoa (*Acca sellowiana* O. Berg Burret) sometidos a un tratamiento cuarentenario de frío. *Agronomía Colomiana*, 23(2): 276-282.

Vuotto, M., Basile, A., Moscatiello, V., De Sole, P., Castaldo-Cobianchi, R., Laghi, E. & Ielpo, M.T.L. 2000. Antimicrobial and antioxidant activities of Feijoa sellowiana fruit. *International Journal of Antimicrobial Agents*, 13: 197-201.

Yam, K.L. & Lee, D.S. 1995. Design of modified atmosphere packaging for fresh produce.

Chapter 1. Mathematical models for the representation of some physiological and quality changes during fruit storage[1]

Abstract

In fruits and vegetables, certain physiological processes, such as respiration and transpiration, and quality properties, such as color, firmness or weight, are used as consumer-based criteria of acceptability and shelf life indicators. Changes in the rates of oxygen consumption, carbon dioxide and water vapor generation and product quality properties result from a series of biochemical processes. These processes are affected by internal conditions such as the ripening state and by external conditions such as temperature or environmental gas concentration. Understanding the time-progress of these processes and properties, according to variables that affect the product, and the mathematical models that regulate them, would be beneficial in selecting the most appropriate storage and preservation conditions to meet determined quality and shelf-life requirements. In this chapter, the effect of postharvest storage conditions on biochemical and physiological processes related to respiration and transpiration and on quality property changes is described. Then, equations developed by many authors that describe the changes in these processes and properties according to storage conditions are reported.

Key words: Color, firmness, postharvest storage, respiration, transpiration

1.1 Introduction

Consumers of fruits and vegetables have recently developed greater interest in the importance of the quality of these products (Batt, 2006; Fearne et al., 2006; Hewett, 2006). Thus, it has become increasingly essential for producers and distributors to use tools for the rapid and easy monitoring of the changes in fruit quality during the postharvest period.

---

[1] This chapter (with minor modifications) was published as:
Castellanos, D.A. & Herrera, A.O. 2015. Mathematical models for the representation of some physiological and quality changes during fruit storage. *Journal of Post-Harvest Technology,* 3(1), 18-35. http://dx.doi.org/10.5281/zenodo.47675

An effort has been made to correlate changes in product properties during the postharvest period (mainly during storage) with quality and shelf-life decline (Schouten et al., 2007; Lukasse and Polderdijk, 2003). These correlations could be beneficial in the development of models with the capacity to predict product future behavior under a wide range of conditions. The objective of this article is to review the models that describe respiration and transpiration processes, color evolution and firmness as a function of storage conditions in fruits in the postharvest stage.

1.2 The effect of environmental conditions on quality properties

Fruits, once harvested, are subject to chemical modifications that are mainly affected by environmental conditions, such as temperature. The concentration of gases, such as oxygen, carbon dioxide, ethylene and water vapor, directly affect the biochemical processes that these products undergo during ripening. These conditions should be considered in the postharvest storage of fruits by establishing the most suitable limits to reduce the deterioration rate (Kader et al., 1989; Lee & Kader, 2000). Herein, some factors are presented.

1.2.1 Temperature

Temperature is the factor that most substantially affects the rate of various metabolic reactions. Once the temperature increases, respiration, enzymatic processes and several reactions related to sensory properties such as firmness, color and flavor also increase, leading to a state of senescence. Likewise, as the temperature decreases, these processes slow down.

Fruits must be preserved at the lowest temperature that the product can tolerate to delay the ripening rate without lowering it more than the critical storage temperature to avoid chilling injury (CI) problems in the fruit (Kader, 2002; Thomson et al., 2002). Some products such as avocados, bananas, grapes, lemons, limes, papayas and tomatoes do not tolerate low temperatures, and their optimum storage temperature is approximately 10 °C (Kader 1997; Lukatkin et al., 2012; Saltveit, 2003). For example, softening is enhanced in tomatoes stored to low temperatures due to CI and loss of turgor pressure (Biswas et al. 2014). When mangos were stored at 12 °C, mild cold damage was caused in the skin of the fruit, expressed as red spots around lenticels (Pesis et al., 2000). In the case of Pawpaw fruits, storage temperature of 4 °C led to a fail to ripen (Galli et al., 2009).

An increase in temperature also results in an increase in the transpiration rate and moisture loss and a simultaneous increase in the capacity of the air around the product to contain water and decrease in its relative humidity (Kang & Lee 1998). Moreover, low temperature storage causes a decrease in the activity of the enzymes 1-aminocyclopropane-1-carboxylic (ACC) oxidase and ACC synthase, which participate in the conversion reactions of ACC to ethylene, reducing its production. By transferring the fruit to room temperature, ACC oxidation continues, and more ethylene will be produced, enhancing ripening (Larrigaudiere et al., 1997; Zhou et al., 2001). Each 10 °C of temperature increase results in a double to triple increase of certain respiration-related biological reaction rates (Sandhya, 2010). Temperature fluctuation must also be considered given that can cause extensive damage due to condensation and metabolic and ripening disorders (Tano, et al., 2007).

1.2.2 Oxygen

Oxygen is fundamental for aerobic respiration and numerous metabolic reactions. A decrease in the oxygen concentration results in a decrease in the rate of the reactions in which it is involved. In fruits, when the O_2 concentration around the fruit is decreased below 8%, ripening slows down (Sandhya, 2010). A low oxygen level slows down ripening by inhibiting ethylene generation and function; at O_2 levels of 2.5%, ethylene generation is reduced by approximately half (Satyan et al., 1992; Ščetar et al., 2010). O_2 concentrations of approximately 2% or less may result in anaerobic respiration reactions that lead to undesirable products, according to each particular anaerobic compensation point that can vary depending on several factors such as specie, cultivar, etc. Moreover, fruits exposed to such low O_2 levels may lose their normal ripening ability once placed again at normal levels (Ke & Kader, 1989; Sandhya, 2010).

1.2.3 CO_2

CO_2 is produced by the oxidation of respiration substrates. The CO_2 production rate is proportional to the respiratory intensity (RI), and an increase in its concentration generally causes various effects on fruits and vegetables in the postharvest state. CO_2 concentrations greater than 1% in the atmosphere around the fruit retard ripening and lead to a decrease in RI (Watada et al., 1996). High CO_2 levels (for example in MA storage) may enhance the inhibition of the growth of microorganisms that are responsible for product deterioration (Bennik et al., 1998). Kubo et al. (1990) observed an RI decrease in some climacteric fruits

and broccoli after exposure to a 60% CO_2 atmosphere but an RI increase in eggplants, cucumbers, peas, spinach and lettuce. Enzymatic activity declined in pears stored under 10% CO_2 (Kerbel et al., 1988). Liu et al. (2004) demonstrated that in bananas stored under 60% CO_2, respiratory climacteric was suppressed, and the pyruvate, 2-oxoglutarate, and malate contents decreased.

1.2.4 Ethylene

Ethylene is a naturally synthesized hormone in plants and is associated with the onset of ripening (Watkins, 2003); it is physiologically active at concentrations of 0.1 ppm and below. Non-climacteric fruits generate a small amount of ethylene as a product of their metabolic processes (Wu, 2010). In climacteric fruits such as bananas, mangos or apples, which complete their ripening in the postharvest state, ethylene exposure contributes to the acceleration of their ripening. These fruits also produce higher quantities of ethylene because of their metabolic processes (Kader, 1988). In this type of fruit, ethylene is the main volatile component produced (50 – 75% of the total carbon content of all volatiles), and by not having a strong aroma, it does not contribute to typical fruit characteristic flavor (Kader, 1999). Exposure to high CO_2 (for example, air + 20% CO_2) or low O_2 (for example, 0.25% O_2) concentrations greatly suppresses C_2H_4 biosynthesis in climacteric fruit tissue. A decrease in O_2 levels to concentrations less than 8% leads to a significant inhibition of the C_2H_4 biosynthesis in fresh fruits and vegetables (Kader, 1986). 'Golden Delicious' apples maintained at 2.5% O_2 have exhibited a suppressed internal C_2H_4 concentration and ACC (1-aminocyclopropane-1-carboxylic acid) accumulation (Gorny & Kader, 1996).

Finally and although is not the purpose of this review, is good to consider the influence of storage conditions under modified atmosphere packaging. Barrier properties of the package containing the fruit (permeability) coupled with respiration will determine the concentration of gases in the atmosphere that surrounds it and this in turn will affect fruit physiological behavior, so that is necessary to take into account the interaction between film and produce when selecting one that offers favorable storage conditions.

1.3 Use of models to represent physiological and quality changes in harvested fruits according to storage conditions

The use of models is an efficient tool to predict characteristic changes in a biological system affected by various environmental conditions, without the need to assess these conditions

in real time. For the successful use of a model, it is necessary that the model can accurately represent the desired physical phenomenon. A model requires previous validation, which means that its parameters must have been identified or adjusted based on experimental data (Tijskens and Schouten, 2009).

Many models have been developed to assess changes in fruits stored under various conditions (Caleb et al., 2012; Hertog et al., 2003; Hertog et al., 2004; Lukasse & Polderdijk, 2003; Schouten et al., 2007; Verdijck & Lukasse, 2000). However, few models consider the interactions among the principal storage variables (temperature, storage atmosphere composition, relative humidity, product ripening during storage, etc.). Each particular fruit has properties that reflect its quality and ripening changes; in general, properties that are easy to measure, representative throughout the product's shelf-life non-destructive, if possible, and affected by storage conditions should be investigated. For certain products, color, texture, moisture, weight loss and respiration rates are the most used properties (Hertog et al., 2001; Jha, 2010; Mangarat & Goswami, 2011; Tijskens & Schouten, 2009).

1.3.1 Respiratory intensity (RI)

Respiration is a metabolic process that provides the plant with the necessary energy to perform its biochemical processes. Respiration substrates oxidized to produce CO_2 and water. Fruit shelf-life after harvest depends on RI; fruits such as mango and banana that have an increased RI are severely perishable (Paliyath & Murr, 2008b). The energy released during respiration is associated with the energy required to completely oxidize a mole of hexose (Brownleader, 1997; Taiz & Zeiger, 2012). A mole of hexose releases approximately 2880 kJ during respiration. Each glucose molecule is oxidized to 6 CO_2 molecules, using 32 molecules of adenosine diphosphate (ADP) and six molecules of O_2 to form 12 water molecules (Eq. 1.1). Under normal physiological conditions, 50% to 60% of this energy is chemically captured to form 32 molecules of adenosine triphosphate (ATP), which are required for subsequent cell metabolic processes. The respiratory metabolism is limited at low partial O_2 pressure, which leads to a decrease in the chemical energy produced during respiration (Mir & Beaudry, 2002).

$$C_6H_{12}O_6(s) + 6O_2 \rightarrow 6CO_2 + 6H_2O + energy \quad (1.1)$$

By the time carbohydrates such as glucose or fructose are completely oxidized, the O_2 volume used per unit time will be practically the same as the volume of generated CO_2 per

unit time (Kader et al., 1987; Renault et al., 1994). For organic acid oxidation, more CO_2 volume is produced than the used O_2. From the above, the respiratory quotient (RQ) is defined as the ratio of CO_2 produced to O_2 consumed per unit time. The RQ values range between 0.7 and 1.3 for the majority of vegetables (Kader & Salveit, 2003). High RQ values usually indicate anaerobic respiration in produce tissues that produce ethanol. In such tissues, a rapid change in the RQ can be used as an indication of the shift from aerobic to anaerobic respiration (Salveit, 2004).

Many mathematical models have described the respiration process and how O_2 and CO_2 levels affect this process. These models can be grouped into two large categories: empirical models (lineal, polynomial or exponential) and models based on Michaelis-Menten enzyme kinetics (Fonseca et al., 2002). The simplest empirical model is the lineal model. In this model, the O_2 consumption rate is determined by its concentration only, as shown in Eq. 1.2:

$$r_{O_2} = a_1 + a_2 y_{O_2} \quad (1.2)$$

Where r_{O2} is the O_2 consumption rate, y_{O2} is the O_2 mole fraction (or, in general, the O_2 concentration in appropriate units) and a_1 and a_2 are constants. Fishman et al. (1996) used this type of equation to model mango respiration.

In exponential models, the O_2 concentration is the only one mainly considered in determining the respiration rate (Eq. 1.3), although the CO_2 concentration could also be considered (Eq. 1.4):

$$r_{O_2} = a_1 + a_2 \exp\left(a_3 y_{O_2}\right)^{a_4} \quad (1.3)$$

$$r_{O_2} = a_1 + a_2 \exp\left(a_3 y_{O_2} y_{CO_2}\right)^{a_4} \quad (1.4)$$

Where y_{CO2} is the CO_2 mole fraction (or, as before, the CO_2 concentration in appropriate units), y_{O2} is the O_2 concentration and a_1, a_2, a_3 and a_4 are constants. Eq. 1.3 has been used to model the respiration of tomatoes (Cameron, et al., 1989), blueberries (Beaudry et al., 1992; Emond et al., 1993) and strawberries (Talasila et al., 1992). Eq. 1.4 has been used to model the respiration of apples, slightly processed under modified atmosphere (MA;

Rocculi et al., 2006), and slightly processed packed kiwi, banana and pears (Del Nobile et al., 2007).

Some authors like Finnegan et al. (2013) propose that respiration rate will not be constant throughout the storage time, and that this will be increased with increasing physiological age of the fruit, representing this process through a model based on exponential decay (for CO_2 production):

$$r_{CO_2} = r_{CO_2}^{eq} + \left(r_{CO_2}^{i} - r_{CO_2}^{eq}\right) e^{-\alpha t} \quad (1.5)$$

Where r_{CO2} is the respiration rate at any time (t); $r_{CO_2}^{i}$ is the initial respiration rate; $r_{CO_2}^{eq}$ is the respiration rate at equilibrium time; t is the storage time and α is a constant coefficient.

Polynomial models include equations of different orders and multiple adjustable coefficients that consider the O_2 concentration and time. Gong & Corey (1994) used a polynomial equation to determine tomato respiration according to O_2 concentration. Dash et al. (2012) used second-order polynomial equations, obtained by regression, to determine O_2 consumption and CO_2 generation in packed sapote based on O_2 and CO_2 concentrations. Morales-Castro et al. (1994) considered O_2 and CO_2 concentrations, temperature and time for the respiration of sweet corn and obtained polynomial equations by regression to calculate CO_2 generation and O_2 consumption. Previous models however, do not provide an analytical representation of the mechanisms of the respiration processes being useful in very specific cases, so that other models based on the Michaelis-Menten equations have been used as a good alternative to describe the effect of O_2 and CO_2 concentrations during respiration (Fonseca et al., 2002; Geysen et al., 2005; Gomes et al., 2010; Ho et al., 2013). Eq. 1.6 illustrates the simplest mechanism of enzymatic kinetics; the model is based on a limiting enzymatic reaction where the substrate is O_2:

$$r_{O_2} = \frac{r_{O_2}^{max} y_{O_2}}{K_m + y_{O_2}} \quad (1.6)$$

Where r_{O2} is the O_2 consumption rate (or CO_2 production, r_{CO2}, $cm^3\ kg^{-1}\ d^{-1}$), r^{max} is the maximum rate of O_2 consumption or CO_2 production ($cm^3\ kg^{-1}\ d^{-1}$) and K_m is the dissociation constant of the enzyme-substrate complex (dimensionless). This equation has been used

to model the respiration of apples (Andrich et al., 1998; Lakakul et al., 1999), blueberries (Song et al., 2002) and cauliflower (Ratti et al., 1996).

The basic Michaelis-Menten equation is transformed into one of the following equations depending on the type of inhibition produced by the generated CO_2 (Fonseca et al., 2002; Gomes et al., 2010; Heydari et al., 2010; Lee et al., 1996; Maneerat et al., 1997; Peppelenbos & van't Leven 1996):

Competitive inhibition:

$$r_{O_2} = \frac{r_{O_2}^{max} y_{O_2}}{K_m\left(1+\frac{y_{CO_2}}{K_{mc_{CO_2}}}\right)+y_{O_2}} \quad (1.7)$$

Non-competitive enzyme inhibition but competitive inhibition for the enzyme-substrate complex (uncompetitive):

$$r_{O_2} = \frac{r_{O_2}^{max} y_{O_2}}{K_{m_{O_2}}+y_{O_2}\left(1+\frac{y_{CO_2}}{K_{mu_{CO_2}}}\right)} \quad (1.8)$$

Non-competitive inhibition:

$$r_{O_2} = \frac{r_{O_2}^{max} y_{O_2}}{(K_m+y_{O_2})\left(1+\frac{y_{CO_2}}{K_{mn_{CO_2}}}\right)} \quad (1.9)$$

A mixed non-competitive and competitive inhibition for the enzyme-substrate complex:

$$r_{O_2} = \frac{r_{O_2}^{max} y_{O_2}}{K_m\left(1+\frac{y_{CO_2}}{K_{mc_{CO_2}}}\right)+y_{O_2}\left(1+\frac{y_{CO_2}}{K_{mu_{CO_2}}}\right)} \quad (1.10)$$

K_{mcCO2}, K_{muCO2} and K_{mnCO2} are constants representing the competitive enzyme, non-competitive enzyme and non-competitive inhibitions, respectively. Competitive inhibitions occur when the inhibitor (CO_2) and the substrate compete for binding to the same active site on the enzyme. Thus, at high CO_2 concentrations, there is a lower maximum RI. Non-competitive enzyme inhibition occurs when the inhibitor reacts with the enzyme-substrate complex; in this case, the maximum RI is not very affected by high CO_2 concentrations.

This type of enzymatic kinetics has been successfully used for many products (Bhande et al., 2008; Heydari et al., 2010; Mangarat & Goswami, 2011; McLaughlin & O'Beirne, 1999). Non-competitive inhibition occurs when the inhibitor reacts not only with the enzyme but also with the enzyme-substrate complex (Lee et al., 1996; Maneerat et al., 1997).

Temperature has an effect on respiration processes and shall be considered in mathematical models (Fonseca et al., 2002). All the constants appearing in equations1.6 to 1.10, together with the maximum O_2 consumption rate and CO_2 generation, depend on the temperature. This dependence has been described in the Arrhenius equation (Fonseca et al., 2002; Gomes et al., 2010) as follows (in this case for the maximum oxygen consumption rate):

$$r_{O_2}^{max} = r_{O_2\theta}^{max} e^{-Ea/RT} \quad (1.11)$$

Where $r_{O2\theta}^{max}$ is the maximum O_2 consumption rate at infinite temperature, E_a is the activation energy (kJ mol^{-1}), R is the universal gas constant (kJ mol^{-1} K^{-1}) and T is the temperature (K). Other authors (Oluwafemi et al., 2012; Iqbal et al., 2009) have used the O_2 consumption rate and CO_2 generation rate as solely depending on temperature, using a reference temperature in the Arrhenius equation (T_{ref}, in K):

$$r_{O_2} = r_{O_2 ref} e^{\left(-\frac{Ea}{R}\right)\left(\frac{1}{T}-\frac{1}{T_{ref}}\right)} \quad (1.12)$$

1.3.2 Transpiration rate (TR) and moisture loss

A low relative humidity can increase transpiration damage and lead to excessive dehydration, RI increase and finally to a loss of product quality. Alferez et al. (2005) and Kader (1985) state that relative humidity should be maintained at approximately 85-95% during handling and storage. Lower values cause fruit dehydration with subsequent weight loss, while higher values could speed up fruit spoilage because part of the water vapor can build up in the product packaging due to storage temperature fluctuations, favoring microbial growth (Kader, 1988). However, there are fruits such as papaya or 'mountain papaya' that can be well preserved at less than 40% relative humidity (Baiyewu & Amusa, 2005).

During ripening, there is a continuous loss of water due to transpiration and disassembly of the different components of the cell wall (Brummell, 2006; Kissinger et al., 2005), degradation of pectic compounds and changes in turgor pressure (Abera et al., 2014; Saladie et al., 2007). Thus, their permeability to water that leaves the cell increases, which also produces wilting and excessive pulp smoothness when the loss is high (Wills et al., 2007). Cellular membrane deterioration is also a key factor for the weight loss. It is critical the first day at harvest in all the produce due to the effect of cutting and to the high respiration rate and transpiration associated with cutting, stress and handling. Some authors have not considered the first day in order to have a linear trend in weight loss (Conesa et al., 2014). Thus, TR is the quantity of water loss from a plant tissue per unit time. This parameter is affected by the own properties of the fruit (morphological characteristics, surface-to-volume ratio, ripening state, damage) and by environmental factors (temperature, relative humidity, air speed and pressure; Kader, 1992). The TR of a fruit is initially expressed by its weight loss (Leonardi et al., 1999):

$$r_{H_2O}^{trs} = \frac{W_0 - W}{t(W_0/1000)} \quad (1.13)$$

Where $r_{H_2O}^{trs}$ is the TR (g kg^{-1} h), t is the transpiration time (h), W_0 is the initial weight of the fruit (g) and W is the weight of the fruit at the given time t (g).

The most basic model to determine TR considers that the driving force for transpiration is the difference in water vapor pressure between the product surface and its surroundings. This relationship is expressed through the following equation (Becker & Fricke, 1996):

$$r_{H_2O}^{trs} = k_i(p_s - p_{at}) \quad (1.14)$$

Where k_i is the transpiration coefficient, (p_s – p_{at}) is the deficit in vapor pressure, p_s is the vapor pressure at the surface of the product and p_{at} is the vapor pressure in its surroundings. The values of k_i for different products can be found in the ASHRAE Handbook (2006).

Mahajan et al. (2008) developed a model for TR based on the above considerations. Their model considers a) the difference between the relative humidity of the medium and the fruit water activity and b) the effect of temperature on the transpiration process:

$$r_{H_2O}^{trs} = k_i(a_{wat} - a_w)\left(1 - e^{-bT}\right) \quad (1.15)$$

Where a_w is the fruit's average water activity, a_{wat} is the water activity of the medium (RH/100), k_i is the mass transference coefficient, T is the temperature (°C) and b is a constant. The weight of the fruit at a given time-point can be calculated by combining equations 1.13 and 1.15, which results in the following equation (Sousa-Gallager et al., 2013):

$$W = W_0 - k_i(a_{wat} - a_w)\left(1 - e^{-bT}\right)\left(\frac{tW_0}{1000}\right) \quad (1.16)$$

The amount of water that the fruit loses during transpiration can be related to the respiratory heat and to the heat convection through the energy balance of the process (Becker & Fricke, 2001; Kang & Lee, 1998; Song et al., 2002):

$$qW + hA_p(T_{at} - T_p) = m_{H_2O,gen}\lambda + c_p W\frac{dT_p}{dt} \quad (1.17)$$

Where q is the respiratory heat (kJ kg^{-1} h^{-1}), W is the weight of the product (kg), h is the convective heat transfer coefficient (kJ m^{-2} $°C^{-1}$ h^{-1}), c_p is the specific heat of the product (kJ kg^{-1} $°C^{-1}$). λ is the latent heat of moisture evaporation (kJ kg^{-1}), A_p is the surface area of the produce (m^2), T_{at} is the ambient temperature (°C), T_p is the produce temperature (°C) and $m_{H2O,gen}$ is the mass of lost water/water vapor generated (kg h^{-1}).

The heat transferred through natural convection from ambient air and the heat generated from respiration inside the product both increase the temperature of the fruit, as sensible heat, and are converted to the latent heat of moisture evaporation in transpiration (Kang & Lee, 1998). This water loss in the produce can be expressed as:

$$m_{H_2O,gen} = \frac{qW + hA_p(T_{at} - T_p) - c_p W\frac{dT_p}{dt}}{\lambda} \quad (1.18)$$

Respiration heat is obtained by the oxidation of glucose into products and energy (Eq. 1.1). Thus, the respiration heat (in kJ kg^{-1} h^{-1}) can be estimated by the respiration reaction and by considering the respiration rate as the average of the O_2 consumption rate (R_{O2}, in mol kg^{-1} h^{-1}) and CO_2 conversion (R_{CO2}; Kang & Lee, 1998):

$$q = \left(\frac{2816}{6\ mol}\right)\left(\frac{R_{O_2}+R_{CO_2}}{2}\right) \quad (1.19)$$

The above expression is multiplied by a correction factor to correct for the respiration energy dissipated as heat and to consider that glucose is not the only substrate during respiration (Song et al., 2002). For a 100% conversion (supposing that glucose is the only substrate), α will be 1. The latent heat of moisture evaporation λ (in kJ kg^{-1}) is obtained from the equation (Brooker, 1967):

$$\lambda = 2502{,}535 - 2{,}386(T - 273{,}16) \quad (1.20)$$

Where T is expressed in Kelvin.

Finally, the transpiration rate (in moles per kg of fruit and storage day) can be expressed as water loss in the stored fruit by multiplying the mass of generated water vapor (product water loss) with the ideal gas equation:

$$R_{H_2O}^{trs} = m_{H_2O,gen}\left(\frac{RT}{WPM_{H_2O}}\right) \quad (1.21)$$

Where M_{H2O} is the molar mass of water in kg mol^{-1}, R is the gas constant, T is the refrigeration temperature, W is the weight of the fruit and P is the pressure.

The establishment of the existing difference between the vapor pressure of water of the product surface area (p_s) and the vapor pressure of water in the produce surroundings is necessary to effectively use transpiration models. The vapor pressure of the surface area of the product will be a consequence of the surface temperature (T_{ps}) and the effect of the vapor pressure deficit (VPD) caused by the dissolved substances. Thus, the vapor pressure of the surface will be (Becker & Fricke, 1996)

$$p_s = VPD * p_{sT_{ps}} \quad (1.22)$$

The VPD values for different vegetables were determined by Chau et al. (1987) and Beck et al. (1995).

1.3.3 Firmness change

Firmness declines as ripening continues up to a minimum level when product senescence is reached. Firmness loss can be attributed to various factors, including disassembly of polysaccharide networks, pectin degradation, hydrolysis of starch, celluloses and hemicellulose in cellular walls (Paliyath & Murr, 2008a; Van Dijk & Tijskens, 2000), and as some authors suggest (Biswas et al., 2014; Saladie et al., 2007), decline in cellular turgor and water loss by transpiration as consequence of these changes in cell architecture. Fruits such as peaches, pears, tomatoes and strawberries can excessively lose their firmness because they have increased levels of endo-polygalacturonase activity (which cleaves the pectin sequence at intermediate points in contrast to exo-polygalacturonase, which removes galacturonic acid fractions at terminal sequence points). Other fruits such as apples maintain their firmness because they do not undergo this activity (Daas et al., 2000). During postharvest storage, some compounds are affected while others are not. Thus, firmness (F, measured in N or in kg_f) can be considered to have a fixed (F_{fix}) and a variable (F_{var}) component:

$$F = F_{fix} + F_{var} \quad (1.23)$$

The compounds that do not undergo degradation or that are broken down slowly, such as celluloses and hemicelluloses, contribute to the fixed firmness. The compounds that undergo degradation, such as pectins, or that are lost, such as moisture, contribute to the loss of turgor pressure, and from this to the variable firmness (Biswas et al., 2014).

Gwanpua et al. (2012) developed a firmness model considering that its variable part depends on the degradation of pectins (P) by pectic enzymes (E_{pect}), which results in galacturonic acid (G) through a simple irreversible reaction (similar to the proposal of Tijskens & Schouten, 2009):

$$P + E_{pect} \xrightarrow{k_{pect}} G + E_{pect} \quad (1.24)$$

Thus, the firmness is:

$$F = F_{fix} + \gamma[P] \quad (1.25)$$

Where [P] is the pectin concentration (nmol^{-3} m^3), F_{fix} is the fixed firmness component and is not affected by enzymatic degradation and Υ (N m^3 nmol^{-1}) is a correction factor that relates firmness (F) to the non-hydrolyzed pectin during enzymatic degradation ([P]).

The presence of ethylene (Eth) in the fruit directly affects the pectic enzyme concentration (Lin et al., 2009). This relationship, which includes complex mechanisms, has been explained in a simplified manner by Gwanpua et al. (2012), as a group of amino acids (E_{pre}) that are converted by ethylene in pectic enzymes (E_{pect}).

$$\mathrm{E_{pre}} + \mathrm{Eth} \xrightarrow{\mathrm{k_{Epect}}} \mathrm{E_{pect}} + \mathrm{Eth} \quad (1.26)$$

Pectic enzyme degradation (E_{pect}) into other compounds (E_{denz}) should also be considered (Johnston et al. 2009). In that case:

$$\mathrm{E_{pect}} \xrightarrow{\mathrm{k_{Edenz}}} \mathrm{E_{denz}} \quad (1.27)$$

Changes in the concentration of pectins and pectic enzymes over time are described through first order kinetics equations:

$$\frac{\mathrm{d[P]}}{\mathrm{dt}} = -\mathrm{k_{pect}[P]\left[E_{pect}\right]}, \text{ where } \mathrm{[P](t=0) = [P]_0} \quad (1.28)$$

$$\frac{\mathrm{d[Eth]}}{\mathrm{dt}} = \frac{\mathrm{r_{Eth}^{max} y_{O_2}}}{\mathrm{K_{m_{O_2,Eth}} + y_{O_2}\left(1 + \frac{y_{CO_2}}{K_{mu_{CO_2,Eth}}}\right)}} + \mathrm{P_{Eth} A([Eth]_{out} - [Eth])},$$

$$\text{where } \mathrm{[Eth](t=0) = [Eth]_0} \quad (1.29)$$

Where [P] is the pectin concentration (nmol^3 m^{-3}), [E_{pect}] is the concentration of pectic enzymes, [Eth] is the endogenous ethylene concentration, k_{pect} is the pectin degradation rate constant (s^{-1}) and k_{Epect} and k_{Edenz} are the pectic enzymes generation and degradation rate constants, respectively (Gwanpua et al., 2012).

The changes in ethylene concentration are calculated based on the O_2 and CO_2 concentrations in the surroundings of the product using a Michaelis-Menten modified model of non-competitive inhibition for CO_2 (Eq. 1.30), which is similar to Eq. 1.3 (Génard & Gouble, 2005; Gwanpua et al., 2012; Sanders & de Wild, 2003). Génard & Gouble (2005)

in their simulation model ETHY, considers that the respiration process has not a significant influence on the generation of ethylene and that its emission is highly dependent on temperature, only slightly sensitive to air O_2 concentrations and almost insensitive to CO_2 concentrations. The above suggests that the respiratory climacteric may not be required for ripening and apparently is not important for modelling.

$$\frac{d[Eth]}{dt} = \frac{r_{Eth}^{max} y_{O_2}}{K_{m_{O_2,Eth}} + y_{O_2}\left(1 + \frac{y_{CO_2}}{K_{mu_{CO_2,Eth}}}\right)} + P_{Eth} A([Eth]_{out} - [Eth]),$$

$$\text{where } [Eth](t = 0) = [Eth]_0 \quad (1.30)$$

Where r_{Eth}^{max} is the maximum ethylene generation rate (nmol m^{-3} s^{-1}), $K_{mO2,Eth}$ is the Michaelis constant for ethylene production, $K_{muCO2,Eth}$ is the constant for the non-competitive inhibition for CO_2, y_{O2} is the molar fraction of O_2 in the surroundings of the product. CO_2 is the molar fraction of CO_2, P_{Eth} is the permeability of ethylene in the product peel (m^{-2} s^{-1}), A is the surface area of the product (m^2) and $[Eth]_{out}$ is the concentration of ethylene around the product (nmol^{-3} m^3). The constants r_{Eth}^{max}, $K_{mO2,Eth}$ and $K_{muCO2,Eth}$ depend on temperature through an Arrhenius relationship such as that in Eq. 1.29 (Gwanpua et al., 2012).

Other authors have described the variable part of firmness through a first-order model (Eq. 1.31, Hertog et al., 2004; Lana et al., 2005; Pinheiro et al., 2013; Schouten et al., 2007) or a logistic model (Eq. 1.32, Hertog et al., 2003). In these models, these authors considered that the variable part depends on respiration, the O_2 and CO_2 concentrations in the surroundings of the product and the temperature. F_0 is the initial firmness, and F_{fix} is the equilibrium firmness. k represents the firmness loss rate and can depend on O_2 and CO_2 levels through Michaelis-Menten relationships (Peppelenbos et al., 1996; Hertog et al., 2001; Hertog et al., 2004) that consider respiration as oxidative and fermentative (Eq. 1.33) or can depend only on temperature through a Arrhenius relationship such as that in Eq. 1.34 (Sila et al., 2004; Schwaab & Pinto, 2007):

$$F = F_{fix} + (F_0 - F_{fix})e^{-kt} \quad (1.31)$$

$$F = \frac{F_{fix}}{1 + (F_0 - F_{fix})e^{-kt}/F_0} \quad (1.32)$$

$$k = \frac{k_f^{max} r_{CO_{2(f)}}^{max}}{1 + {}^{y_{O_2}}/_{K_{m_{CO_{2(f)}}}}} + \frac{k_O^{max} r_{O_2}^{max} y_{O_2}}{K_{mO_2} + y_{O_2}\left(1 + {}^{y_{CO_2}}/_{K_{mu_{CO_2}}}\right)} \quad (1.33)$$

$$k = k_{ref} e^{\left(-\frac{E_a}{R}\right)\left(\frac{1}{T} - \frac{1}{T_{ref}}\right)} \quad (1.34)$$

In these equations, k_f^{max} and k_O^{max} are the maximum rates of firmness loss related to fermentative and oxidative processes, respectively, and $K_{mu_{CO_2}}$ is the Michaelis-Menten constant for firmness loss inhibition related to oxidation by CO_2. k_f^{max} and k_O^{max} are functions of temperature attributed to Arrhenius relationships, and $r_{CO_{2(f)}}^{max}$ and $r_{O_2}^{max}$ are the maximum rates of anaerobic CO_2 production and O_2 consumption, respectively, which are also temperature-dependent through Arrhenius equations (Eq. 1.34). k_{ref} is the constant reference rate for the reference temperature (T_{ref}), E_a is the activation energy and R is the gas constant. Castellanos & Algecira (2012) used a simplified version of equation (33) for 'Sucrier' banana storage. In this case, the contribution of the fermentative process to the firmness loss rate was negligible because the O_2 concentrations during storage were greater than zero. For other fruits, such as avocados (Hertog et al., 2003), a similar approach was applied.

1.3.4 Color change

Color change in fruits is the most evident indicator of ripening (Will et al., 2007). Chlorophyll (Chl) is degraded by the action of three Chl catabolic enzymes, chlorophyllase, pheophorbide-α-oxygenase (PAO) and red Chl catabolite reductase (RCCR; Dangl et al., 2000; Hortensteiner, 2006), and reveals carotenoids, such as lycopene and carotene, that are present in the cortex, which result in the characteristic fruit color. Likewise, chloroplast transformation in chromoplasts through remodeling of the internal membrane system with the formation of carotenoid-accumulating structures, also results in color changes in the produce cells (Egea, et al., 2010). In some fruits, there are other compounds, products of secondary metabolism, such as anthocyanins that are responsible for the color of grapes, blueberries and apples (Paliyath & Murr, 2008b).

The color of an object can be described by various color models such as the RGB (red, green and blue) model, which is used in color monitors, Hunter Lab, CIE (International Commission on Illumination) *L*a*b**, CIE XYZ, CIE *L*u*v**, CIE Yxy. These differ in the color

space symmetry and in the coordinate system used to define the points in this space. The tristimulus methods of the CIE and of the similar Hunter model are of the greatest importance for instrumental measurements. According to CIE concepts, the human eye has three-color receptors: red, green and blue and all of their combinations. Many food studies use CIE *L*a*b** color coordinates and their derived psychophysical parameters C* (chroma) and h (hue; tone) or Hunter Lab coordinates (HunterLab, 2008). McGuire (2012) noted that it is difficult to separately interpret the values of the coordinates *a** and *b** and that, most likely, these are not independent variables. He proposed the use of C^*_{ab} and h_{ab} as more suitable color measurements. It is also important to clearly establish the brightness, calibration standards and viewing angle to accurately interpret color data.

The CIE 1976 *L*a*b** (CIELAB) color space is defined when the coordinates for luminosity, L*, and chromaticity, *a**, *b**, are presented in a three-dimensional space. L* represents the luminosity of the color or clarity and is the vertical axis with values ranging between 100, for white, and zero, for black. The axes for *a** and *b** have no specific numeric limits. Positive values for *a** represent red/magenta, and negative values represent green. Similarly, positive values for *b** represent yellow, and negative values represent blue (HunterLab, 2008).

The following equation defines the total color difference (ΔE^*_{ab}) between two different points measured in the same sample using the geometrical distance in a spherical space:

$$\Delta E^*_{ab} = ((L^*)^2 + (a^*)^2 + (b^*)^2)^{1/2} \quad (1.35)$$

The psychophysical parameters chroma, C^*_{ab}, and tone (hue), h_{ab}, stem from luminosity-chromaticity coordinates (L*, *a**, *b**) defined by CIELAB space as follows:

$$C^*_{ab} = (\,(a^*)^2 + (b^*)^2)^{1/2} \quad (1.36)$$

$$h_{ab} = \arctan\left(\frac{b^*}{a^*}\right) \quad (1.37)$$

Several authors have proposed different equations to represent the change in color coordinates L*, *a** and *b** as a function of time using zero-order (Eq. 1.38), first-order (1.39), second-order polynomial (Eq. 1.40) and logistic models (Eq. 1.41).

$$C = C_0 + kt \quad (1.38)$$

$$C = C_0 \exp(-kt) \quad (1.39)$$

$$C = k_1 t^2 + k_2 t + k_3 \quad (1.40)$$

$$C = C_0 + \frac{C_{fix}}{1+\exp\left(-k\left(t-t_{1/2}\right)\right)} \quad (1.41)$$

In Eqs. 1.39-1.41, C is the color coordinate, C_0 is the initial value of the color coordinate, C_{fix} is the equilibrium value of the color coordinate, t is the storage time, $t_{1/2}$ is the time required to reach a half of the equilibrium value, k, k_1, k_2, k_3 are parameters of change dependent on storage conditions (T, O_2 and CO_2 levels).

Ren et al. (2006) assessed the kinetics of color changes in broccoli stored under refrigeration. These authors observed that *b** and ΔE^*_{ab} changes could be presented by a first-order exponential model (1.39) where the k parameter is temperature-dependent and can be expressed by an Arrhenius relationship. In addition, these authors describe changes during storage time for *a** and h_{ab} using second-order polynomial functions (Eq. 1.40). In studies about postharvest storage of banana fruits (Castellanos & Algecira, 2012; Chen & Ramaswamy, 2002), peel color changes were described by Hunter Lab system color coordinates based on the O_2 concentration and temperature over time. Lightness was described by a logistic growth model (Eq. 1.41), *a** was described using a zero-order model (Eq. 1.38), and *b** was described using a first-order model (Eq. 1.39). Chen & Ramaswamy (2002) also presented the ΔE^*_{ab} value using a logistic model (Eq. 1.41), where all the constant rates only depend on temperature. The regression coefficients (R^2) for all the coordinates and ΔE^*_{ab} were higher than 0.96. Jha et al. (2007) defined a ripening index for mango that was independent of color coordinates. These authors considered the ripening index obtained by the total soluble solids and the optimum value, or 100 %. For mangoes, they consider the ripening index to be a function of *a** and *b** color coordinates according to the following equation:

$$I_m = j_1 + j_2 a^* + j_3 b^* + j_4 a^* b^* \quad (1.42)$$

Where j_1, j_2, j_3 and j_4 are the equation constants.

Gómez and Camelo (2002) also defined an average color index based on the L*, *a** and *b** coordinates of the CIELAB space, equally dependent on the storage conditions.

$$I_{cm} = \frac{2000 \times a^*}{L^* \times ((a^*)^2 + (b^*)^2)^{0,5}} \quad (1.43)$$

For the postharvest storage of tomatoes and limes, Hertog et al. (2004) and Pranamornkith (2009), respectively, presented a logistic model for the color tone h_{ab} based on time (Eq. 1.44). This behavior can be viewed as the consequence of two parallel processes: the exponential increase of enzymatic activity during ripening and the effect of enzymatic activity on color (Tijskens and Evelo 1994).

$$h(t) = h_{+\infty} + \frac{h_{-\infty} - h_{+\infty}}{1 + e^{kt(h_{-\infty} - h_{+\infty})\frac{h_{-\infty} - h_0}{h_0 - h_{+\infty}}}} \quad (1.44)$$

Here, $h_{-\infty}$ and $h_{+\infty}$ are the tone minimum and maximum values (balanced) in degrees, h_0 is the tone value at time zero and k is the constant temperature-dependent rate in d^{-1}. This dependency is represented by an Arrhenius relationship (Eq. 1.11).

Dixon & Hewett (1998) studied two apple varieties with a first-order model (Eq. 1.39). These authors studied the time-evolution of tone values h_{ab} depending only on temperature and used a combined Arrhenius model and Boltzmann enzyme distribution function to calculate the constant rate, k_h:

$$k_h = k_h^{max} \exp\left({-E_a}/{RT}\right) + \exp\left({\Delta S}/{R}\right)\exp\left({-\Delta H}/{RT}\right) \quad (1.45)$$

where k_h is the constant rate of h_{ab} change, kh^{max} is the maximum rate of change, E_a is the activation energy (kJ mol^{-1}), R is the gas constant (kJ mol^{-1} $K^{-1)}$, T is the temperature (K), ΔS is the entropy change (kJ mol^{-1} K^{-1}) and ΔH is the enthalpy change (kJ mol^{-1}).

No effort has been made to model the functions of other quality indicators, such as aroma and taste, based on environmental conditions because of the great difficulties involved. This unexplored area creates a wide range of new possibilities in which multidisciplinary groups of scientists and engineers specialized in fresh food preservation field can work in the future.

1.4 Conclusions

Properties such as color, firmness and moisture provide valuable information for the monitoring of quality changes in postharvest fruits because of their reliability and rapid and easy measurement. These changes are consequences of many biochemical and physiological processes that occur during fruit ripening, such as respiration and transpiration. In addition, these changes depend on the external conditions to which the fruit is exposed. Understanding the mechanisms in which these conditions affect quality changes processes is of great importance because it allows their appropriate modification to maintain quality and maximize preservation time.

To date, many authors have developed and used various mathematical models for particular cases of respiration and transpiration. They have presented, in a trustworthy manner, the progression of respiration and transpiration processes as well as the progression of quality properties, such as temperature activity, O_2, CO_2 and H_2O concentrations around products during postharvest storage. Based on this information, it is possible to monitor these progressions during storage and determine the availability (or quality) of the product at a given time. In addition, it is possible to simulate specific storage situations and to obtain concrete values of these quality properties when previously requested.

However, the application of these particular models is often limited. Only a few models for general use have been developed, such as the Michaelis-Menten enzyme kinetics model for the description of respiration (and in some cases of the firmness loss rate) or the combined model of mass transfer and respiration heat. Thus, more studies by multidisciplinary groups of chemists, biologists and engineers are necessary to develop more general and complex models for the description of quality properties.

These models should consider the characteristics of the product under study, for example, if it is climacteric or not, and how the conditions to which the product is exposed affect the biochemical and physiological processes. These processes result in respiration, transpiration and quality properties changes. Moreover, it is necessary that these models also consider other quality indicators such as aroma and taste.

1.5 References

Abera, M.K., Verboven, P., Herremans, E., Defraeye, T., Fanta, S.W., Ho, Q.T., Carmeliet, J. & Nicolai, B.M. 2014. 3D Virtual pome fruit tissue generation based on cell growth modeling. *Food Bioprocess Technology*, 7: 542-555.

Alferez, F., Zacarias, L. & Burns, J.K. 2005. Low relative humidity at harvest and before storage at high humidity influence the severity of postharvest peel pitting in citrus. *Journal of the American Society for Horticultural Science*, 130(2): 225-231.

Andrich, G., Zinnai, A., Balzini, S., Silvestri, S. & Fiorentini, R. 1998. Aerobic respiration rate of Golden Delicious apples as a function of temperature and p_{O2}. *Postharvest Biology and Technology*, 14: 1–9.

ASHRAE. 2006. *ASHRAE Handbook*. Fundamentals, Chapter 9: Thermal properties of foods.

Baiyewu, R.A. & Amusa, N.A. 2005. The effect of temperature and relative humidity on Pawpaw fruit rot in South-Western Nigeria. *World Journal of Agricultural Sciences*, 1(1): 80-83.

Batt, P.J. 2006. Fulfilling customer needs in agribusiness supply chains. *Acta Horticulturae*, 699: 83–89.

Becker, B.R. & Fricke, B.A. 1996. Transpiration and respiration of fruits and vegetables. In: *New Developments in Refrigeration for Food Safety and Quality. International Institute of Refrigeration*, Paris, and American Society of Agricultural Engineers, St. Joseph, MI, pp. 110-121.

Becker, B.R. & Fricke, B.A. 2001. A numerical model of commodity moisture loss and temperature distribution during refrigerated storage. *Acta Horticulturae*, 566: 431-436.

Bennik, M.H.J., Vorstman, W., Smid, E.J. & Gorris L.G.M. 1998. The influence of oxygen and carbon dioxide on the growth of prevalent Enterobacteriaceae and Pseudomonas species isolated from fresh and modified atmosphere stored vegetables. *Food Microbiology*, 15: 459-469.

Beaudry, R.M., Cameron, A.C., Shirazi, A. & Dostal-Lange D.L. 1992. Modified atmosphere packaging of blueberry fruit: effect of temperature on package O_2 and CO_2. *Journal of the American Society for Horticultural Science*, 117: 436–441.

Bhande, S.D., Ravindra, M.R. & Goswami, T.K. 2008. Respiration rate of banana fruit under aerobic conditions at different storage temperatures. *Journal of Food Engineering*, 87: 116–123.

Biswas, P., East A.R., Hewett, E.W. & Heyes, J.A. 2014. Interpreting textural changes in low temperature stored tomatoes. *Postharvest Biology and Technology*, 87: 140-143.

Brownleader, M.D., Harborne, J.B. & Dey, P.M. 1997. Carbohydrate metabolism: primary metabolism of monosaccharides. In: *Plant Biochemistry*, Dey, P. M., & Harborne, J. B. (Eds.), Academic Press, San Diego, pp. 111-141.

Brooker, D.B. 1967. Mathematical model of the psychrometric chart. *Transactions of the American* Society *of* Agricultural *Engineers*, 558-560.

Brummell, D.A. 2006. Cell wall disassembly in ripening fruit. *Functional Plant Biology*, 33: 103-119.

Caleb, O.J., Mahajan, P.V., Opara, U.L. & Witthuhn, C. 2012. Modelling the respiration rates of pomegranate fruit and arils. *Postharvest Biology and Technology*, 64: 49–54.

Cameron, A.C., Boylan-Pett, W. & Lee, J. 1989. Design of modified atmosphere packaging systems: modeling oxygen concentrations within sealed packages of tomato fruits. *Journal of Food Science*, 54: 1413–1416, 1421.

Castellanos, D.A. & Algecira, N.A. 2012. Modeling change in color and firmness of baby banana (*Musa acuminata* AA) in modified atmosphere packaging. *Agronomía Colombiana*, 30(1): 84-94.

Chau, K.V., Romero, R.A., Baird, C.D. & Gaffney, J.J. 1987. *Transpiration coefficients of fruits and vegetables in refrigerated storage*. ASHRAE Report 370-RP. Atlanta, GA, USA.

Chen, C. R. & Ramaswamy, H. S. 2002. Color and texture change kinetics in ripening bananas. *LWT*, 35: 415–419.

Conesa, M.R., Garcia-Salinas, M.D., de la Rosa, J.M., Fernandez-Trujillo, J.P., Domingo, R. & Perez-Pastor, A. 2014. Effects of deficit irrigation applied during fruit growth period of late mandarin trees on harvest quality, cold storage and subsequent shelf life. *Scientia Horticulturae*, 165: 344-351.

Daas, P.J.H., Voragen, A.G.J. & Schols, H.A. 2000. Characterization of non-esterified galacturonic acid sequences in pectin with endopolygalacturonase. *Carbohydrate Research*, 326: 120-129.

Dangl, J.F., Dietrich, R.A. & Thomas, H. 2000. *Senescence and programmed cell death. In: Biochemistry and molecular biology of plants*, Buchanan, B., Gruissem, W. & Jones, R. (Eds.), American society of plant physiologist Press, Rockville, pp. 1057-1059.

Dash, K.K., Goswami, T.K. & Dek, S.C. 2012. Modeling for the modified atmosphere packaging of Sapota fruit. *Agricultural Engineering International: CIGR Journal*, 14(2): 102-109.

Del Nobile, M.A. Licciardello, F., Scrocco, C., Muratore, G. & Zappa, M. 2007. Design of plastic packages for minimally processed fruits. *Journal of Food Engineering*, 79: 217-224.

Dixon, J. & Hewett, E.W. 1998. Temperature affects postharvest color change of apples. *Journal of the American Horticultural Sciences*, 123(2): 305-310.

Egea, I., Barsan, C., Bian, W., Purgatto, E., Latché, A., Chervin, C., Bouzayen, M. & Pech J.C. 2010. Chromoplast differentiation: current status and perspectives. *Journal of Plant Physiology*, 51(10): 1601-1611.

Emond, J.P., Chau, K.V. & Brecht, J.K. 1993. Modeling respiration rates of blueberry in a perforation-generated modified atmosphere package. In: *Proceedings of the 6th international controlled atmosphere research conference*, Blanpied, G.D., Barstch, J. A. & Hicks, J.R. (Eds.), Ithaca, NY, USA, pp. 134-144.

Fearne, A., Barrow, S. & Schulenberg, D. 2006. Implanting the benefits of buyer-supplier collaboration in the soft fruit sector. *Supply Chain Management*, 11(1): 3-5.

Finnegan, E., Mahajan, P.V., O'Connell, M., Francis, G.A. & O'Beirne, D. 2013. Modelling respiration in fresh-cut pineapple and prediction of gas permeability needs for optimal modified atmosphere packaging. *Postharvest Biology and Technology*, 79: 47-53.

Fishman, S., Rodov, V. & Ben-Yehoshua, S. 1996. Mathematical model for perforation effect on oxygen and water vapor dynamics in modified-atmosphere packages. *Journal of Food Science*, 61: 956–961.

Fonseca, S.C., Oliveira, F.A.O. & Brecht, J.K. 2002. Modeling respiration rate of fresh fruits and vegetables for modified atmosphere packages: a review. *Journal of Food Engineering*, 52: 99-119.

Galli, F., Archbold, D.D. & Pomper, K.W. 2009. Pawpaw fruit chilling injury and antioxidant protection. *Journal of the American Society for Horticultural Sciences*, 134(4): 466-471.

Génard, M. & Gouble, B. 2005. ETHY. A theory of fruit climacteric ethylene emission. *Plant Physiology*, 139: 531-545.

Geysen, S., Verlinden, B.E., Conesa, A. & Nicolaï, B.M. 2005. Modeling respiration of strawberry (cv. Elsanta) as a function of temperature, carbon dioxide, low and superatmospheric oxygen concentration. *Frutic*, 5: 12-16.

Gomes, M.H., Beaudry, R.M., Almeida, D.P.F. & Malcata, F.X. 2010. Modeling respiration of packaged fresh-cut 'Rocha' pear as affected by oxygen concentration and temperature. *Journal of Food Engineering*, 96: 74-79.

Gómez, P.A. & Camelo, A.F.L. 2002. Calidad postcosecha de tomates almacenados en atmósferas controladas [Postharvest quality of tomato fruits stored under controlled atmospheres]. *Horticultura Brasileira*, 20(1): 38-43.

Gong, S. & Corey, K.A. 1994. Predicting steady state oxygen concentrations in modified atmosphere packages of tomatoes. *Journal of the American Society for Horticultural Sciences*, 119: 546-550.

Gorny, J.R. & Kader, A.A. 1996. Controlled-atmosphere suppression of ACC synthase and ACC oxidase in Golden Delicious apple during long-term cold storage. *Journal of the American Society for Horticultural Sciences*, 121: 751-755.

Gwanpua, S.G., Verlinden, B.E. Hertog, M.L.A.T., Bulens, I., Van de Poel, B., Van Impe, J., Nicolai, B.M. & Geeraerd, A.H. 2012. Kinetic modeling of firmness breakdown in 'Braeburn' apples stored under different controlled atmosphere conditions. *Postharvest Biology and Technology*, 67: 68-74.

Hertog, M.L.A.T.M., Nicholson, S.E. & Banks, N.H. 2001. The effect of modified atmospheres on the rate of firmness change in 'Braeburn' apples. *Postharvest Biology and Technology*, 23(3): 175-184.

Hertog, M.L.A.T.M., Nicholson, S.E. & Whitmore, K. 2003. The effect of modified atmospheres on the rate of quality change in Hass avocado. *Postharvest Biology and Technology*, 29: 41–53.

Hertog, M.L.A.T.M., Nicholson, S.E. & Jeffery, P.B. 2004. The effect of modified atmospheres on the rate of firmness change of 'Hayward' kiwifruit. *Postharvest Biology and Technology*, 31: 251–261.

Heydari, A., Shayesteh, K., Eghbalifam, N. & Bordbar, H. 2010. Studies on the respiration rate of banana fruit based on enzyme kinetics. *International Journal of Agriculture and Biology*, 12: 145–149.

Hewett, E.W. 2006. Progressive challenges in horticultural supply chains: Some future challenges. *Acta Horticulturae*, 712(I): 39–49.

Ho, Q.T., Verboven, P., Verlinden, B.E., Schenk, A. & Nicolai, B.M. 2013. Controlled atmosphere storage may lead to local ATP deficiency in apple. *Postharvest Biology and Technology*, 78: 103-112.

HunterLab. 2008. CIE L*a*b* Color Scale. Applications Notes. *Insight on Color*. Vol. 8 No. 7. Available in: http://www.hunterlab.com/appnotes/an07_96a.pdf Accessed on: April 2014.

Iqbal, T., Rodrigues, F.A.S., Mahajan, P.V. & Kerry, J.P. 2009. Mathematical modeling of O_2 consumption and CO_2 production rates of whole mushrooms accounting for the effect of temperature and gas composition. *International Journal of Food Science and Technology*, 44: 1408–1414.

Jha, S.N. 2010. Color measurements and modeling. In: *Nondestructive Evaluation of Food Quality. Theory and practice*, Jha, S.N. (Ed.), Springer-Verlag, Berlin Heidelberg, pp. 17-40.

Jha, S.N., Chopra, S. & Kingsly, A.R.P. 2007. Modeling of color values for nondestructive evaluation of maturity of mango. *Journal of Food Engineering*, 78: 22–26.

Johnston, J.W., Gunaseelan, K., Pidakala, P., Wang, M. & Schaffer, R.J. 2009. Coordination of early and late ripening events in apples is regulated through differential sensitivities to ethylene. *Journal of Experimental Botany*, 60: 2689–2699.

Kader, A.A. 1985. Quality factors. Definition and evaluation for fresh horticultural crops. In: *Postharvest technology of Horticultural crops*, Kader, A. (Ed.), CRC, Inc. Boca Raton, FA, USA, pp: 118–121.

Kader, A.A. 1986. Biochemical and physiological basis for effects of controlled and modified atmospheres on fruits and vegetables. *Food Technology*, 40(5): 99-104.

Kader, A.A. 1988. Influence of preharvest and postharvest environment on nutritional composition of fruits and vegetables. In: *Horticulture and human health, contributions of fruits and vegetables*, Quebedeaux, B. & Bliss, F.A. (Eds.), Prentice-Hall, Englewood Cliffs, NJ, USA, pp. 18-32.

Kader, A.A. 1992. Postharvest biology and technology: an overview. In: *Postharvest Technology of Horticultural Crops, Publication 3311*, Kader, A.A. (Ed.), University of California, Division of Agriculture and Natural Resources, Davis, CA, USA, pp. 70–85.

Kader, A. A. 1997. A summary of CA requirements and recommendations for fruits other than apples and pears. In: *Proceedings of the 7th international controlled atmosphere research conference,* Kader, A.A. (Ed.), University of California, Davis, CA, USA, Vol. 3, pp. 1–34.

Kader, A.A. 1999. Fruit maturity ripening and quality relationships. *Acta Horticulturae*, 485: 203-208.

Kader, A.A. 2002. Postharvest biology and technology: an overview. In: *Postharvest Technology of Horticultural Crop, publication number 3311*, Kader, A.A. (Ed.), Regents of the University of California, Division of Agricultural and Natural Resources, Oakland, CA, USA, pp. 39–48.

Kader, A.A. & Salveit, E.M. 2003. Respiration and Gas Exchange, In: *Postharvest Physiology and Pathology of Vegetables*, Bartz, J.A. & Brencht, J.K. (Eds.). Marcel Dekker, Inc. New York, USA, pp. 1-23.

Kader, A.A, Zagory, D. & Kerbel, E.L. 1989. Modified atmosphere packaging of fruits and vegetables. *Critical Reviews of Food Science and Nutrition*, 28: 1–30.

Kang, J.S. & Lee, S. 1998. A kinetic model for transpiration of fresh produce in a controlled atmosphere. *Journal of Food Engineering*, 35: 65–73.

Ke, D. & Kader, A.A. 1989. Tolerance and response of fresh fruits to oxygen levels at or below 1%. *International Controlled Atmosphere Conference 5th Proc*., June 14-16, 1989. Vol. 2, Other Commodities and Storage Recommendations Wenatchee, Washington, USA, pp: 209-16.

Kerbel, E.L., Kader, A.A. & Romani, R.J. 1988. Effects of elevated CO_2 concentrations on glycolysis in intact 'Bartlett' pear fruit. *Plant Physiology*, 86: 1205-1209.

Kissinger, M., Tuvia-Alkalai, S., Shalom, Y. & Fallik, E. 2005. Characterization of physiological and biochemical factors associated with postharvest water loss in ripe pepper fruit during storage. *Journal of the American Society for Horticultural Sciences*, 130(5): 735-741.

Kubo, Y., Inaba, A. & Nakamura, R. 1990. Respiration and C_2H_4 production in various harvested crops held in CO_2-enriched atmospheres. *Journal of the American Society for Horticultural Sciences*, 115: 975–978.

Lakakul, R., Beaudry, R.M. & Hernandez, R.J. 1999. Modeling respiration of apple slices in modified atmosphere packages. *Journal of Food Science*, 64: 105-110.

Lana, M.M., Tijskens, L.M.M. & van Kooten, O. 2005. Effects of storage temperature and fruit ripening on firmness of fresh cut tomatoes. *Postharvest Biology and Technology*, 35(1): 87–95.

Larrigaudiere, C., Graell, J., Salas, J. & Vendrell, M. 1997. Cultivar differences in the influence of a short period of cold storage on ethylene biosynthesis in apples. *Postharvest Biology Technology*, 10: 21-27.

Lee, D.S., Song, Y. & Yam, K.L. 1996. Application of an enzyme kinetics based respiration model to permeable system experiment of fresh produce. *Journal of Food Engineering*, 27: 297-310.

Lee, S.K. & Kader, A.A. 2000. Preharvest and postharvest factors influencing vitamin C content of horticultural crops. *Postharvest Biology and Technology*, 20(3): 207–220.

Leonardi, C., Baille, A. & Guichard, S. 1999. Effects of fruit characteristics and climatic conditions on tomato transpiration in greenhouse. *Journal of Horticultural Science and Biotechnology*, 74(6): 748–756.

Lin, Z., Zhon, S. & Grierson, D. 2009. Recent advances in ethylene research. *Journal of Experimental Botany*, 60: 3311–3336.

Liu, S., Yang, Y., Murayama, H., Taira, S. & Fukushima, T. 2004. Effects of CO_2 on respiratory metabolism in ripening banana fruit. *Postharvest Biology Technology*, 33: 27–34.

Lukasse, L.J.S. & Polderdijk, J.J. 2003. Predictive modelling of post-harvest quality evolution in perishables, applied to mushrooms. *Journal of Food Engineering*, 59: 191-198.

Lukatkin, A.S., Brazaityte, A., Bobinas, C. & Duchovskis, P. 2012. Chilling injury in chilling-sensitive plants: a review. *Agriculture*, 99:111–124.

Mahajan, P.V., Oliveira F. A.R. & Macedo, I. 2008. Effect of temperature and humidity on the transpiration rate of whole mushrooms. *Journal of Food Engineering*, 84: 281–288.

Maneerat, C., Tongta, A., Kanlayanarat, S. & Wongs-Aree, C. 1997. A transient model to predict O_2 and CO_2 concentrations in modified atmosphere packaging of banana at various temperatures. In: *Proceedings of the 7th international controlled atmosphere research conference: Vol. 5,* Gorny, J.R. (Ed.), Davis, CA, USA, pp. 191–197.

Mangaraj, S. & Goswami, T.K. 2011. Modeling of respiration rate of litchi fruit under aerobic conditions. *Food Bioprocess Technology*, 4: 272–281.

McLaughlin, C.P. & O'Beirne, D. 1999. Respiration rate of a dry coleslaw mix as affected by storage temperature and respiratory gas concentrations. *Journal of Food Science*, 64(1): 116–119.

Mir, N. & Beaudry, R. 2002. Atmosphere control using oxygen and carbon dioxide. In: *Fruit Quality and its biological basis*, Knee, M. (Ed.), Sheffield Academic Press. Chapter 6, pp-122–156.

Morales-Castro, J., Rao, M.A., Hotchkiss, J.H. & Downing, D.L. 1994. Modified atmosphere packaging of sweet corn on cob. *Journal of Food Processing and Preservation*, 18: 279-293.

Paliyath, G. & Murr, D.P. 2008a. Common fruits, vegetables and flowers and their quality characteristics. In: *Postharvest biology and technology of fruits, vegetables and flowers*, Paliyath, G., Murr, D.P., Handa, A.K. & Lurie, S. (Eds.), Wiley-Blackwell, USA, pp. 19-50.

Paliyath, G. & Murr, D.P. 2008b. Biochemistry of fruits. In: *Postharvest biology and technology of fruits, vegetables and flowers,* Paliyath, G., Murr, D.P., Handa, A.K. & Lurie, S. (Eds.), Wiley-Blackwell. USA, pp. 19-50.

Peppelenbos, H.W., Tijskens, L.M.M., Van't Leven, J. & Wilkinson, E.C. 1996. Modeling oxidative and fermentative carbon dioxide production of fruits and vegetables. *Postharvest Biology and Technology*, 9: 283–295.

Peppelenbos, H.W. & Van't Leven, J. 1996. Evaluation of four types of inhibition for modelling the influence of carbon dioxide on oxygen consumption fruits and vegetables. *Postharvest Biology and Technology*, 7: 27-40.

Pesis, E., Aharoni, D., Aharon, Z., Ben-Arie, R., Aharoni, N. & Fuchs, Y. 2000. Modified atmosphere and modified humidity packaging alleviates chilling injury symptoms in mango fruit. *Postharvest Biology and Technology*, 19(1): 93–101.

Pinheiro, J., Alegria, C., Abreu, M., Gonçalves, E.M. & Silva, C.L.M. 2013. Kinetics of changes in the physical quality parameters of fresh tomato fruits (*Solanum lycopersicum*, cv. 'Zinac') during storage. *Journal of Food Engineering*, 114: 338-345.

Pranamornkith, T. 2009. *Effects of postharvest treatments on storage quality of lime (Citrus latifolia Tanaka) fruit*. PhD thesis. Massey University, New Zealand. Available in: http://mro.massey.ac.nz/bitstream/handle/10179/1162/02_whole.pdf?sequence=1

Ratti, C., Raghavan, G.S.V. & Gariepy, Y. 1996. Respiration rate model and modified atmosphere packaging of fresh cauliflower. *Journal of Food Engineering*, 28: 297–306.

Ren, K., Tu, K., Pan, L. & Chen, Y. 2006. Kinetic models of broccoli color changes during chilled storage. *Journal of Food Processing and Preservation*, 30: 180–193.

Renault, P., Houal, L., Jacquemin, G. & Chambroy, Y. 1994. Gas exchange in modified atmosphere packaging. 2: Experimental results with strawberries. *International Journal of Food Science and Technology*, 29: 379–394.

Saladie, M., Matas, A.J., Isaacson, T., Jenks, M.A., Goodwin, S.M., Niklas, K.J., Ren, X. L., Labavitch, J. M., Shackel, K. A., Fernie, A.R., Lytovchenko, A., O'Neill, M.A., Watkins, C. B. & Rose, J.K.C. 2007. A reevaluation of the key factors that influence tomato fruit softening and integrity. *Plant Physiology*, 144: 1012-1028.

Saltveit, M.E. 2003. Is it possible to find an optimal controlled atmosphere? *Postharvest Biology Technology*, 27: 13-13.

Saltveit, M.E. 2004. Respiratory metabolism. *The Commercial Storage of Fruits, Vegetables, and Florist and Nursery Stocks*. Agriculture Handbook 66.

Sanders, M.G. & de Wild, H.P.J. 2003. The relation between in vivo ethylene production and oxygen partial pressure. *Postharvest Biology and Technology*, 30: 143–151.

Sandhya, K.V.K. 2010. Modified atmosphere packaging of fresh produce: Current status and future needs. *LWT, Food Science and Technology*, 43: 381-392.

Satyan, S.H., Scott, K.J. & Graham, D. 1992. Storage of banana bunches in sealed polyethylene tubes. *Journal of Horticultural Science*, 67: 283-287.

Ščetar, M., Kurek, M. & Galić, K. 2010. Trends in fruit and vegetable packaging-a review. *Croatian Journal of Food Technology, Biotechnology and Nutrition*, 5(3-4): 69-86.

Schouten, R.E., Huijben, T.P.M., Tijskens, L.M.M. & van Kooten, O. 2007. Modeling quality attributes of truss tomatoes: Linking color and firmness maturity. *Postharvest Biology and Technology*, 45(3): 298–306.

Schwaab, M. & Pinto, J.C. 2007. Optimum reference temperature for re-parameterization of the Arrhenius equation. Part 1: Problems involving one kinetic constant. *Chemical Engineering Science*, 62(10): 2750–2764.

Sila, D.N., Smout, C., Vu, T. S. & Hendrickx, M. E. 2004. Effects of high-pressure pretreatment and calcium soaking on the texture degradation kinetics of carrots during thermal processing. *Journal of Food Science*, 69(5), E205–E211.

Sloof, M., Tijskens, L.M.M. & Wilkinson, E. C. 1996. Concepts for modelling the quality of perishable products (Review).*Trends in Food Science and Technology*, 7: 165–171.

Song, Y., Vorsa, N. & Yam, K.L. 2002. Modeling respiration-transpiration in a modified atmosphere packaging system containing blueberry. *Journal of Food Engineering*, 53: 103-109.

Sousa-Gallagher, M.J., Mahajan, P.V. & Mezdad, T. 2013. Engineering packaging design accounting for transpiration rate: Model development and validation with strawberries. *Journal of Food Engineering*, 119(2): 370-376.

Taiz, L. & Zeiger, E. 2012. *Plant Physiology*, 5th Ed. Sinauer Associates, Inc., Sunderland Massachusetts.

Talasila, P.C., Chau, K.V. & Brecht, J.K. 1992. Effects of gas concentrations and temperature on O_2 consumption of strawberries. *Transactions of the American Society of Agricultural Engineers*, 35: 221–224.

Tano, K., Oulé, M.K., Doyon, G., Lencki, R.W. & Arul, J. 2007. Comparative evaluation of the effect of storage temperature fluctuation on modified atmosphere packages of selected fruit and vegetables. *Postharvest Biology and Technology*, 46(3): 212–221.

Thompson, J.F., Mitchell, F.G. & Kasmire, R.F. 2002. Cooling horticultural commodities. In: *Postharvest Technology of Horticultural Crops*; Third edition, publication number 3311, Kader A.A. (Ed.), Regents of the University of California, Division of Agricultural and Natural Resources, Oakland, CA, USA, pp. 97-112.

Tijskens, L.M. & Evelo, R. G. 1994. Modelling colour of tomatoes during postharvest storage. *Postharvest Biology and Technology*, 4: 85-98.

Tijskens, L.M.M. & Schouten, E. 2009. Modeling Quality Attributes and Quality-related Product Properties. In: *Postharvest Handling: A Systems Approach*, Florkowski, W. and Bruckner, B. (Eds.), San Diego: Academic Press. USA, pp. 483-512.

Van Dijk, C. & Tijskens, L.M.M. 2000. Mathematical modeling of enzymatic reactions as related to texture after storage and mild preheat treatment. In: *Minimally processed fruits and vegetables*, Alzamora, S.M., Tapia, M.S. & Lopez-Malo, A. (Eds.), Aspen Publishers. Maryland, USA, pp. 127–152.

Verdijck, G.J.C. & Lukasse, L.J.S. 2000. Control of quality evolution of agricultural products in climatized storage and transport using product quality evolution models. *Journal A*. 41(3): 37–43.

Watada, A.E., Ko, N.P. & Minott, D.A. 1996. Factors affecting quality of fresh-cut horticultural products. *Postharvest Biology and Technology*, 9: 115–125.

Watkins, C.B. 2003. In: Principles and practices of postharvest handling and stress In: *Apples: Botany, Production and Uses*, Ferree, D.C. & Warrington, I.J. (Eds.), CAB Publishing. UK, pp. 585-614.

Wills, R.B.H., McGlasson, W.B., Graham, D. & Joyce, D.C. 2007. *Postharvest. An introduction to the physiology and handling of fruit, vegetables and ornamentals*. University of new South Wales Press Ltd. Australia, pp. 29-50.

Wu, C.T. 2010. An overview of postharvest biology and technology of fruits and vegetables. *Technology on Reducing Post-harvest Losses and Maintaining Quality of Fruits and Vegetables*. Proceedings of 2010 AARDO Workshop. Held at Taiwan Agricultural Research Institute, Council of Agriculture, Taiwan, ROS. pp. 2-11.

Zhou, H.W., Dong, L., Ben-Arie, R. & Lurie, S. 2001. The role of ethylene in the prevention of chilling injury in nectarines. *Journal of Plant Physiology*, 158: 55-61.

Chapter 2. Modelling the evolution of O_2 and CO_2 concentrations in MAP of a fresh product. An first example with tomato[2]

Abstract

Through modelling of modified atmosphere packaging (MAP) systems, it is possible to predict evolution of gas composition in the package headspace and ease the selection of favorable conditions for the optimal preservation of the packed product. However, it is necessary to adequately describe the associated phenomena: product respiration and gas exchange through the package. A mathematical model was established to describe the evolution of the O_2 and CO_2 concentrations in a MAP system, considering packages with perforations and of variable volume and taking as an example tomato. Respiration rates were described using Michaelis–Menten kinetics while gas exchange through the package and its perforations was described with Fick equations of diffusion. The influence of temperature was considered to follow Arrhenius' law. In order to validate the model proposed, an experiment was conducted packaging the fruits in PP, PLA and LDPE perforated bags for 12 days at 13.5°C. The prediction capacity of the model agrees with the experimental data, with a coefficient of determination (R^2) equal to 0.89-0.98 for O_2 concentrations and 0.83-0.97 for CO_2 concentrations. The model was used to set a specific O_2 concentration in the headspace by define the required package surface area or perforation diameter.

Keywords: Packaging, mathematical model, permeability, respiration rate, Michaelis-Menten, Arrhenius

[2] This chapter (with minor modifications) was published as:
Castellanos, D.A., Cerisuelo, J.P., Hernández-Muñoz, P., Herrera, A.O. & Gavara, R. 2016. Modelling the evolution of O_2 and CO_2 concentrations in MAP of a fresh product: application to tomato, *Journal of Food Engineering,* 168: 84-95. http://dx.doi.org/10.1016/j.jfoodeng.2015.07.019

Nomenclature

a_i, b_i	constants Eq. 2.10
A	effective exchange area of the packaging film (m^2)
A_h	cross sectional area of the perforations (cm^2)
d	diameter of the perforation (cm)
d_e	effective diameter of the perforations (cm)
D_i	diffusion coefficient of gas *i* in air or a film ($cm^2\ d^{-1}$)
E_a	activation energy (kJ mol^{-1})
J_i	total permeation flow of gas *i* through the package (mol d^{-1})
J_{fi}	flow of gas *i* across the package film (mol d^{-1})
J_{hi}	total flow of gas *i* through the perforations (mol d^{-1})
J_{pi}	fluid-dynamic flow of gas *i* through the perforations (mol d^{-1})
K_{mO2}, K_{mCO2}	dissociation constants of the enzyme-substrate complex
K_{muCO2}, $K_{mu'CO2}$	constants of uncompetitive inhibition for consumption of O_2 and generation of CO_2, respectively
K_{Tri}	transmission rate of gas *i* through the perforations ($cm^3\ d^{-1}$)
L	film thickness (mm)
L_h	effective transmission length (cm)
MMU	Michaelis-Menten Kinetics with uncompetitive inhibition
n_i	moles of gas *i*
P	pressure (atm)
p_i	partial pressure of gas *i* inside the package (atm)
p_{iout}	partial pressure of gas *i* outside the package (atm)
Q_i	film permeability coefficient for gas *i* (cm^3 mm $m^2\ d^{-1}\ atm^{-1}$)
R	universal gas constant (0.008314 kJ $mol^{-1}\ K^{-1}$)
r_i	respiration rate of gas *i*
r_{O2}, r_{CO2}	consumption of O_2 and generation of CO_2 rates ($cm^3\ kg^{-1}\ d^{-1}$)
r_{O2max}, r_{CO2max}	maximum consumption of O_2 and generation of CO_2 rates ($cm^3\ kg^{-1}\ d^{-1}$)
t	packaging time (d)
T	temperature (°C, K)
V	Free package volume - headspace (cm^3)
W	product weight (kg)
y_{O2}, y_{CO2}, y_{N2}	O_2, CO_2 and N_2 concentrations inside the package
y_{O2out}, y_{CO2out}, y_{N2out}	O_2, CO_2 and N_2 concentrations outside the package
$y_{O2\ eq}$, $y_{CO2\ eq}$, $y_{N2\ eq}$	Equilibrium O_2, CO_2 and N_2 concentrations inside the package

2.1 Introduction

The use of systems with modified atmosphere packaging (MAP) at refrigeration temperatures has been established as a technique with the potential to extend the shelf life of fresh fruits and vegetables maintaining their quality properties (Sandhya, 2010; Techavises & Hikida, 2008). In this type of storage the ripening process and product deterioration are delayed by reducing the rate of metabolic reactions and microbial activity as result of lowering the temperature and changing the concentration of the surrounding atmosphere (Floros & Maxos, 2005; Mangaraj, et al., 2014). MAP of fresh products involves the modification of the internal atmosphere of the packaging system due to the dynamic interaction of two simultaneous processes: product respiration (O_2 consumption and CO_2 production) and transfer of gases between external and internal atmospheres through the package walls. These processes generally lead to the reduction of the O_2 concentration and the increase in concentration of CO_2 at the package headspace throughout the storage time, until an eventual equilibrium is achieved (Floros & Maxos, 2005; Heydari, et al., 2012; Mahajan, et al., 2007).

For many fruits and vegetables, favorable levels of O_2 and CO_2 are between 1 and 10 % for each gas (Sandhya, 2010). These favorable gas levels in the system are achieved once the product/package system reaches the steady state, where the mass transfer rate of each gas is equal to the rate of respiration (O_2 input rate is equal to the consumption rate for O_2, and the CO_2 output rate is equal to the generation rate for CO_2). Therefore, it is intended that the permeability characteristics of the used packaging are adequate to achieve the optimal gas composition and the packaging process designed to do it in the shortest time. (Del-Nobile, et al., 2007; Mahajan, et al., 2007). In some cases, the permeability of the packaging material is not high enough, resulting in overall consumption of O_2 and excessive accumulation of CO_2 in the headspace (which give raise to fermentative processes and product deterioration). For this reason, perforations are made in the package walls to increase the mass transfer at adequate rates to counteract respiration processes (González-Buesa, et al., 2009; Kwon, et al., 2013; Techavises & Hikida, 2008).

Conducting multiple trials to provide the conditions that result in the appropriate level of gas for the packed product can be very wasteful, thus, the knowledge and prediction of the processes involved in the evolution of the MAP system, reduce time and cost of trials. Several mathematical models have been developed and proposed to estimate the concentration in the internal atmosphere for perforated packages, integrating the mass

transfer and respiration processes in order to select the most suitable conditions for the product in advance:

Mahajan et al. (2007) developed a model that takes into account the change in the permeability of the packaging film with respect to temperature, using an Arrhenius equation and empirical relationships to describe gas transfer through the perforations, as well as suggesting to describe the respiration rate with Michaelis-Menten and Arrhenius equations. In this model, the total pressure and volume are considered constants, as well as the fact that there is no gas stratification inside the package. González-Buesa et al. (2009) propose a similar model, although more complex than the previous one, and take into account the convective effect on gas transfer through the perforations using Poiseuille's law and the diffusive effect using empirical equations. Empirical simple equations are also used for the product respiration rate. This model considers total pressure variable and package volume constant and does not consider the effect of temperature. Kwon et al. (2013) propose a similar model to Mahajan et al. (2007), but using a modified Fick equation for gas transfer through the perforations. In this model, N_2 is omitted from of the mass balance equations. Mangaraj et al. (2014) propose a model similar to Kwon et al. (2013), but only for non-perforated packages.

From the previous models, two shortcomings can be established: 1) these models were set up for packages of constant volume. Is not considered that for flexible packages such as bags, there is a change in the headspace volume due to the difference in the O_2 and CO_2 permeability of the packaging materials and because of what the respiratory quotient (R_{CO2}/R_{O2}) is different from one for many fresh produce. 2) The transfer of gases through the perforations is not well defined and often, the model does not consider the effect of temperature on this.

Beside the above, a slightly considered aspect in models developed for MAP is how to reach a specific headspace concentration by changing the characteristics of the package. Previously, has been wanted to determine the headspace concentration establishing the package configuration for a given produce. A great implementation of a MAP model would be starting from a target concentration in the headspace, to determine the package configuration required to achieve this purpose.

In this chapter, a mathematical model for the description and prediction of evolution in O_2 and CO_2 concentrations in a MAP system of variable volume is presented. In the model the processes of respiration of the packed product and mass transfer through perforated

packages and depending on storage temperature are considered. For the model trials, an input of a suitable collection of gas permeability and respiration rate parameters was needed. Hence, the gas permeability of three packaging materials (LDPE, MOPP and PLA) to O_2 and CO_2, the gas transmission rates through perforations and the respiration rates of an example fruit (tomato - *Lycopersicon esculentum* M.) were experimentally determined and adjusted to suitable laws. Thereafter, a validation experiment was conducted by packaging tomatoes in bags with different permeation parameters and comparing the results with those predicted by the proposed model. Finally, the developed model was employed to define the packaging characteristics required to achieve a given O_2 concentration.

2.2 Mathematical approach

As mentioned above, there are two processes that lead to changes in the concentration of gases in the headspace of freshly produce packages: the respiration process in the packed fruit results in O_2 consumption and CO_2 production, generating a concentration difference between the headspace and the atmosphere surrounding the package. Hence, there will be a gas exchange through the package walls with O_2 entering and CO_2 leaving, due to the concentration difference, as can be seen in Figure 2.1 (Mahajan, et al., 2007; González-Buesa, et al., 2009).

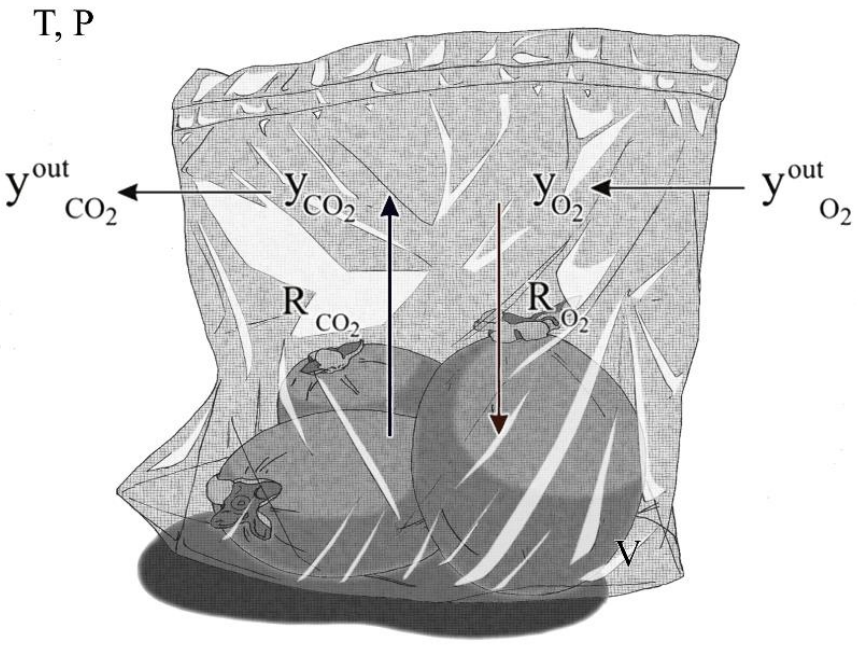

Figure 2.1. O_2 and CO_2 exchange in a MAP system

2.2.1 Respiration rates

For the mathematical description of the respiration process, the enzyme kinetics of Michaelis-Menten have been successfully used for many products, specifically the equation of uncompetitive inhibition (MMU) wherein the inhibitor (here, CO_2) reacts with the enzyme-substrate complex. Therefore, the maximum respiration rate is not influenced by high concentrations of CO_2 (Bhande, et al., 2008; Fonseca, et al., 2002; Heydari, et al., 2010; Kwon, et al., 2013; Mangaraj & Goswami, 2011; Mangaraj, et al., 2014).

As shown before in Chapter 1, according to the MMU kinetics the rates of O_2 consumption (Eq. 1.8) and CO_2 generation are respectively:

$$r_{O_2} = \frac{r_{O_{2max}} y_{O_2}}{K_{m_{O_2}} + y_{O_2}\left(1 + \frac{y_{CO_2}}{K_{mu_{CO_2}}}\right)} \quad (1.8)$$

$$r_{CO_2} = \frac{r_{CO_{2max}} y_{O_2}}{K_{m_{CO_2}} + y_{O_2}\left(1 + \frac{y_{CO_2}}{K_{mu'_{CO_2}}}\right)} \quad (2.1)$$

Where r_{O2} and r_{CO2} are the O_2 consumption and CO_2 production rates, respectively; r_{O2max} and r_{CO2max} are the maximum rates of O_2 consumption or CO_2 production, K_{mO2} and K_{mCO2} are the dissociation constants of the enzyme-substrate complex, and K_{muCO2} and $K_{mu'CO2}$ are the inhibition constants due to CO_2 (Castellanos & Herrera, 2015; Fonseca, et al., 2002; Mangaraj, et al., 2014). The dependence on temperature for the MMU equation parameters has been reported to follow the Arrhenius equation (Eq. 1.11) as described in Chapter 1 (Bhande, et al., 2008; Gomes, et al., 2010) as follows (in this case, for the maximum O_2 consumption rate):

$$r_{O_2}^{max} = r_{O_2\theta}^{max} e^{-Ea/RT} \quad (1.11)$$

Where $r_{O2\theta}^{max}$ is the pre-exponential factor (the maximum O_2 consumption rate at infinite T), E_a is the activation energy, R is the universal gas constant and T is the temperature. Similar equations can be generated for the other parameters in Eqs. 1.8 and 2.1.

2.2.2 Gas exchange in the packaging system

A Inside the package, the atmosphere concentration is the result of the processes of respiration of the fruit and the exchange of gases through the package itself; these two

processes contribute to the variation in the number of moles of a gas *i* in the package (n_i, which in this case can be O_2, CO_2 or N_2) as follows:

$$\frac{dn_i}{dt} = r_i W \frac{P}{RT} + J_i \quad (2.2)$$

Where r_i is the respiration rate for the gas *i*, W is the weight of the packed product, P is the system pressure, T is the storage temperature, R is the ideal gas constant and J_i is the total flow of gas *i* through the package. In case of a plastic package with perforations, J_i has two components:

$$J_i = J_{fi} + J_{hi} \quad (2.3)$$

Being J_{fi} the gas permeation through the continuous packaging film, and J_{hi} the gas transmission through the perforations. Transfer of gas *i* by permeation can be expressed by (Geankoplis, 1993):

$$J_{fi} = -\frac{Q_i A(p_i - p_{i,out})}{L} \frac{P}{RT} \quad (2.4)$$

Where Q_i is the permeability coefficient of gas *i* in the packing material, and p_i and p_{out} are the partial pressures of the gas *i* inside and outside the package, and L is the thickness of the packaging material. The permeability of the packaging films will depend on the storage temperature following Arrhenius' law (Mahajan, et al., 2007; Mangaraj, et al., 2009):

$$Q_i = Q_{iref} e^{\frac{-E_{ai}}{R}\left(\frac{1}{T} - \frac{1}{T_{ref}}\right)} \quad (2.5)$$

Where Q_{iref} is a reference permeability coefficient for gas *i* to a T_{ref}, E_{ai} is the activation energy for gas *i* and R is the ideal gas constant.

The gas *i* transmission through perforations (Eq. 2.6) has been considered as the sum of two mechanisms (Del-Valle, et al., 2003; González, et al., 2008): ordinary diffusion (represented by Fick's law) and the convective fluid-dynamic transfer of gas *i* described by Poiseuille's law, J_{pi}. This latter is due to changes in total pressure caused by respiratory quotients ($RQ = R_{CO2}/R_{O2}$) other than 1, and differences in permeation rates for O_2, CO_2 and N_2.

$$J_{hi} = -\frac{D_i A_h}{L_h}\frac{(p_{i-}p_{i,out})}{RT} + J_{pi} \quad (2.6)$$

Where D_i is the gas *i* diffusivity in the flowing gas, p_i and p_{iout} are the gas *i* partial pressures inside and outside the package, L_h is the effective length of the diffusion channel and A_h the transfer area of the perforations (González et al., 2008; Kwon et al., 2013). The grouping of terms D_iA_h/L_h is the transmission rate of the gas *i* through the perforations, K_{TRi}.

The rate transmission has been represented in terms of the perforation area in cases where the thickness of the packaging film is of the same order or less than the perforation diameter (Chung et al., 2003; Del-Valle et al., 2003; González et al., 2008). In several studies (Del-Valle, et al., 2003; Ghosh & Anantheswaran, 2001; Kwon, et al., 2013) the effective length L_h is taken as the sum of the thickness of the packaging and a correction term for gas diffusion resistance in the perforations, ε (between 0.5 and 1.1 times the effective diameter of the perforations; Eq. 2.7). On the other hand, González, et al., (2008) developed an empirical equation to represent the K_{TRi} coefficients based on the area of the perforation with specific constants for each gas *i* (Eq. 2.18).

$$K_{TRi} = \frac{D_i A_h}{L+\varepsilon} \quad (2.7)$$

$$0.5d_e \leq \varepsilon \leq 1.1d_e$$

$$K_{TRi} = a_i A_h^{b_i} \quad (2.8)$$

In Eq. 2.8, a_i and b_i are specific constants for each gas. In case of having more than one perforation, coefficients are multiplied by the number of perforations. As for the convective exchange of gas through the perforations, for flexible packages (as the bags used for this work) without abrupt changes in RQ or permeation, the system pressure will be equal to the external pressure (there will be a balance of forces which increase or decrease the free package volume) and J_{pi} can be considered equal to 0. It is more practical to represent the gas concentration variation over time in terms of mole fraction, and therefore in Eqs. 2.2-2.6 the partial pressures and the terms of moles of each gas *i* can be replaced accordingly for mole fraction terms assuming ideal gas behavior. Furthermore, the rate of change in the moles of gas *i* at constant temperature and total pressure inside the package, can be expressed as:

$$\frac{dn_i}{dt} = \frac{P}{RT}\left[V\frac{dy_i}{dt} + y_i\frac{dV}{dt}\right] \quad (2.9)$$

2.2.3 Gas balance equations

Considering the above and making the necessary replacements in Eqs. 2.2-2.6, the differential balances of the main gas components in the headspace volume are:

$$\left[V\frac{dy_{O_2}}{dt} + y_{O_2}\frac{dV}{dt}\right] = K_{TRO_2}\left(y_{O_{2Out}} - y_{O_2}\right) + \frac{APQ_{O_2}}{L}\left(y_{O_{2Out}} - y_{O_2}\right) - r_{O_2}W \quad (2.10)$$

$$\left[V\frac{dy_{CO_2}}{dt} + y_{CO_2}\frac{dV}{dt}\right] = K_{TRCO_2}\left(y_{CO_{2Out}} - y_{CO_2}\right) + \frac{APQ_{CO_2}}{L}\left(y_{CO_{2Out}} - y_{CO_2}\right) + r_{CO_2}W \quad (2.11)$$

$$\left[V\frac{dy_{N_2}}{dt} + y_{N_2}\frac{dV}{dt}\right] = K_{TRN_2}\left(y_{N_{2Out}} - y_{N_2}\right) + \frac{APQ_{N_2}}{L}\left(y_{N_{2Out}} - y_{N_2}\right) \quad (2.12)$$

The variation in the free package volume V is estimated by adding the differential equations for each gas and considering that the sum of the mole fractions of O_2, CO_2 and N_2 can be regarded as 1 (presence of other gases such as water vapor or ethylene is negligible for the calculations):

$$y_{O_2} + y_{CO_2} + y_{N_2} = 1 \quad (2.13)$$

Thus, the loss or gain in total volume can be written as:

$$\frac{dV}{dt} = W\left(r_{CO_2} - r_{O_2}\right) + \sum_{i=1}^{n}\left(\left(y_{iOut} - y_i\right)\left(K_{TRi} + \frac{APQ_i}{L}\right)\right) \quad (2.14)$$

2.2.4 Consistency of the system of differential equations

The model requires the input of a number of parameters that are defined by the selection of:

a) The product to pack and the required storage conditions and shelf life period. The parameters of the respiration rate included in Eqs. 1.8 and 2.1, the product weight and the storage time are established.
b) The packaging environmental conditions: Temperature, atmospheric pressure and initial concentration of gases in the external and internal atmospheres are input.
c) The package information, material film and package size (headspace). Then, film thickness and surface area of gas exchange, permeability coefficients (Eq. 2.5 for

each gas), number and size of perforations used in the package and transmission rates of the diverse gases through the perforations (Eq. 2.7 or Eq. 2.8) are defined.

With the parameters above mentioned, the model can calculate the evolution of V and the partial pressures of the three gases (O_2, CO_2 and N_2) using differential equations 2.10-2.14, respectively. Thus, there are four dependent variables (V, y_{O2}, y_{CO2} y y_{N2}) and four mass balance equations, with zero degrees of freedom in the system.

2.3 Materials and methods

2.3.1 Fresh produce

Tomatoes (*Lycopersicon esculentum* M.) were obtained from a commercial grower located in the Canary Islands, Spain, on October 2014. The fruits were harvested at the optimal maturity stage and transported to the laboratories of the Institute of Agro-chemistry and Food Technology (Paterna, Spain) on the following days. After discarding those with evidence of damage, fruits of similar size and shape were selected and stored at 14 ºC. The next day, a few tomatoes were randomly selected for respiration rate calculations. The rest were packed as described in the next subsection.

2.3.2 Packages

Three types of film widely used in food packaging were selected for the manufacturing of bags: low-density polyethylene (LDPE) with a thickness of 0.020 ± 0.002 mm, cast polypropylene (PP) with a thickness of 0.025 ± 0.002 mm (Rediplast, Bogotá, Colombia), and polylactic acid (PLA) with a thickness of 0.025 ± 0.001 mm (Q4 Packaging Systems S.L., Ribaroja - Valencia, Spain). The thickness of the films was determined as the average of five measurements with a Mitutoyo (Kawasaki, Japan) gauge.

2.3.3 Respiration rates

The rates of O_2 consumption and CO_2 generation by tomatoes were determined using a closed system method. One fruit (130 ± 10 g) was placed in an open glass container of 2020 cm^3, during an hour of acclimatization to the temperature of the experiment and then hermetically sealed. The O_2 concentration in the headspace was determined with an optical

analyzer OpTech®-O_2 Platinum (MOCON, Inc., Minneapolis, MN, USA), taking the measure from a Mocon organo-platinum sensor attached to the inside surface of the container. The CO_2 concentration was measured by taking a headspace sample of 10 ml through a rubber seal, which was then analyzed with a Packaging Atmosphere Analyzer, Lippke® CheckMaster 2100 (Paul Lippke Handels-GmbH, Neuwied, Germany) previously calibrated with Gas Chromatography; 10 cm^3 of air were introduced into the container to replace the withdrawn sample. The experiments were made in temperature-controlled cabinets to 16, 24 and 37 °C, setting temperature in ± 0.2 °C and taking measurements at regular intervals for a period of 6 days, avoiding reaching the phase of anaerobic respiration. All measurements were made in triplicate, reporting the average value of each concentration.

Respiration rate at each temperature was calculated using the following equations:

$$r_{O_2}(t) = (V/W)\left(y_{O_2 t-1} - y_{O_2 t+1}\right)/\Delta t \quad (2.15)$$

$$r_{CO_2}(t) = (V/W)\left(y_{CO_2 t+1} - y_{CO_2 t-1}\right)/\Delta t \quad (2.16)$$

Being $r_{O2}(t)$ and $r_{CO2}(t)$ the respiration rates at time t and Δt the time elapsing between two consecutive measurements.

The corresponding experimental data of r_{O2}, r_{CO2}, y_{O2} and y_{CO2} generated at each temperature were substituted in the linearized form of Eqs. 1.8 and 2.1 to estimate the parameters of the MMU equations by multiple linear regressions (Wang, et al., 2009). The temperature dependency was represented by replacing the parameters of the two MMU equations in the linearized form of the Arrhenius equation (Eq. 1.11), estimating the pre-exponential factors and the activation energies for each parameter.

2.3.4 Gas transfer through the package

The O_2 permeation rate (OPR) of the PP, LDPE and PLA films were determined with an isostatic, steady-state method, using a Mocon® Oxtran 2/21 permeation instrument (MOCON, Inc., Minneapolis, MN, USA) for samples with a transfer-area of 0.95 cm^2 and at 1 atm of pressure gradient. The OPR for each film were measured to 10, 15, 18, 21 and 24 °C and converted to permeability coefficients multiplying by the film thickness and dividing

by the pressure in the appropriate units. The CO_2 permeability coefficients were determined using a system of permeation at steady state. A stream of CO_2 (99.9%) and another of a carrier gas (air) with equal flow and pressure were driven to the two chambers separated by the tested film in a permeation cell. The CO_2 permeates from the side with high concentration, through the film and into the CO_2-deficient carrier gas stream. After leaving the sample chamber, the carrier gas passes through a gas chromatograph where the CO_2 concentration is quantified. After a period of stabilization (12 hours), the Q_{CO2} values for each film were measured at 13, 18, 22 and 25 °C. The respective data of the permeability coefficients for O_2 and CO_2 generated were substituted in the linearized form of Arrhenius equation (Eq. 2.7) estimating by linear regression the reference permeability coefficients at T_{ref} = 23 °C and the activation energies for each material. The permeability parameters of the films for N_2 were estimated from information of their respective manufacturers and from specialized literature (Auras & Almenar, 2010; Hasbullah, et al., 2000; Siracusa, 2012; Techavises & Hikida, 2008).

To estimate the gas transmission rates for the perforated films, the theoretical model based on diffusion through perforations (Eq. 2.7) was used and the results were compared with those obtained using the empirical model (Eq. 2.8) of González et al. (2008). The gas diffusion coefficients for Eq. 2.7 were obtained in function of temperature using an Arrhenius-type equation from values reported by Xanthopoulos et al. (2012). The ε value was experimentally determined for O_2 as follows: PP films (whose permeability was already assessed) were perforated and placed in a static permeation cell. The dimensions of each perforation were determined with an optical microscope (Motic® B1-220A, Speed Fair Co., Ltd., Richmond, Canada). 1-8 perforations with an approximate diameter of 132 ± 54 µm or 1-6 perforations of 365 ± 54 µm were made. For calculations, these were estimated to be approximately circular ($A_h = \pi d^2/4$). The PP film (91 cm^2 of exposed area) was hermetically fixed with a rubber seal on the chamber inlet being inside an insulated compartment (780 cm^3) that was filled with N_2. The outside surface was exposed to atmospheric air. O_2 permeating to the inside compartment through the perforations and film accumulated and the O_2 concentration evolution in the inside compartment was measured with the optical analyzer used in the respiration trials for 2 days to 5, 16, 24 and 33 °C. The transmission rate through perforations was calculated from this concentration and discounting the gas exchanged due to film permeability, as follows:

$$\mathrm{K_{TRO_2}} = -\frac{V}{t}\left(\frac{\mathrm{y_{outO_2}} - \mathrm{y_{O_2}(t)}}{\mathrm{y_{outO_2}} - \mathrm{y_{iniO_2}}}\right) - \frac{\mathrm{APQ_{O_2}}}{\mathrm{L}} \quad (2.17)$$

Where V is the chamber volume, A is the film area, L is the film thickness, P is the pressure, Q_{O2} is the film permeability coefficient for O_2, $y_{O2}(t)$ is the O_2 concentration in a time t, y_{outO2} is the atmospheric O_2 concentration and y_{iniO2} is the initial O_2 concentration (zero in all trials). The respective K_{TRO2} generated and the O_2 diffusion coefficient calculated to each temperature were substituted in Eq. 2.7 to determine ε. The same value of ε determined before for O_2 was also used initially for N_2 and CO_2 in the model.

2.3.5 Modelling

Once respiration and permeation parameters were determined, the system of gas-balance differential equations (Eqs. 2.10-2.14) was numerically solved using a calculation routine built in Matlab® (MathWorks, Inc., Natick, MA, USA) from the 'ode15s' function, an implicit multistep method based on numerical differentiation formulas (NDFs). In the routine, a relative error tolerance 'RelTol' of $1x10^{-6}$ and an absolute error tolerance 'AbsTol' of $1x10^{-7}$ were used. After the initial values of the known parameters, product weight, package configuration (transfer area, film thickness and number and diameter of the perforations), concentrations, temperature, pressure and storage time were set, the change in the levels of O_2, CO_2, N_2, and the free package volume were calculated with this routine.

2.3.6 Packaging and validation

In order to validate the developed model, an experiment was conducted packaging tomato fruits in bags of the three films evaluated. Tomato fruits with a total weight of ca. 350 g were randomly selected and packed in PP, LDPE and PLA bags with two configurations: (1) with a perforation of 132 µm of effective diameter and (2) with two perforations of 365 µm of effective diameter made with thin needles and determined with the optical microscope as above. The bags had a total internal surface area of 1000 cm^2 and a total internal volume of 1350 cm^3. A polystyrene support of 200 cm^2 with a volume of 200 cm^3 was placed in each bag to hold the fruit in place and ease sample handling. The fruits had a total volume of 450 cm^3, being then the initial free package volume 700 cm^3 and the effective transfer-area 800 cm^2. The initial headspace gas composition was similar to that of the atmosphere. The packages were stored in a controlled-temperature cabinet to 13.5 ± 2 °C for 12 days, keeping relative humidity constant at 80 ± 2%. For all trials, measurements of the concentrations of O_2 and CO_2 were made throughout the storage time in the same way as

described above for respiration tests: using the optical analyzer for O_2 and taking samples with the atmosphere analyzer for CO_2. All measurements were made in triplicate.

2.4 Results and discussion

2.4.1 Respiration rates

In Figure 2.2 the experimental values and those obtained with the model for O_2 and CO_2 concentrations in the respiration chamber at the different temperatures versus time are depicted. The parameters estimated from the linear regression of the linearized form of Eqs. 1.8, 2.1 (Michaelis-Menten) and 1.11 (Arrhenius) are presented in Table 2.1 together with the corresponding regression coefficients (R^2).

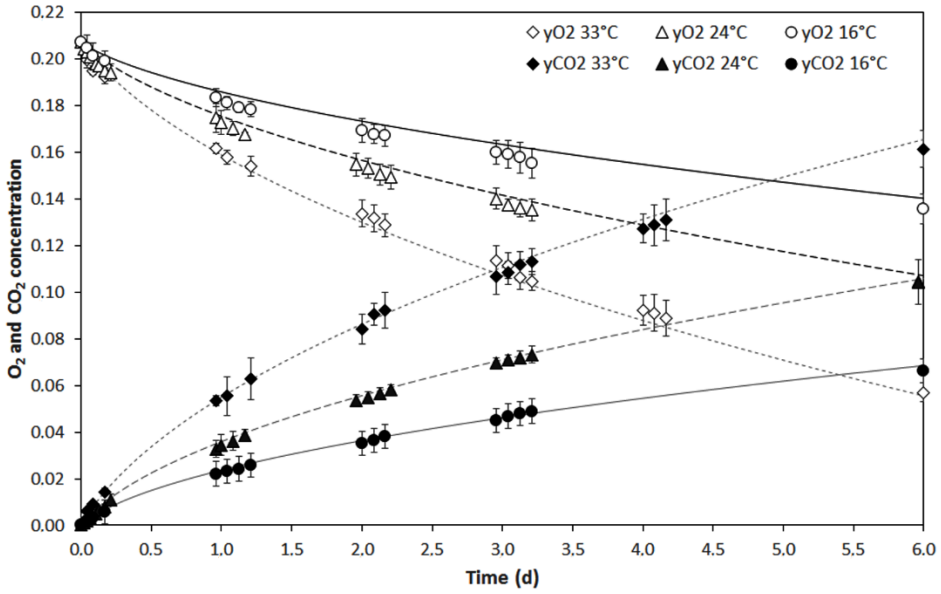

Figure 2.2. Measured (symbols) and modelled (Eqs. 1.8 and 2.1, lines) headspace concentrations of O_2 and CO_2 in the respiration container at different temperatures

As shown in Figure 2.2 and as expected, O_2 concentration in containers decreased while CO_2 concentration increased in all cases. The rate of change in O_2 and CO_2 concentrations with respect to time of storage decreased as O_2 level was decreasing and the CO_2 level was rising in the containers. This profile should be predicted for respiration kinetics that follow the MMU pattern (Eqs. 1.8 and 2.1). As the CO_2 concentration increases, its inhibitory effect is more apparent slowing the respiration rate. In turn, when having less available O_2 to consume, respiration processes will also be reduced. By day 6, the O_2 level reached a

value of 17.1% at 16 °C, 10.0% at 24 °C and 5.7% at 33 °C, while the CO_2 level reached a value of 3.4% at 16 °C, 10.6% at 24 °C and 16.1% at 33 °C. The total coefficient of determination for the MMU model was 0.965 for O_2 and 0.987 for CO_2 with respect to the experimental data evaluated. This is an evidence of the good agreement observed between experimental and predicted values and, therefore, the MMU kinetic model is valid to describe the respiration of tomato observed.

Table 2.1. Pre-exponential factors (V_e) and apparent activation energies (E_a) of Arrhenius (Eq. 1.11) for the MMU parameters (Eqs. 1.8 and 2.1) of tomato and regression coefficients (R^2)

Respiration parameters	*Arrhenius' equation (Eq. 1.11)*		
MMU equations	V_e	E_a *(kJ mol^{-1})*	R^2
O_2 (Eq. 1.8)			
r_{O2max}	2.187×10^9	36.215	0.993
K_{mO2}	4.224×10^5	41.448	0.998
K_{muCO2}	2.414×10^5	40.287	0.997
CO_2 (Eq. 2.1)			
r_{CO2max}	3.833×10^8	31.196	0.997
K_{mCO2}	3.533×10^3	28.739	0.986
$K_{mu'CO2}$	1.330×10^7	51.002	0.996

Respiratory rates increased with increasing storage temperature. The dependence of the MMU parameters with respect to storage temperature was determined using an Arrhenius-type equation (Eq. 1.11) with regression coefficients higher than 0.98 for all parameters. The activation energies were positive in all cases, being the value of MMU parameters for O_2 and CO_2 greater as storage temperature increased.

2.4.2 Gas transfer through the package

The activation energy and pre-exponential factor of Arrhenius-type equation (Eq. 7) of the evaluated materials for O_2 and CO_2 are given in Table 2.2. LDPE had the highest permeability to O_2 and CO_2, followed by PP and PLA that had more comparable values. Experimental ratios Q_{CO2}/Q_{O2} obtained (to T_{ref} = 23 °C) were 6.04 for LDPE, 2.96 for PP and 2.75 for PLA, respectively. Activation energies were comparable to each other for the

three materials evaluated, with positive values in all cases indicating the direct dependence of the permeability coefficient with respect to temperature. E_a for O_2 were larger than those reported for CO_2, being E_{aCO2} the largest for LDPE (22.52 kJ mol^{-1}) and E_{aO2} the largest value for PP (46.71 kJ mol^{-1}). The latter indicates that with increasing temperature, O_2 permeability is increased to a greater extent than CO_2 permeability for the materials evaluated. Regression coefficients were greater than 0.97, showing good correspondence of the Arrhenius parameters with experimental data. The results obtained are comparable to those reported by Mangaraj et al. (2009) and Techavides & Hikida (2008) for LDPE, to those reported by Hasbullah et al. (2000) and Mangaraj et al. (2009) for the PP and to those reported by Auras & Almenar (2010) for PLA.

Table 2.2. Arrhenius activation energies and reference permeability coefficients for the packaging films used

Permeability parameters (Eq. 2.5)	*PP*		*LDPE*		*|PLA*	
O_2		(R^2)		(R^2)		(R^2)
Q_{ref}^* (cm^3 mm m^{-2} d^{-1} atm^{-1})	115.04	(0.998)	230.38	(0.992)	73.05	(0.996)
E_a (kJ mol^{-1})	46.71		39.16		44.39	
CO_2						
Q_{ref}^* (cm^3 mm m^{-2} d^{-1} atm^{-1})	340.25	(0.987)	1391.22	(0.981)	201.07	(0.979)
E_a (kJ mol^{-1})	18.85		22.52		16.72	
N_2**						
Q_{ref}^* (cm^3 mm m^{-2} d^{-1} atm^{-1})	27.39	…	185.79	…	18.30	…
E_a (kJ mol^{-1})	41.70		37.66		11.20	

*T_{ref} = 296.15 K (23°C)

** Estimated from Auras and Almenar (2010), Hasbullah et al. (2000), Siracusa (2012), Techavises and Hikida (2008) and manufacturers.

The permeability parameters for N_2 in Table 2.2 were estimated from the values obtained by Auras & Almenar (2010) for PLA, Hasbullah et al. (2000) and Siracusa (2012) for PP, and Hasbullah et al. (2000) and Techavises & Hikida (2008) for LDPE, and from information provided by the respective manufacturers of each material.

The transmission rate for O_2 with respect to total area of the perforations determined at each temperature can be seen in Figure 2.3. As the total perforated area increases, K_{TR} also increases. The value of K_{TR} for O_2 also rises with the temperature. The process of mass transfer of gas through the perforations is the result of the gas diffusion in the headspace into the perforation, the gas transfer through the perforated channel and the gas diffusion in the external air (or vice versa). Thus, the effective resistance to transport will be

greater than that which would be expected only from the diffusion channel of the perforation (Fick's law) and for this reason is necessary to add a correction term to the film thickness (Chung, et al., 2003; Del-Valle, et al., 2003; Techavises & Hikida, 2008).

In this case, to calculate the transmission rates with the modified Fick's law (Eq. 2.7), the correction term to the effective length ε was initially considered as 0.5 times the diameter of the perforation, equal to those proposed by authors mentioned above.

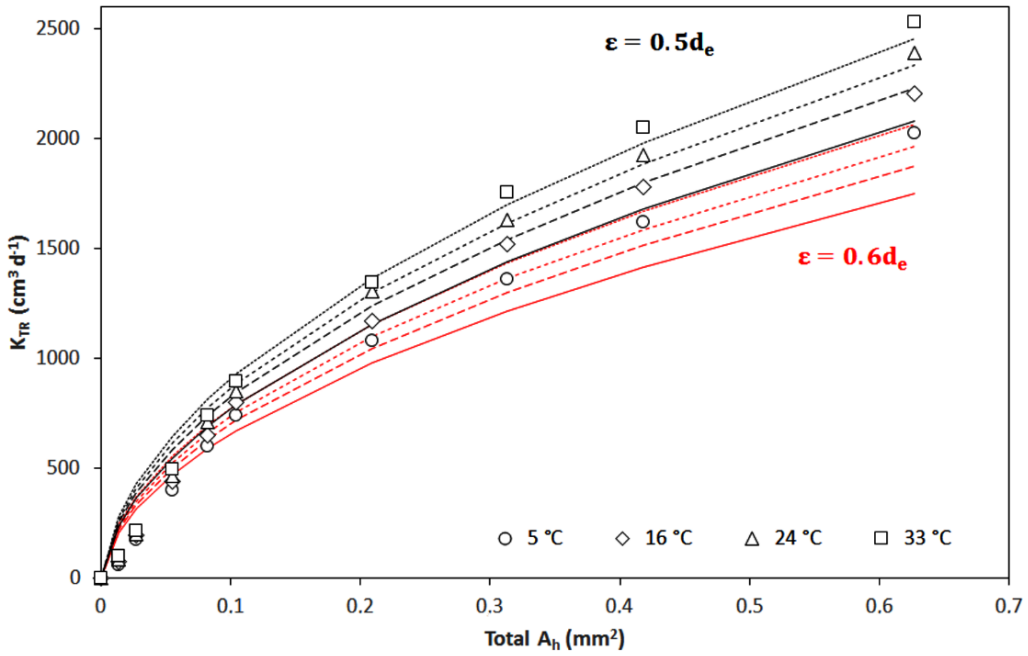

Figure 2.3. Oxygen transmission coefficient as a function of the total area of the perforations at various temperatures. Experimental values (figures) and predicted values (lines; Eq. 2.7) with ε = $0.5d_e$ (black) and ε = $0.6d_e$ (red).

The K_{TR} were also calculated with ε = 0.5d in order to compare these with the experimental results. However, in case of more than one perforation, the K_{TR} calculated for O_2 were much larger than the experimentally determined ones (which had been suggested by Del-Valle et al., 2003). Hence, an effective diameter d_e was used instead, defined as the diameter that would have a perforation with the same total area as the sum of the areas of all perforations in the package. For a perforation, the effective diameter is equal to the diameter, and for two or more it will then be equal to $N^{1/2}d$, where N is the number of perforations. With this correction, K_{TRO2} values for $0.5d_e$ and $0.6d_e$ were recalculated, resulting $0.5d_e$ in K_{TRO2} closest to the experimental values, as shown in Figure 2.3 (R^2 = 0.956 for $0.5d_e$ and R^2 = 0.899 for $0.6d_e$). After finding that ε = $0.5d_e$ is the correction value for L_h which better matches the model to the experimental data for oxygen, the same value was chosen for N_2

and CO_2 (ε for CO_2 was later changed to $0.6d_e$ in the validation of the full model since it provided a better fit to the results, as may be seen below).

Table 2.3. Parameters of Eq. 2.7 and 2.8 for O_2, CO_2 and N_2, and gas transmission coefficients for the experimental perforations arrays used

Eq. 2.7	O_2	CO_2	N_2	Eq. 2.8	O_2	CO_2	N_2
$D_{i/air\ ref}$ ($cm^2\ d^{-1}$)*	17477	12923	17279	*a***	0.880	0.830	1.169
E_a ($kJ\ mol^{-1}$)*	4.196	4.311	4.222	*b***	0.577	0.569	0.558
ε (cm)	$0.5d_e$	$0.6d_e$	$0.5d_e$				
K_{TR} ($cm^3\ d^{-1}$)**				K_{TR} ($cm^3\ d^{-1}$)			
1P × 132 µm	248.39	160.15	247.12	1P × 132 µm	201,27	176.06	223.58
2P × 365 µm	1221.01	762.41	1214.73	2P × 365 µm	985.14	842.98	1038.55

* Reference values (T_{ref} = 23 °C) and activation energies for the calculation of diffusion coefficients in a type-Arrhenius equation as Eq. 2.5 (Xanthopoulos et al., 2012).

** K_{TR} to one perforation of d = 132 µm and two perforations of d = 365 µm (d_e = 516 µm) with L = 25 µm. Estimated to 13.5 °C

*** (González, et al., 2008)

The parameters for calculating the transmission rates of O_2, CO_2 and N_2 with Eq. 2.7 are at the top of Table 2.3. Required parameters in the empirical model of González et al. (2008) are also shown in the top right of Table 2.3. The transmission rates calculated with Eq. 2.7 and Eq. 2.8 for the perforation arrangements evaluated in the model validation are included at the bottom of Table 2.3. The K_{TR} obtained with the modified Fick model (Eq. 2.7) were lower than those calculated with the empirical model of González et al. (2008) and had a better fit to the experimental data in the validation of the model, especially in the case of the K_{TR} values for CO_2. The model of González et al. (2008) was adjusted from experiments using much smaller perforation diameters than those evaluated in this work, and therefore their extrapolation to larger diameters may result in underestimated K_{TR} values, further that dependence on temperature is not so well appreciated by this model. For the reasons stated above, the modified Fick equation (Eq. 2.7) was used to describe the permeation through the perforations in the model.

2.4.3 Modelling and Validation

To verify the suitability of the proposed model, and determine their predictive reliability to track the evolution of package atmospheres, the results of the validation experiment with packed tomatoes at 13.5 °C were compared with those predicted by the model from Eqs. 2.10-2.14 to the same initial conditions. As shown in Figure 2.4 (a, b and c), the model adequately describes the evolution of O_2 and CO_2 concentrations for all the films and perforations evaluated. This agreement is also evidenced by the one in the determined parameters included in Table 2.4 and the range of correlation coefficients obtained: R^2 = 0.89-0.98 for O_2 and 0.83-0.97 for CO_2.

Table 2.4. Experimental and predicted equilibrium concentrations of O_2 and CO_2 for the packages evaluated and coefficients of determination (R^2) of the model in each case

	$y_{O2\ eq\text{-}exp}$	$y_{O2\ eq\text{-}pre}$	R^2	$y_{CO2\ eq\text{-}exp}$	$y_{CO2\ eq\text{-}pre}$	R^2
PP						
(1) 1P × 132 µm	0.122	0.115	0.895	0.050	0.043	0.914
(2) 2P × 365 µm	0.178	0.174	0.833	0.032	0.035	0.832
PLA						
(1) 1P × 132 µm	0.104	0.114	0.981	0.058	0.051	0.955
(2) 2P × 365 µm	0.175	0.175	0.971	0.034	0.036	0.907
LDPE						
(1) 1P × 132 µm	0.131	0.123	0.893	0.017	0.018	0.929
(2) 2P × 365 µm	0.170	0.167	0.854	0.017	0.017	0.883

For all the packages evaluated, an O_2 and CO_2 equilibrium concentration was achieved (Figure 2.4, Table 2.4). The CO_2 concentration reached an equilibrium value in practically all cases after 3 days of storage, while O_2 equilibrium concentration was reached between day 2 and day 9, depending on the material-perforations combination of each bag. PLA bags (1P x 132 um) took the longest time, reaching 10.4% of O_2 (11.4% predicted by the model) at day 9. In general, higher CO_2 (and lower O_2) concentrations were achieved with PLA bags closely followed by PP and finally by LDPE (Table 2.2). This partly due to the difference in permeability between the three films and partly to the contribution of mass transfer through the film is significant to the overall mass transfer (film and perforations) through the package.

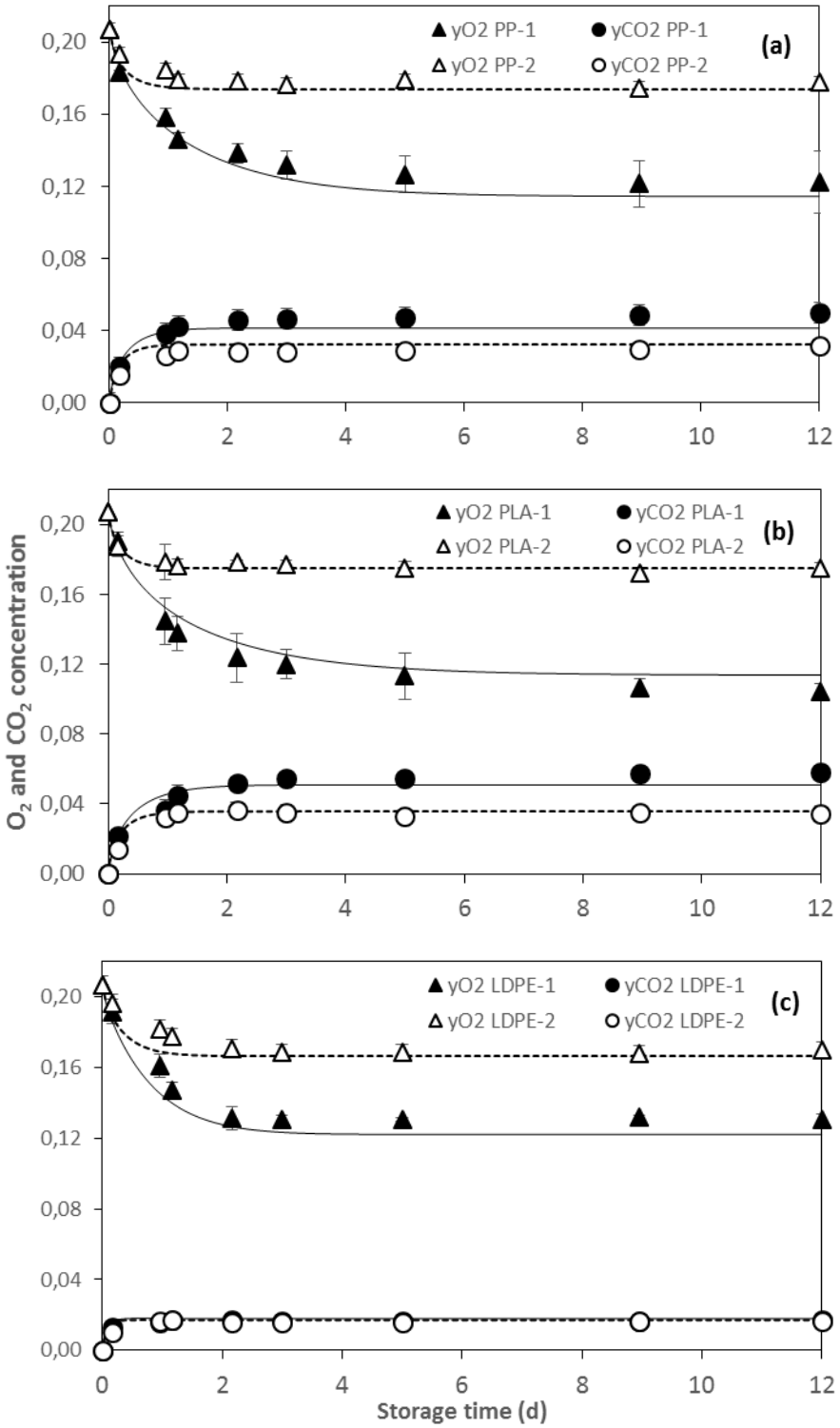

Figure 2.4. Experimental and predicted evolution of O_2 and CO_2 composition for (a) PP, (b) PLA and (c) LDPE bags with (1, black figures and continuous lines) one perforation of 132 µm and (2, white figures and dash lines) two perforations of 365 µm.

For PLA, the less permeable film, the permeation through the film represents 76.8% of the total transfer of CO_2 for the first configuration of perforated package (1P x 132 µm) and

40.4% for the second configuration (2P x 365 µm). For PP, the permeation rate represents 84.4% for the first configuration and 52.5% for the second configuration and for LDPE, more permeable the film, the permeation rate represents 96.8% for the first configuration and 86.0% for the second configuration. For O_2 the same pattern is observed. A plot of residuals as function of O_2 and CO_2 concentrations predicted by the model (Figure 2.5) show fairly random patterns in both cases; therefore it is possible to say that all major variables have been included and that equations used are appropriate to adequately describe the exchange of gases in the bags.

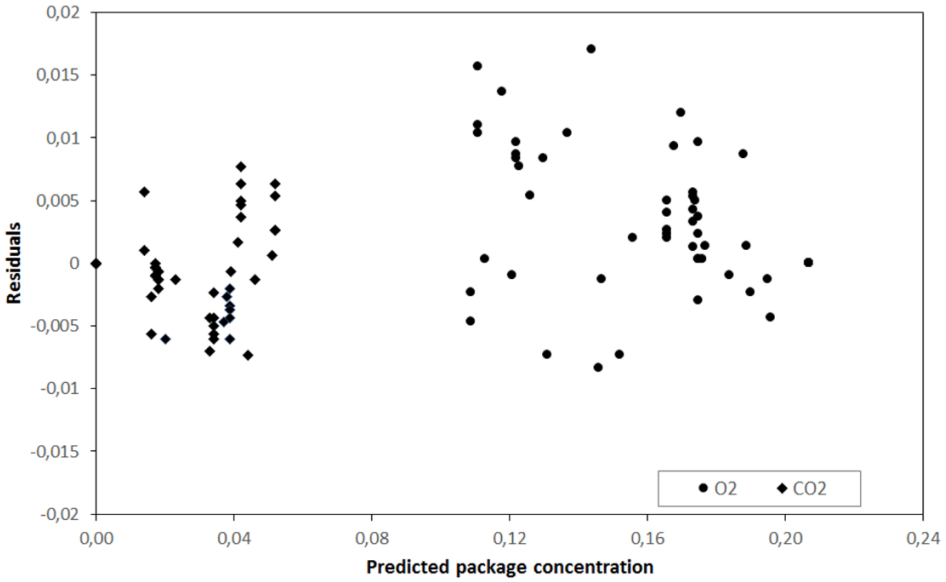

Figure 2.5. Residual versus predicted concentration of O_2 and CO_2.

As mentioned above, a value of $\varepsilon = 0.5d_e$ (Eq. 2.5) was estimated to calculate the O_2 and N_2 transmission rates, and $\varepsilon = 0.6d_e$ for CO_2. These values of ε allowed adequately describing the contribution of the perforations to the total transfer of gases through the package. For CO_2, $\varepsilon = 0.5d_e$ resulted in overestimated K_{TRCO2} values and CO_2 concentrations in the headspace lower than those experimentally determined. Similar results were observed with the empirical model proposed by González et al. (2008), which also overestimates K_{TRCO2}, predicting lower CO_2 concentrations than those in the actual values (González-Buesa, et al., 2009).

An additional experiment was done by packaging tomatoes in unperforated PP bags also at 13.5 °C and measuring O_2 concentration in the headspace. As can be seen in Figure 2.6, the evolution of the O_2 level was well described by the model. O_2 concentration in PP bags falls below 6% at day 6 without reaching an equilibrium value. Predicted O_2

concentration for PLA bags falls below 4% at day 6 also, without reaching equilibrium, while for LDPE bags an equilibrium O_2 concentration of 9.5% was predicted to be achieved at day 5. The model can describe also, the gas evolution in the headspace for packages without perforations.

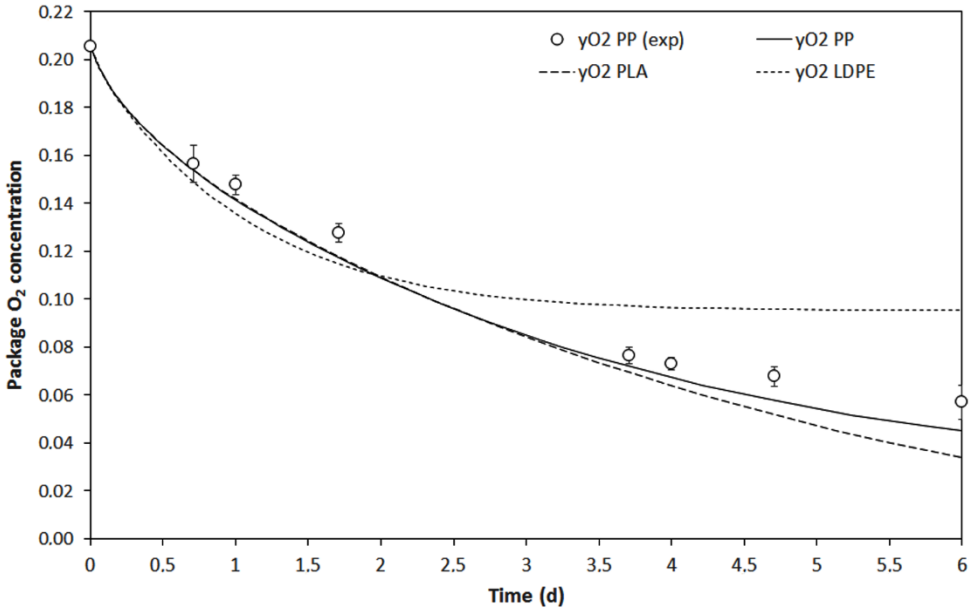

Figure 2.6. Evolution of O_2 concentration in PP bags (dots) and predicted evolution of O_2 concentration in PP, PLA and LDPE bags (lines) without perforations.

One aspect that has not been properly considered in the models reported for MAP (González-Buesa, et al., 2009; Mahajan, et al., 2007; Mangaraj, et al., 2015), is the volume change in flexible packages. Given the difference in the permeation rates of gases through the films, the perforations and the respiration rates, there will be a change in the free volume package that can result in either the swelling or, more frequently, the collapsing of the package due to a massive loss of gas in the headspace. In the model, the evolution in the free package volume was calculated, although no experimental values were measured. As can be seen in Figure 2.7, predicted values of V for PP and PLA bags are relatively close to the initial volume, with a slight gain for PLA bags with two perforations (2P x 365 um) and headspace reductions for the other combinations. Headspace in LDPE bags is greatly reduced for both combinations, being higher for bags with a perforation (1P x 132 um). This is due to the higher value in the ratio Q_{CO2}/Q_{O2} (equal to 6.04) with respect to PP (2.96) and PLA (2.75). In LDPE bags, a much faster rate of CO_2 permeation out into the external atmosphere can be foreseen, which results in lower CO_2 concentrations in the headspace

and a minor effect of inhibition on the MMU kinetics with higher consumption rates of O_2 that is not replaced by CO_2. Therefore, the free package volume is continuously decreasing.

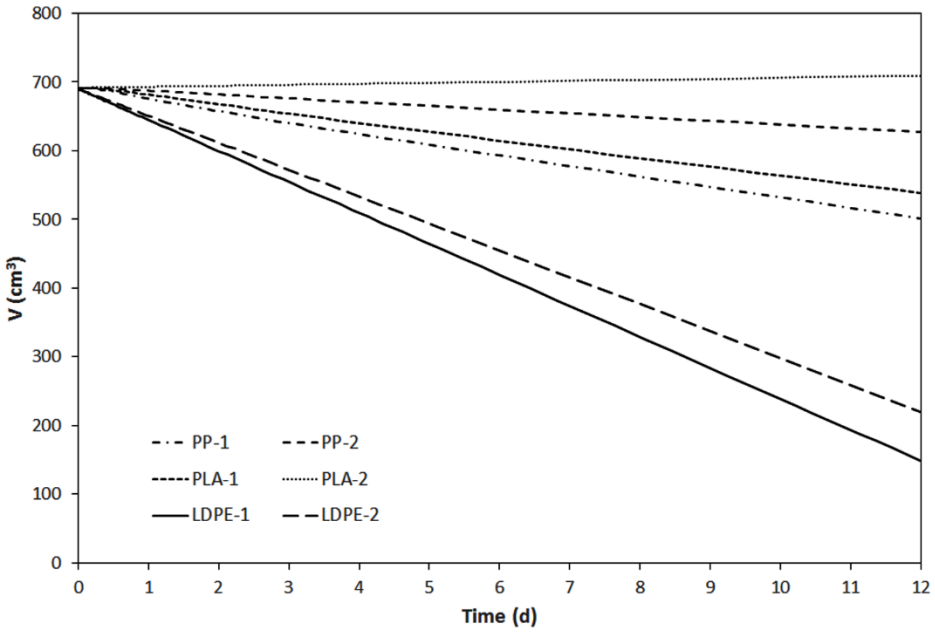

Figure 2.7. Predicted evolution in free package volume for PP, PLA and LDPE bags with (1) one perforation of 132 µm and (2) two perforations of 365 µm.

By reducing the amount of O_2, the N_2 concentration will be increasing in the headspace, producing a continuous concentration difference with respect to the external atmosphere so that the N_2 will be flowing out of the package and also reducing the volume. This collapsing phenomenon also occurs in some of the other bags, as shown in Figure 2.7, but to a much lesser extent since Q_{CO2}/Q_{O2} is not so large. The reduction in the free package volume was evidenced in all the cases described above, especially in LDPE bags, where it was quite noticeable, but as mentioned, not measured. This change in the headspace volume could be measured extracting the gas within the package with a syringe or another precise device along the storage time.

2.4.4 Setting a specific concentration in the headspace

As shown in Figure 2.4, if the gas transfer rate is enough to compensate the produce respiration after a certain time an atmosphere of equilibrium is reached inside the package and Eqs. 2.10-2.11 may be rewritten as:

$$\left(K_{TRO_2} + \frac{APQ_{O_2}}{L}\right)\left(y_{O_{2}Out} - y_{O_2\,eq}\right) - r_{O_2}W - y_{O_2\,eq}\frac{dV}{dt} = 0 \quad (2.18)$$

$$\left(K_{TRCO_2} + \frac{APQ_{CO_2}}{L}\right)\left(y_{CO_{2}out} - y_{CO_2\,eq}\right) + r_{CO_2}W - y_{CO_2\,eq}\frac{dV}{dt} = 0 \quad (2.19)$$

Where $y_{O2\,eq}$ and $y_{CO2\,eq}$ are the equilibrium O_2 and CO_2 concentrations. The change in the free package volume over time dv/dt, is substituted from Eq. 2.14.

The meaning of Eqs. 2.18 and 2.19 is that to reach a certain constant concentration of gas, a given transfer capacity by the package will be required to match the respiration of the fruit. To achieve this transfer capacity, the type of packaging material, the package surface area and the number and size of perforations can be modified. Knowing the produce respiration, is possible define a packaging system to achieve a self-sustaining controlled atmosphere with favorable gas levels.

To pack a product in MAP with a certain equilibrium gas concentration, is necessary to begin by defining the product type and quantity. Storage conditions are then defined: temperature, pressure and concentration of the atmosphere, $y_{O2\,out}$ and $y_{CO2\,out}$. Then a packaging material and its thickness can be selected. Once defined all this, the gas permeability coefficients in the package, the gas diffusion coefficients in the atmosphere and the parameters of the MMU equations are established. At this point depending on the size of the package is defined or not, two possible settings arise. In the first setting, if the size is not defined, is possible to achieve the required transfer capacity of the package simply by increasing the surface area. In this case, the K_{TR} values of each gas are zero in the absence of perforations and three variables will be taken: the equilibrium O_2 and CO_2 concentrations, $y_{O2\,eq}$ and $y_{CO2\,eq}$, and the required surface area. As there are three variables and two independent equations, fixing one, zero degrees of freedom are left and the remaining two variables are determined in the calculation. That is, if it is wanted to set the equilibrium O_2 concentration in the MAP system, the equilibrium CO_2 concentration is already defined and cannot be set. As is not possible to isolate A and $y_{O2\,eq}$ in Eqs. 2.18-2.19, is necessary to calculate their value iteratively. In the second setting, if the size of the package is defined, the surface area will be constant and to achieve the required transfer capacity is necessary to make perforations. In this case, the equilibrium gas concentrations, $y_{O2\,eq}$ and $y_{CO2\,eq}$, and the transmission coefficients through the perforation, K_{TRO2}, K_{TRCO2} and K_{TRN2}, will be taken as variables. However, from Eq. 2.7 can be seen that just as the diffusion coefficients of each gas in the atmosphere, the thickness of the bag and the ε correction term are already defined, the real variables are the diameter and the number of perforations in the package. If the number of perforations is fixed, only the diameter is

variable and if the perforation diameter is fixed, only the number of these may be varied. Then, three variables will be taken: the equilibrium O_2 and CO_2 concentrations, $y_{CO2\ eq}$ and $y_{O2\ eq}$, and the diameter or the number of perforations. As in the first setting, when one of the concentrations is fixed, zero degrees of freedom are left, and the remaining concentration and the diameter or the number of perforations are determined in the calculation.

Consider the following example: Majidi et al. (2014) used a concentration of 5% O_2 and 3% CO_2 at 13 °C to store tomato in controlled atmosphere. To try to meet this requirement a simulation was done using the same bags and packing the same amount of fruit (ca. 350 g) as the previous validation test, with a target concentration of 5% O_2 and CO_2 approaching 3% that cannot be reached exactly because the reasons given above. Having the material type (PP, LDPE and PLA) and bag size defined arise two possible settings: 1) the transfer capacity of the package is greater than the respiration rate of the fruit; in this case the package can be cut down until it reaches the required transfer capacity. 2) The transfer capability is lower than the respiration rate, so is required to make perforations until it reaches the required transfer capacity.

For the first setting, the surface area required to achieve the target O_2 concentration and the equilibrium CO_2 concentration were calculated by double iteration. These results are at the top of Table 2.5. The surface area required for LDPE (478 cm^2) is fewer than that available in the bags (800 cm^2) so by cutting the bag to achieve the required area, the target O_2 concentration can be reached. Required areas for the PP and PLA bags are greater than the available so it is necessary to make perforations. For the second setting, the diameter required for the perforation and $y_{CO2\ eq}$ were also calculated by double iteration. The results are in the bottom of the Table 2.5. The PP bags would need one perforation of 36 µm and the PLA bags one perforation of 50 µm. In all cases, the target concentration of 5% O_2 is achieved. In Figure 2.8, simulation of how the equilibrium concentrations inside the package are reached starting from an initial atmospheric concentration is shown. Would be required between 7 and 11 days of storage to reach equilibrium depending on the package material. However, this time depends on the initial concentration and if this is closer to the desired concentration, equilibrium is reached more quickly. If the initial O_2 concentration were 5 % in the headspace (and 3% of CO_2), the equilibrium levels would be reached on day 9 as shown in Figure 2.9, compared to 11 days with an initial O_2 equal to 20.8 %.

Table 2.5. Package configuration required to achieve an equilibrium O_2 concentration of 5% ($y_{O2\ eq}$ = 0.05) and equilibrium O_2 and CO_2 concentrations predicted by the model

Target concentration			
$y_{O2\ eq}$		0.05	
Bag	*PP*	*LDPE*	*PLA*
Available surface area (cm^2)	800	800	800
Thickness (mm)	0.025	0.018	0.025
Setting 1 (unperforated bag)			
Reached concentrations			
$y_{O2\ eq}$	0.05	0.05	0.05
$y_{CO2\ eq}$	0.036	0.024	0.039
Required surface area (cm^2)	1070	478	1550
Decision	Add perforations	Cut the bag	Add perforations
Setting 2 (perforated bag)			
Reached concentrations			
$y_{O2\ eq}$	0.05	-	0.05
$y_{CO2\ eq}$	0.041	-	0.052
Required perforations	1	-	1
Perforation diameter (µm)	36	-	50

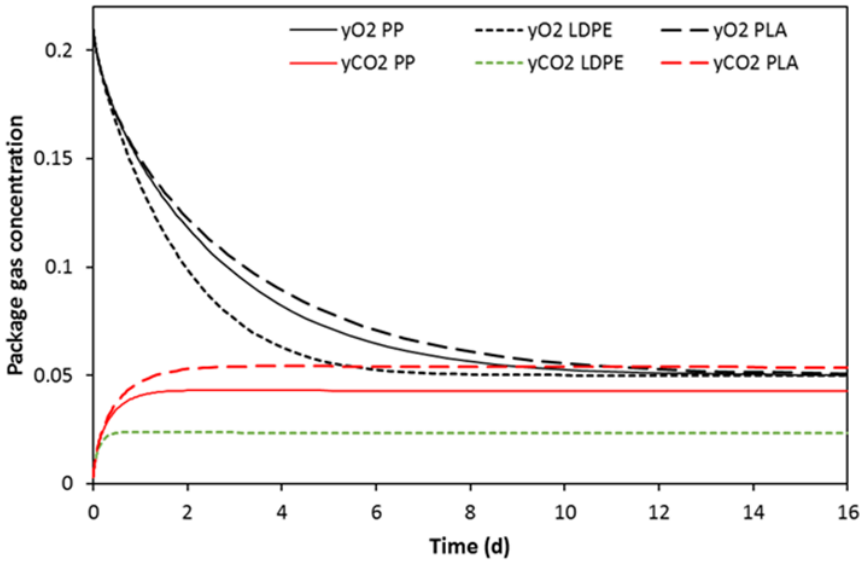

Figure 2.8. Predicted evolution of O_2 and CO_2 concentrations in unperforated LDPE and perforated PP and PLA bags setting an equilibrium O_2 concentration of 5 % ($y_{O2\ eq}$ = 0.05)

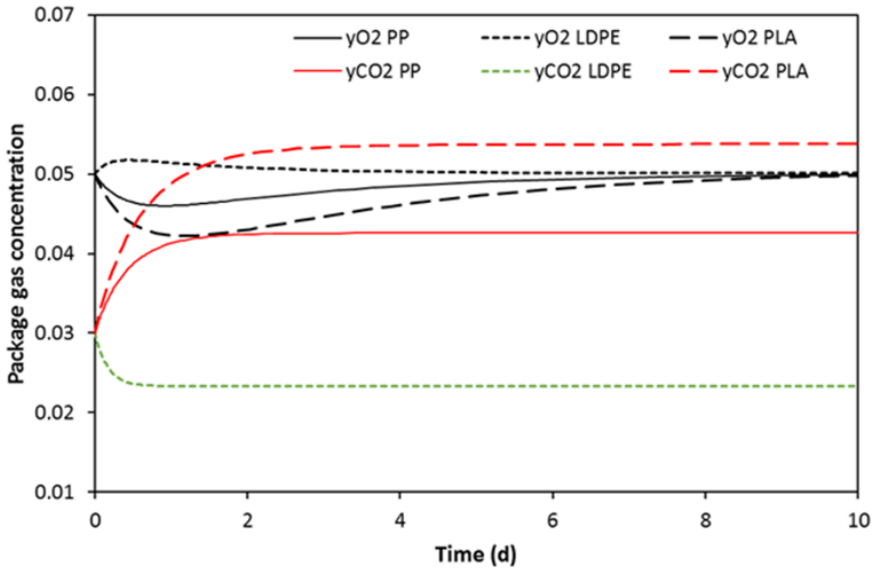

Figure 2.9. Predicted evolution of O_2 and CO_2 concentrations in unperforated LDPE and perforated PP and PLA bags setting an equilibrium O_2 concentration of 5 % ($y_{O2\ eq}$ = 0.05) with the same initial concentration.

2.5 Conclusions

A mathematical model to describe the evolution of O_2 and CO_2 concentrations in a MAP system with perforations and variable volume, taking into account the diffusive gas permeation through the packaging film and the perforations, the respiration rate of the packed product and the storage temperature, was successfully established.

The capacity of the model was verified with experimental data, achieving good prediction results for tomato packed in three types of perforated films. The model is based on analytical expressions for calculating respiration rates (MMU enzyme kinetics) and gas transfer through the package of films (Fick's law) and of perforations (modified Fick's law), so it can be easily used to predict the behavior of other products packed in a wider range of packaging materials.

The model can also be used to set a specific equilibrium concentration of O_2 or CO_2 by properly modifying the configuration of the package and hence its transfer capacity.

2.6 References

Auras, R. & Almenar, E. 2010. Permeation, sorption and diffusion in poly(lactic acid). In: Auras, R., Lim, L.T., Selke, S.E.M. & Tsuji, H. (Eds.). *Poly(Lactic Acid): synthesis, structures, properties, processing and application*. New York: Wiley & Sons, pp. 164-170.

Bhande, S.D., Ravindra, M.R. & Goswami, T.K. 2008. Respiration rate of banana fruit under aerobic conditions at different storage temperatures. *Journal of Food Engineering,* 87(1): 116-123.

Castellanos, D.A. & Herrera, A.O. 2015. Mathematical models for the representation of some physiological and quality changes during fruit storage. *Journal of Post-Harvest Technology,* 3(1): 18-35.

Chung, D., Papadakis, S.E. & Yam, K.L. 2003. Simple models for evaluating effects of smalls leaks on the gas barrier properties of food packages. *Packaging Technology and Science,* 16: 77-86.

Del-Nobile, M.E., Licciardello, F., Scrocco, C., Muratore, G. & Zappa, M. 2007. Design of plastic packages for minimally processed fruits. *Journal of Food Engineering,* 79: 217-224.

Del-Valle, V., Almenar, E., Lagarón, J.M., Catalá, R. & Gavara, R. 2003. Modelling permeation through porous polymeric films for modified atmosphere packaging. *Food Additives and Contaminants,* 20: 170-179.

Floros, J.D. & Maxos, K.I. 2005. Introduction to modified atmosphere packaging. In: Han, J. (Ed.) *Innovations in Food Packaging*. New York: Elsevier Academic Press, pp. 159-172.

Fonseca, S.C., Oliveira, F.A.O. & Brecht, J.K. 2002. Modelling respiration rate of fresh fruits and vegetables for modified atmosphere packages: a review. *Journal of Food Engineering,* 52: 99-119.

Geankoplis, C.J. 1993. *Transport Processes and Unit Operations*. Third Ed. New Jersey: Prentice Hall.

Ghosh, V. & Anantheswaran, R.C. 2001. Oxygen transmission rate through micro-perforated films: Measurement and model comparison. *Journal of Food Process Engineering*, 24: 113-133.

Gomes, M.H., Beaudry, R.M., Almeida, D.P.F. & Malcata, F.X. 2010. Modelling respiration of packaged fresh-cut 'Rocha' pear as affected by oxygen concentration and temperature. *Journal of Food Engineering*, 96: 74-79.

González-Buesa, J., Ferrer-Mairal, A., Oria, R., Salvador, M.L. 2009. A mathematical model for packaging with microperforated films of fresh-cut fruits and vegetables. *Journal of Food Engineering*, 95: 158-165.

González, J., Ferrer, A., Oria, R. & Salvador, M.L. 2008. Determination of O_2 and CO_2 transmission rates through microperforated films for modified atmosphere packaging of fresh fruits and vegetables. *Journal of Food Engineering*, 86: 194-201.

Hasbullah, R., Gardjito, Syarief, A.M. & Akinaga, T. 2000. Gas permeability characteristics of plastic films for packaging of fresh produce. *Journal of the Society of Agricultural Structures, Japan*, 31(2): 5-11.

Heydari, A., Alemzadeh, I. & Vossoughi, M. 2012. Study and Mathematical Modeling of Transient Gas Compositions for Modified Atmosphere Packaging. In: Öchsner, A., Da Silva, L.F.M. & Altenbach, H. (Eds.), *Analysis and Design of Biological Materials and Structures*. Berlin Heidelberg: Springer-Verlag, pp. 163-174.

Heydari, A., Shayesteh, K., Eghbalifam, N., Bordbar, H. & Falahatpisheh, S., 2010. Studies on the respiration rate of banana fruit based on enzyme kinetics. *International Journal of Agriculture & Biology*, 12(1): 145-149.

Kwon, M.J., Jo, Y.H., An, D.S., & Lee, D.S. 2013. Applicability of Simplified Simulation Models for Perforation-Mediated Modified Atmosphere Packaging of Fresh Produce. *Mathematical Problems in Engineering*, doi: 10.1155/2013/267629

Mahajan, P.V., Oliveira, F.A.R., Montanez, J.C. & Frias, J. 2007. Development of user-friendly software for design of modified atmosphere packaging for fresh and fresh-cut produce. *Innovative Food Science and Emerging Technologies,* 8: 84-92.

Majidi, H., Minaci, S., Almassi, M. & Mostofi, Y. 2014. Tomato quality in controlled atmosphere, modified atmosphere packaging and cold storage. *Journal of Food Science and Technology,* 51(9): 2155-2161.

Mangaraj, S., Goswami, T.K. 2011. Modeling of Respiration Rate of Litchi Fruit under Aerobic Conditions. *Food and Bioprocess Technology*, 4: 272-281.

Mangaraj, S., Goswami, T.K., Mahajan, P.V. 2009. Applications of plastic films for modified atmosphere packaging of fruits and vegetables: a review. *Food Engineering Reviews*, 1: 133-158.

Mangaraj, S., Goswami, T.K. & Mahajan, P.V. 2014. Development and validation of a comprehensive model for map of fruits based on enzyme kinetics theory and Arrhenius relation. *Journal of Food Science and Technology*, 52(7): 4286-4295.

Saltveit, M.E. 2004. Cucumber. In: Gross, K.C., Wang, C.Y. & Saltveit, M.E. (Eds.), The commercial storage of fruits, vegetables, and florist and nursery stocks. Beltsville: USDA/ARS (USDA. Agricultural handbook, 66).

Sandhya, K.V.K. 2010. Modified atmosphere packaging of fresh produce: Current status and future needs. LWT - Food Science and Technology 43, 381-392.

Siracusa, V. 2012. Food Packaging Permeability Behaviour: A Report. *International Journal of Polymer Science*, doi: 10.1155/2012/302029

Techavises, N. & Hikida, Y. 2008. Development of a mathematical model for simulating gas and water vapor exchanges in modified atmosphere packaging with macroscopic perforations. *Journal of Food Engineering*, 85: 94-104.

Wang, Z.W., Duan, H.W. & Hu, C.Y. 2009. Modelling the respiration rate of guava (Psidium guajava L.) fruit using enzyme kinetics, chemical kinetics and artificial neural network. *European Food Research and Technology*, 229: 495-503.

Xanthopoulos, G., Koronaki, E. & Boudouvis, A. 2012. Mass transport analysis in perforation-mediated modified atmosphere packaging of strawberries. *Journal of Food Engineering*, 111: 326-335.

Chapter 3. Modelling respiration of feijoa fruits and application in modified atmosphere packaging[3]

Abstract

A proper description of the process of respiration is important in the design and establishment of package systems for preserving fresh fruits and vegetables. In this work a model based on both Michaelis-Menten enzyme kinetics and chemical kinetics equations was developed and assessed in order to describe the respiration rates of feijoa fruits (*Acca sellowiana* Berg) from experimental data obtained at different temperatures by a closed system method. The temperature effect in the O_2 consumption and CO_2 production was described using Arrhenius-type relationships. After this, the fresh fruits were packed in perforated low-density polyethylene (LDPE) and polypropylene (PP) bags for 8 days at 12°C and 80% RH to validate the usefulness of the model to represent the gas evolution in modified atmosphere packaging (MAP). In the tests, maximum respiration rates of 3650-4230 $cm^3\ kg^{-1}\ d^{-1}$ were obtained at 24 °C whereas at 6 °C, O_2 consumption and CO_2 production rates were up to 6 times lower. It was possible to describe properly the respiration kinetics using a Michaelis-Menten uncompetitive equation with coefficients of determination above 0.9. The overall model was validated in the MAP test being possible to predict successfully the O_2 and CO_2 evolution inside the LDPE and PP bags.

Key words: Michaelis-Menten, Arrhenius, uncompetitive inhibition, chemical kinetics, fruit storage

[3] This chapter (with minor modifications) is a part of the article published as:
Castellanos, D.A., Mendoza, R., Gavara, R. & Herrera, A.O. 2016. Respiration and Ethylene Generation Modeling of 'Hass' Avocado and Feijoa Fruits and Application in Modified Atmosphere Packaging, *International Journal of Food Properties,*
http://dx.doi.org/10.1080/10942912.2016.1160921

Nomenclature

a, b	apparent reaction orders
A	effective exchange area of the packaging film (m^2)
A_h	cross sectional area of the perforations (cm^2)
CK	chemical Kinetics
d	diameter of the perforation (cm)
d_e	effective diameter of the perforations (cm)
D_{O2}, D_{CO2}	diffusion coefficients of O_2 and CO_2 in air ($cm^2\ d^{-1}$)
E_a	activation energy ($kJ\ mol^{-1}$)
k_{O2}, k_{CO2}	rate coefficients ($cm^3\ kg^{-1}\ d^{-1}$)
K_{mO2}, K_{mCO2},	dissociation constants of the enzyme-substrate complex
K_{muCO2}, $K_{mu'CO2}$	constants of uncompetitive inhibition for consumption of O_2 and generation of CO_2, respectively
l	film thickness (mm)
MM	Michaelis-Menten simple kinetics
MMU	Michaelis-Menten Kinetics with uncompetitive inhibition
P	system pressure (atm, kPa)
p_{O2}	partial pressure of O_2 (atm, kPa)
Q_{O2}, Q_{CO2}	film permeability coefficients to O_2 and CO_2 ($cm^3\ mm\ m^2\ d^{-1}\ atm^{-1}$)
R	universal gas constant (0.008314 $kJ\ mol^{-1}\ K^{-1}$ or 82.057 $atm\ cm^3\ mol^{-1}\ K^{-1}$)
r_{O2}, r_{CO2}	O_2 consumption and CO_2 production rates ($cm^3\ kg^{-1}\ d^{-1}$)
r_{O2max}, r_{CO2max}	maximum O_2 consumption and CO_2 production rates ($cm^3\ kg^{-1}\ d^{-1}$)
RQ	respiratory quotient, r_{CO2}/r_{O2}
t	packaging/storage time (d)
Δt	time elapsing between two successive measurements
T	temperature (°C, K)
V	free package volume - headspace (cm^3)
W	fruit weight (kg)
y_{O2}, y_{CO2}	O_2 and CO_2 concentrations inside the package
y_{O2out}, y_{CO2out}	O_2 and CO_2 concentrations outside the package
ε	Correction term for gas transmission through perforations (mm)

3.1 Introduction

Feijoa (*Acca sellowiana* Berg) is a tropical fruit with significant growth in production over recent years. However, once this produce is harvested, it undergo rapid decay in its quality properties so the use of suitable storage methods is fundamental.

Feijoa or pineapple guava is an evergreen shrub of the Myrtaceae family, native to Southern Brazil and Northern Uruguay (Dos Santos, et al., 2009; East, et al., 2009). Commercial production of feijoa is centered in New Zealand, Georgia, Azerbaijan, Colombia and the United States (California), with Brazil and Uruguay as emergent countries (Dos Santos, et al., 2009). The fruit is recognized for its exceptional nutritional qualities with a high content of iodine and vitamin C, antioxidant compounds such as flavonoids and polyphenols, anticancer and antimicrobial activity (Bontempo, et al., 2007). Feijoa is a climacteric fruit with a limited postharvest life, ripening after 1-2 weeks of harvest at 16-17 °C. It has a commercial storage life of four weeks at 4-5 °C, with a maximum shelf life of 5 days at 20 °C, although the fruit may have chilling injury when stored at temperatures below 5 °C (Parra & Fischer, 2014). The fruit respiration rate (r_{CO2}) oscillates between 177 and 355 cm^3 kg^{-1} d^{-1} at a temperature of 4-5 °C; and may change to between 1662 and 3325 (climacteric peak) cm^3 kg^{-1} d^{-1} at 20-23 °C. Its ethylene generation rate is between 0.1-1.2 cm^3 kg^{-1} d^{-1} at 20-23 °C (Parra & Fischer, 2014; Velho, et al., 2011).

Given the short shelf life of this fruit, it is necessary to use proper storage systems such as modified atmosphere packaging (MAP) or controlled atmospheres (CA) to preserve its quality properties longer (East, et al., 2009; Sandhya, 2010). However, the successful use of these systems depends on the previous consideration of the respiration processes. As fruits ripen, they will consume oxygen from its surroundings and generate CO_2 and in consequence, the desired conditions to be achieved involve a change in the atmosphere surrounding the fresh produce, reducing O_2 and increasing CO_2. In this way, it is possible to influence produce´s metabolism and/or the activity of decay-causing microorganisms to increase storability (Fonseca, et al., 2002; Mangaraj, et al., 2015). Nevertheless, to achieve the wanted gas levels it is necessary to know the rate at which the stored product will consume O_2 and will be producing CO_2 towards this atmosphere to determine the suitable package permeability in MAP or gas flow required in CA depending on the system conditions (Mahajan, et al., 2007; Sandhya, 2010).

Several authors have developed mathematical models to describe respiration in fruits, many of them based on Michaelis-Menten kinetics (Caleb, et al., 2012; Fonseca, et al., 2002; Mangaraj, et al., 2015). However, only some of them take into account the combined effect of the concentrations of O_2 and CO_2 in the atmosphere surrounding the product and the storage temperature. For feijoa, some data on respiration have been published before,

but there are no models available yet to describe the consumption of O_2 and production of CO_2 in relation to storage time, temperature and level of these gases.

In this chapter, a mathematical model to describe the respiration process of feijoa fruits is presented, and its application in the modelling of a MAP system is evaluated. Respiration rates of the fruit were estimated at different temperatures by using Michaelis-Menten enzyme kinetics and Chemical kinetics equations together with Arrhenius' law. The data predicted by these equations were compared with experimental data aiming to select the most suitable ones according to their accuracy and reliability. After this, the usefulness of the respiration equations was validated through the MAP model presented in Chapter 2 to predict the evolution of O_2 and CO_2 in the packaging headspace of a MAP system containing feijoa fruits.

3.2 Materials and Methods

3.2.1 Fruit samples

The fruits were obtained from commercial growers located in Tibasosa, department of Boyacá, in Colombia. Samples were harvested at physiological maturity stage, 20 weeks from flowering time for feijoa (Parra & Fischer, 2014) and later transported to the Postharvest Laboratory, Faculty of Agricultural Sciences, Universidad Nacional de Colombia (Bogotá, Colombia) in the following days. In the laboratory, fruits with evidence of damage were discarded, and fruits with similar characteristics were then selected to ensure uniformity in the size, weight and color of the sample group. The fruits were subjected to cleaning and disinfection and then were dried at room temperature. After, the samples were randomly divided into two groups. The first group was used to experimentally measure the respiration rates, and the second group was used for the MAP tests.

3.2.2 Determination of the respiration rates

The rates of O_2 consumption and CO_2 generation at different temperatures by fruits were determined using a closed system method. Two feijoa fruits (150 ± 20 g), were placed in open glass containers of 2020 cm^3 during an hour of acclimatization at the experiment temperature and then hermetically sealed. O_2 and CO_2 concentrations in the headspace were measured by taking a 5 cm^3 gas sample through a rubber seal on the top of the container, which was analyzed with an electronic analyzer Oxybaby® 6i (Witt-Gasetechnik

GmbH & Co. KG, Witten, Germany) previously calibrated with Gas Chromatography. 5 cm^3 of air was introduced into the container to replace the withdrawn sample. The tests were performed in temperature-controlled cabinets to 6, 10, 17 and 24 °C, setting temperature in ± 0.2 °C and taking measurements at regular intervals for maximum 3 days, avoiding reaching the phase of anaerobic respiration. All measurements were performed in triplicate, reporting the average value of each concentration.

Respiration rate to each temperature was estimated using the following equations as posed in Chapter 2:

$$r_{O_2}(t) = (V/W)\left(y_{O_2 t-1} - y_{O_2 t+1}\right)/\Delta t \quad (2.15)$$

$$r_{CO_2}(t) = (V/W)\left(y_{CO_2 t+1} - y_{CO_2 t-1}\right)/\Delta t \quad (2.16)$$

Where $r_{O2}(t)$ and $r_{CO2}(t)$ are the respiration rates at time t, Δt is the time elapsing between two successive measurements. y_{O2t-1}, y_{CO2t-1} are the O_2 and CO_2 mole fractions determined in the previous measurement than reported at time t and y_{O2t+1}, y_{CO2t+1} are the O_2 and CO_2 mole fractions determined in the subsequent measurement than reported at time t, respectively.

To describe the experimental behavior of the respiration process in the fruits (and the effect of atmospheric O_2 and CO_2 levels), various equations have been proposed. Among these equations stand out the Michaelis-Menten equations based on the enzyme kinetics principle and the chemical kinetics equations based on the reaction order, which have been used due their suitable representation of this biochemical process and good fit of experimental data (Bhande, et al., 2008; Fonseca, et al., 2002; Wang, et al., 2009).

The simplest Michaelis-Menten Kinetics (MM) is shown in Eq. 1.6. As described in Chapter 1, this equation is based on a limiting enzymatic reaction where the substrate is O_2. The respiration rate, in this case the O_2 consumption rate r_{O2}, is (Fonseca, et al., 2002; Heydari, et al., 2010):

$$r_{O_2} = \frac{r_{O_{2max}} y_{O_2}}{K_{m_{O_2}} + y_{O_2}} \quad (1.6)$$

A similar equation can be defined for the CO_2 production rate, also in function of y_{O2}.
In some studies (Bhande, et al., 2008; Heydari, et al., 2010; Mangaraj & Goswami, 2011), the inhibitory effect by CO_2 on respiration has been considered using the Michaelis-Menten kinetics with uncompetitive inhibition (MMU) due the CO_2 (Fonseca, et al., 2002; Mangaraj & Goswami, 2011). As presented in Chapters 1 and 2, the uncompetitive inhibition equations for the respiration process in terms of O_2 consumption and CO_2 generation are respectively:

$$r_{O_2} = \frac{r_{O_{2max}} y_{O_2}}{K_{m_{O_2}} + y_{O_2}\left(1 + \frac{y_{CO_2}}{K_{mu_{CO_2}}}\right)} \quad (1.8)$$

$$r_{CO_2} = \frac{r_{CO_{2max}} y_{O_2}}{K_{m_{CO_2}} + y_{O_2}\left(1 + \frac{y_{CO_2}}{K_{mu'_{CO_2}}}\right)} \quad (2.1)$$

The Chemical Kinetics (CK) equations have been applied to represent the O_2 consumption and the CO_2 production in fresh produce where respiration can be described as a simpler process than an enzymatic kinetics. These equations have been successfully applied in beans (Chen, et al., 2016) and guava (Wang, et al., 2009). In the CK equations, apparent reaction orders are considered to explain the effect of O_2 and CO_2 concentrations on the respiration rates (Wang, et al., 2009):

$$r_{O_2} = k_{O_2} y_{O_2}^{a_{O2}} y_{CO_2}^{b_{O2}} \quad (3.1)$$

$$r_{CO_2} = k_{CO_2} y_{O_2}^{a_{CO2}} y_{CO_2}^{b_{CO2}} \quad (3.2)$$

The respiration rate in the product changes with temperature. In the Michaelis-Menten enzyme kinetics, it can be considered that the parameters outlined above will vary depending on storage temperature (Bhande, et al., 2008; Mangaraj, et al., 2015). Similarly, in the CK equations the rate coefficients are temperature-dependent (Wang, et al., 2009). As previously mentioned, the dependence of MM/MMU parameters and CK rate coefficients on storage temperature has been expressed using Arrhenius-type equations as follows (in this case, for the maximum O_2 consumption rate for example):

$$r_{O_2}^{max} = r_{O_2\theta}^{max} e^{-Ea/RT} \quad (1.11)$$

Similar equations can be written for the other parameters in Eqs. 1.8, 2.1, 3.1 and 3.2.

To determine the O_2 consumption and CO_2 production rates of feijoa fruits, the Michaelis-Menten Uncompetitive enzyme kinetics (MMU; Eqs. 1.8 and 2.1) and the chemical kinetics equations (CK; Eqs. 3.1 and 3,2) were used, evaluating at the end the expression that better fits the experimental data obtained. The experimental values of r_{O2}, r_{CO2}, y_{O2} and y_{CO2} generated at each temperature were substituted in the linearized form of the MMU and CK equations to obtain the respective parameters by multiple linear regressions. The temperature dependency was determined by replacing the parameters of each equation in the linearized form of the Arrhenius equation (Eq. 1.11) estimating the pre-exponential factors and the activation energies for each parameter.

The MMU and CK equations were compared by using an adjusted R^2 (Mendoza, et al., 2016; Sanders & De Wild, 2003), which allows the comparison between non-linear models and compensates for possible bias due to different number of parameters. As before, the temperature influence was estimated by replacing the parameters of each equation in the linearized form of the Arrhenius' law and obtaining the pre-exponential factors and the activation energies for each parameter.

At this stage, after obtaining the various parameters, the respiration equations that best represented the evolution of gases, were selected to perform the validation experiment in a system of modified atmosphere packaging.

3.2.3 Application in MAP and validation

After finding the parameters of the equations of respiration and selecting the most suitable one in each case, an experiment was conducted packaging feijoa fruits in two types of perforated bags to validate their capacity to describe the gas evolution in a MAP system. 181.3 ± 9.1 g of feijoa were packed in PP bags and 189.5 ± 8.3 g of feijoa were packed in LDPE bags. The initial volume headspace was 359.8 ± 10.6 cm^3 for feijoa and PP, and 503.3 ± 9.8 cm^3 for feijoa and LDPE respectively. In the experiment, cast-polypropylene (PP) bags with a thickness of 0.025 ± 0.002 mm and low-density polyethylene bags with a thickness of 0.018 ± 0.001 mm (both, Rediplast, Bogotá, Colombia) were used. The bags had a total internal surface area of 1000 cm^2 and an effective transfer-area of 800 cm^2. In each bag, a single perforation of 0.280 mm effective diameter was made to ensure the O_2 level in the headspace did not reach 0% by previously simulating the evolution of the system

using the respiration and ethylene production equations and the differential balance equations for each gas (Eq. 14-16) described below. The perforation size was measured using an optical microscope (Motic® B1-220A, Speed Fair Co., Ltd., Richmond, Canada). Packages with the fruits inside were stored in a controlled-temperature cabinet to 12 ± 0.2 °C for 8 days, keeping relative humidity constant at 80 ± 1%.

For all tests, measurements of O_2 and CO_2 in the packages were performed throughout the storage time in the same way as described above in the respiration tests. All measurements were made in triplicate. The initial headspace gas composition in the packages was similar to that of the atmosphere.

O_2 and CO_2 permeability coefficients of both films were experimentally determined with steady state methods as previously described in Chapter 2, using a Mocon® Oxtran 2/21 permeation instrument (MOCON, Inc., Minneapolis, MN, USA) for O_2 and a chamber specially built with a permeation cell and connected to a gas chromatograph.

As mentioned above, a perforation was made in each package to avoid exhausting O_2 in the headspace before the end of the experiment and get an anaerobic phase. As mentioned in Chapter 2, the gas transmission through the perforation in each package follows a modified Fick's diffusion equation (Eq. 2.7) incorporating a term of correction ε for gas diffusion resistance in the perforation (Castellanos, et al., 2016; Chung, et al., 2003).

The change over time of O_2 and CO_2 concentrations in the MAP system can be described using the differential gas balance equations presented in Chapter 2:

$$\left[V\frac{dy_{O_2}}{dt} + y_{O_2}\frac{dV}{dt}\right] = K_{TRO_2}\left(y_{O_{2Out}} - y_{O_2}\right) + \frac{APQ_{O_2}}{L}\left(y_{O_{2Out}} - y_{O_2}\right) - r_{O_2}W \quad (2.10)$$

$$\left[V\frac{dy_{CO_2}}{dt} + y_{CO_2}\frac{dV}{dt}\right] = K_{TRCO_2}\left(y_{CO_{2Out}} - y_{CO_2}\right) + \frac{APQ_{CO_2}}{L}\left(y_{CO_{2Out}} - y_{CO_2}\right) + r_{CO_2}W \quad (2.11)$$

In the system, the change of the N_2 concentration in the packaging system is estimated with Eq. 2.12 and the change in the headspace volume is estimated with Eq. 2.14. In the MAP model, it was considered that there is no gas stratification in the packaging headspace and the total pressure is the same as atmospheric.

The differential equations were numerically solved using a calculation routine built in Matlab® (MathWorks, Inc., Natick, MA, USA) from the 'ode15s' function (an implicit

multistep method based on numerical differentiation formulas, NDFs). After the initial gas conditions were defined, in this case atmospheric levels, and the initial values of product weight, package arrangement, temperature, pressure and storage time were set, the change in the concentrations of O_2 and CO_2 were calculated with this routine. In the calculation, the respiration parameters obtained for the equations previously selected were included. The data generated in the calculation routine from the model were then compared with the experimental gas measurements in the packages.

3.3 Results and discussion

3.3.1 Respiration rates

In Figure 3.1, the respiration rates of feijoa fruits as a function of O_2 within the hermetic containers are shown. In Figure 3.2, the evolution of O2 and CO2 concentrations in the container headspace is also shown. The consumption rate of O_2 and the production rate of CO_2 were influenced, as shown in the figures, by the O_2 concentration in the atmosphere surrounding the product. The rates of O_2 consumption and CO_2 production were higher to the initial concentrations of O_2 (air) and became lower as the O_2 was consumed within the package. By decreasing the O_2 concentration, the slope of the concentration curves of O_2 and CO_2 becomes close to zero.

For respiration rate in feijoa fruits, Velho et al. (Velho, et al., 2011) obtained a r_{CO2} value of the same order but 40 % smaller, ca. 1750 $cm^3\ kg^{-1}\ d^{-1}$ at 23 °C and p_{O2} = 21 kPa for feijoa grown in Santa Catarina, Brazil. At 6 °C and p_{O2} = 15 kPa, the r_{CO2} obtained was 1150 $cm^3\ kg^{-1}\ d^{-1}$, ca. 2.5 times higher than that obtained by East et al. (East, et al., 2009) for 'Unique' feijoa grown in New Plymouth, New Zealand, 360 $cm^3\ kg^{-1}\ d^{-1}$ at 5 °C and p_{O2} = 21 kPa, and ca. 2 times higher than the value obtained by Velho et al. (Velho, et al., 2011), 700 $cm^3\ kg^{-1}\ d^{-1}$ at 4 °C and p_{O2} = 21 kPa. These differences can be attributed to the different cultivars and cultivation zones of the fruits used in each particular study.

Respiratory behavior of feijoa fruits was represented using the MMU and CK equations estimating the respective parameters from experimental data. The parameters of these equations are found in Table 3.1. The O_2 consumption and CO_2 production rates increased directly with the temperature (Figure 3, subplots a and b), reaching lower concentrations of O_2 (and higher CO_2) at higher temperatures as shown in Figure 3.2. Temperature-dependence of MMU parameters, r_{max}, K_m and K_{mu}, and of CK parameter k, was set up obtaining the respective pre-exponential factors and the apparent activation energies by

linear regression of the Arrhenius equation (Table 3.1). The positive values of the activation energies for the three parameters indicate a direct relationship between the temperature and respiration rates.

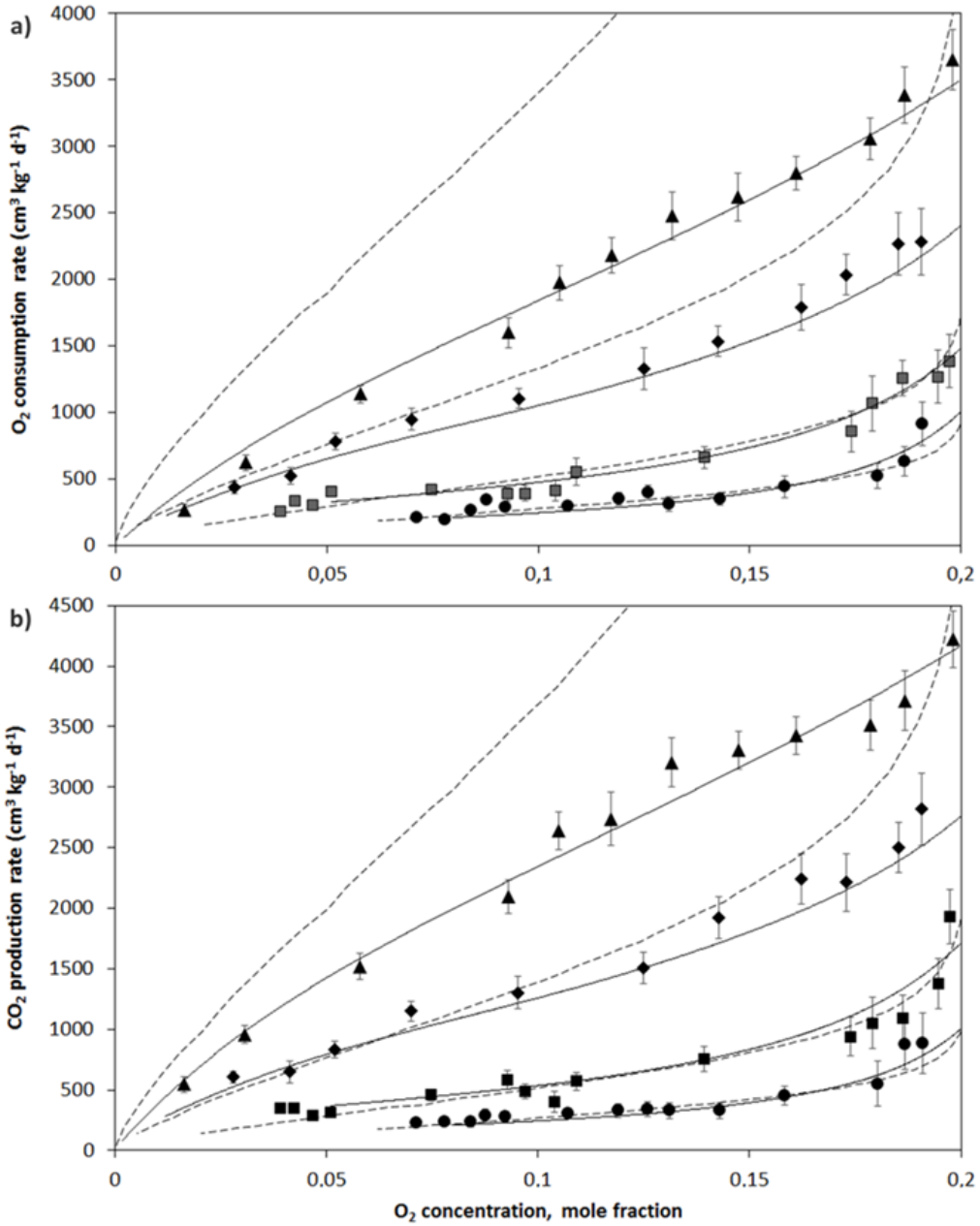

Figure 3.1. O_2 consumption (a) and CO_2 production (b) rates as a function of O_2 concentration within the experimental container headspace at 6 °C (●), 10 °C (■), 17 °C (♦), 24 °C (▲) and predicted values using the Chemical Kinetics (---) and Michelis-Menten Uncompetitive (—) equations for feijoa fruits. Bars represent SD.

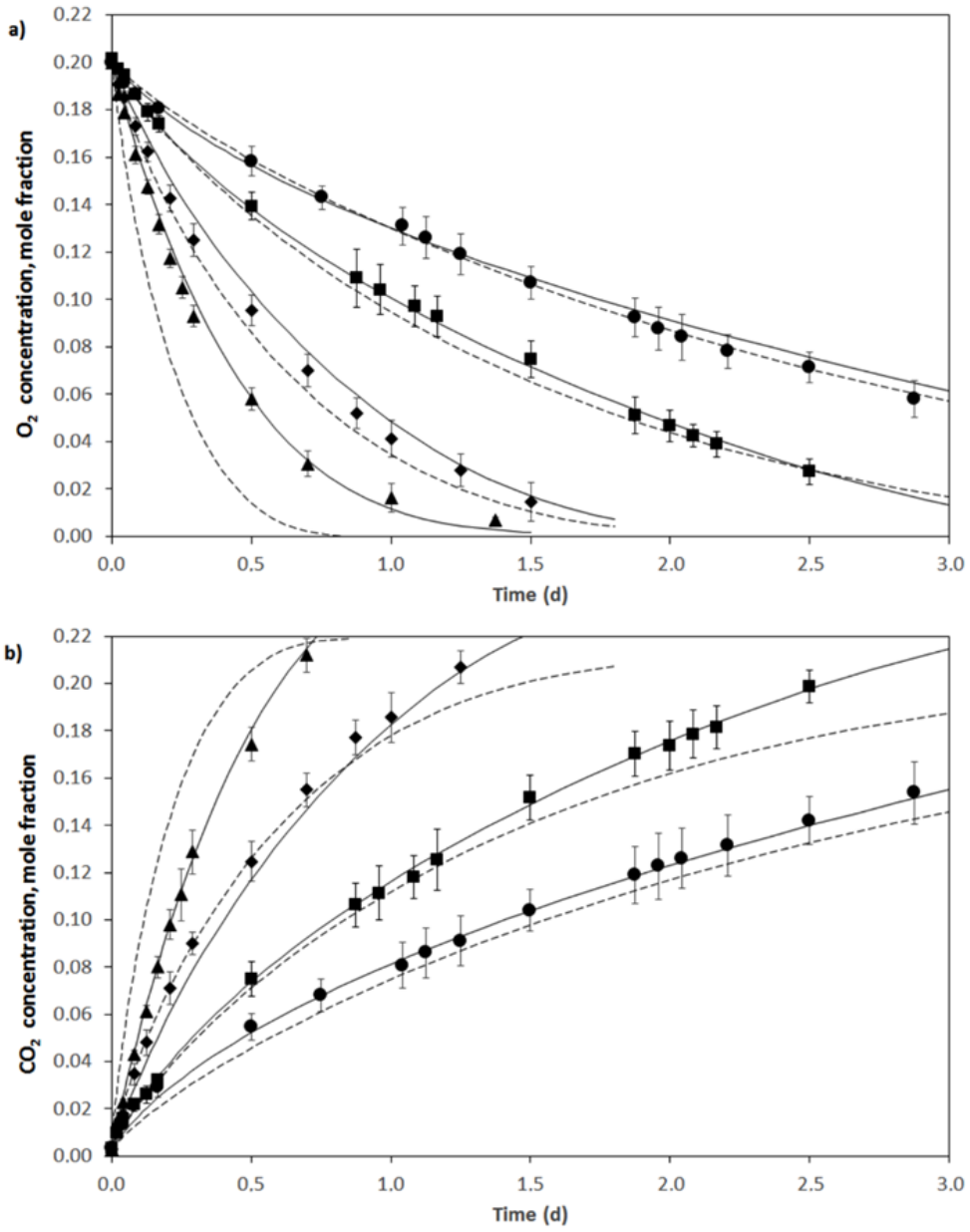

Figure 3.2. O_2 and CO_2 evolution within the experimental container headspace at 6 °C (●), 10 °C (■), 17 °C (♦), 24 °C (▲) and predicted values using the Chemical Kinetics (---) and Michelis-Menten Uncompetitive (—) equations for feijoa fruits. Bars represent SD.

Apparent reaction orders *a* and *b* in the CK equation were found to be independent of the test temperature (Table 3.1). Reaction orders are not integers indicating the complexity in the reaction mechanism of the respiration process. The negative values in the reaction order *b* in both O_2 consumption and CO_2 rates is marking the inhibitory effect of CO_2 concentration itself. At higher concentrations of CO_2, respiration rates will be lower. This

inhibitory effect by CO_2 is well established considering the good fit obtained with the MMU equation.

After obtaining the parameters of each equation, the predicted evolution in the O_2 consumption and CO_2 production rates as a function of O_2 concentration at the different test temperatures was calculated for both fruits. Predicted r_{O2} and r_{CO2} are shown as lines in Figure 1 while predicted y_{O2} and y_{CO2} are shown also as lines in Figure 3.2 respectively. Both equations adequately represent the respiratory behavior of the fruit according to the coefficients of determination R^2 of each equation (Table 3.1) and considering the fitness between the experimental and predicted data was good.

Table 3.1. Estimated parameters of O_2 consumption and CO_2 production rates for the Michaelis-Menten Uncompetitive (MMU) and Chemical Kinetics (CK) equations

Model	*O_2*	*CO_2*
Michaelis-Menten Uncompetitive		
r_{max} (cm^3 kg^{-1} d^{-1})		
$r_{max\text{-}ref}$ (cm^3 kg^{-1} d^{-1})	$9.60 \pm 0.42 \times 10^{15}$	$3.59 \pm 0.24 \times 10^{14}$
E_a (kJ mol^{-1})	68.51 ± 3.12	60.43 ± 4.09
K_m		
$K_{m\text{-}ref}$	$7.09 \pm 0.33 \times 10^{10}$	$2.99 \pm 0.20 \times 10^{7}$
E_a (kJ mol^{-1})	65.07 ± 3.00	46.76 ± 3.16
K_{mu}		
$K_{mu\text{-}ref}$	$5.27 \pm 0.24 \times 10^{11}$	$7.60 \pm 0.51 \times 10^{14}$
E_a (kJ mol^{-1})	70.92 ± 3.24	88.15 ± 5.96
R^2	0.977	0.974
Chemical Kinetics Equations		
a	0.71 ± 0.04	0.74 ± 0.05
b	-0.20 ± 0.01	-0.22 ± 0.02
k (cm^3 kg^{-1} d^{-1})		
k_{ref} (cm^3 kg^{-1} d^{-1})	$1.66 \pm 0.08 \times 10^{21}$	$9.54 \pm 0.68 \times 10^{21}$
E_a (kJ mol^{-1})	97.57 ± 4.79	101.63 ± 7.28
R^2	0.927	0.923

r_{max}: maximum respiration rate (O_2 consumption or CO_2 production). $r_{max\text{-}ref}$: pre-exponential factor, maximum rate (at infinite T). K_m: Michaelis constant. $K_{m\text{-}ref}$: pre-exponential factor, Michaelis constant. K_{mu}: Inhibition constant by CO_2. $K_{mu\text{-}ref}$: pre-exponential factor, inhibition constant. *a*, *b*: apparent reaction orders. k: rate coefficient. k_{ref}: pre-exponential factor, rate coefficient. E_a: apparent activation energies. R^2: coefficient of determination.

The MMU equation (R^2 = 0.977 for O_2 and 0.974 for CO_2) gets closer to the experimental data compared with the CK equation (R^2 = 0.917 for O_2 and 0.923 for CO_2), especially at

17 and 24 °C where is clearly shown that the CK equation deviates from the experimental behavior.

With the CK equation, it was possible to describe acceptably the respiratory behavior of the fruits, although the predicted values deviate from the experimental data for the highest temperatures. This is due the temperature influence is only expressed in the k parameter, while in the MMU equation is expressed in three different parameters and confirms the strong influence of the temperature on the respiration. The values predicted by the MMU equation were closer to the experimental data of evolution in the O_2 consumption and CO_2 production rates, and in the gas levels in the packaging headspace as shown in Figures 3.1 and 3.2. In addition, values estimated with the MMU equations do not lose accuracy at higher temperatures. The goodness of fit offered by the MMU equation is consistent with the findings for several products in other works (Bhande, et al., 2008; Heydari, et al., 2010). The above is not surprising considering the enzymatic nature of this process.

At this point, it is worth mentioning that the parameters of respiration obtained from experimental data particular to fruits evaluated. This means, from a cultivar, maturity stage and physiological characteristics defined (in this case, fruits of local cultivars and of physiological maturity as outlined in the Materials and Methods). A more advanced maturity stage, for example, results in higher respiration rates. These variables related to the stored product itself affect the processes of O_2 consumption an CO_2 production (Caleb, et al., 2012; Fonseca, et al., 2002; Mangaraj, et al., 2015). Likewise, they also have an impact on the predictive power of the developed model when it is desired to describe the behavior of another set of fruits with different characteristics. In the Michaelis-Menten kinetics, the effect of these variables will be represented in the pre-exponential factors of the respiration parameters and for samples with a different maturity or ripening stage, or with changes in their structure, for example, these pre-exponential factors will variate compared with the estimated factors for the fruits initially evaluated. For this reason, it is necessary to take into account these considerations in the application of the respiration equations to predict the produce behavior in the MAP system.

3.3.2 Validation in MAP

All gas transfer parameters through the packages used in the MAP experiment are found in Table 3.2. The permeability coefficients of the two packaging materials to O_2 and CO_2 were estimated according to the procedure explained in Chapter 2. Gas exchange through the perforation made in each package was calculated in Eq. 2.7 taking a correction factor

ε equal to 0.5 times the diameter of the perforation (Castellanos, et al., 2016; Chung, et al., 2003), and obtaining the respective diffusion coefficients of O_2 and CO_2 in air at 12 °C from data reported in (Xanthopoulos, et al., 2012).

Table 3.2. Parameters for calculating the gas exchange in the packages for the validation in MAP to 12 °C

Parameter	*O_2*	*CO_2*
Film permeability coefficients		
Q_i/PP (cm^3 mm m^{-2} d^{-1} atm^{-1})	55.3	253.2
Q_i/LDPE (cm^3 mm m^{-2} d^{-1} atm^{-1})	124.7	977.6
Parameters of permeation in the perforation		
D_i/air (cm^2 d^{-1})	16364	12081
ε = 0.5d (mm)	0.14	
$A_h = \pi d^2/4$ (cm^2)	6.16×10^{-4}	

Q_i/PP, Q_i/LDPE: Polypropylene and polyethylene permeability coefficients taken from Castellanos et al. (2016). D_i/air: gas diffusion coefficient in air, adapted from Xanthopoulos, et al. (2012). d: perforation diameter. ε: term of correction. A_h: perforation area.

In all packages, O_2 concentration decreased and CO_2 concentration increased up to constant levels in the packaging headspace as shown in Figure 3.3. Equilibrium O_2 and CO_2 levels were reached approximately one and a half days after of beging the storage. The reached equilibrium O_2 and CO_2 concentrations were lower for LDPE bags compared with PP bags given the greater permeability of the former to each gas (Table 3.2). With the MMU respiration equations obtained and chosen above, and with the gas exchange parameters in the packaging system, the differential equations 2.10-2.14 were numerically solved. From this, predicted gas concentrations were calculated for the MAP system to test conditions.

As can be seen in Figure 3.3 the gas evolution over time was well described by the integrated model. The predicted data suggest an increase and then a slight decrease in CO_2 concentration before reaching equilibrium levels inside the LDPE bags, which do not occurs in the PP bags. For O_2, a predicted decrease in the concentration occurs and then constant levels are reached in the same way that experimental behavior. The predicted equilibrium values were similar to those obtained experimental data as can be seen in Table

3.3. The differences between experimental and predicted data are between 0.014-0.017 for O_2 and 0.001-0.008 for CO_2.

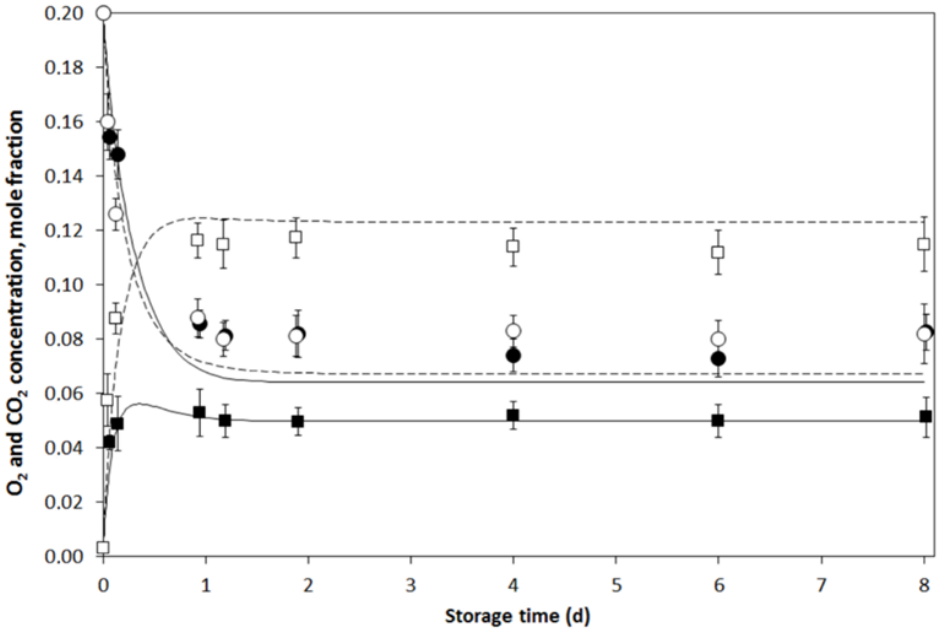

Figure 3.3. Evolution in the headspace gas concentration for feijoa fruits packed in PP (O_2 ○; CO_2 □) and LDPE (O_2 ●; CO_2 ■) bags with one perforation x 280 µm at 12 °C and predicted values by the model (PP ---; LDPE —). Bars represent SD.

Table 3.3. Experimental and predicted equilibrium concentrations of O_2, CO_2 and C_2H_4 for the validation in MAP to 12°C

Packaging film	$y_{O2\ eq\text{-}exp}$	$y_{O2\ eq\text{-}pre}$	R^2	$y_{CO2\ eq\text{-}exp}$	$y_{CO2\ eq\text{-}pre}$	R^2
PP	0.082 ± 0.011	0.068	0.905	0.115 ± 0.010	0.123	0.902
LDPE	0.083 ± 0.007	0.064	0.906	0.051 ± 0.007	0.050	0.970

PP: cast polypropylene bags. LDPE: low-density polyethylene bags. R^2: coefficient of determination of the model in each case.

The coefficients of determination of the model were above 0.9 for all cases highlighting a good degree of fit with respect to the experimental behavior. Overall, with the integrated model, using the MMU equation for respiration and gas permeation parameters through the packages and perforations, the gas evolution in the MAP system for feijoa fruits was properly described according to the information in Figure 3.3 and Table 3.3.

The most important application of the developed model for the evaluated fruits is to setting a specific concentration in the headspace of the MAP system. In designing the MAP system, it is wanted to find the most favorable conditions for the produce preservation. In other words, steady and favorable concentrations of gases in the package headspace and that these equilibrium concentrations to be achieved in the shortest time possible (Castellanos, et al., 2016). From the developed MAP model for feijoa fruits, the permeability parameters required to achieve a defined equilibrium concentration of O_2 and CO_2 can be defined using the differential balance equations (Eqs. 2.10-2.14) and considering that in the period of equilibrium, the change of each gas over time will be zero. The time required to reach the equilibrium concentration depends on the difference between the target concentration and the initial concentration of gas in the MAP system. The less the difference between these concentrations, the equilibrium time will be lower in turn. Once the parameters of respiration are known, the MAP system can be manipulated to balance these processes and achieve the target gas concentration that is more favorable for the fruit. This manipulation of the system is done by altering its capacity to transfer gases according with the growers and dealers possibilities. First, the choice of a packing material to increase or decrease the permeability coefficients. If the packaging material has been defined, it is then possible alter the size of the package and thus increase its surface area and the packaging headspace. If the package size is already defined, then perforations can be made to increase the transfer capacity and achieve the required level of gas.

3.4 Conclusions

The Michaelis-Menten kinetics equation with CO_2 uncompetitive inhibition adequately describes the respiration process for feijoa fruits obtaining good fit between the predicted and experimental O_2 and CO_2 evolution compared to the chemical kinetics equations. The respiration and parameters were properly correlated with storage temperature using Arrhenius equations.

With the developed equations of O_2 consumption and CO_2 production, an integrated model to describe the evolution of O_2 and CO_2 concentrations in a MAP system was successfully established and validated. In the MAP model, analytical expressions for calculating gas transfer through the packaging film and the perforations were properly used.

3.5 References

Bhande, S.D., Ravindra, M.R. & Goswami, T.K. 2008. Respiration rate of banana fruit under aerobic conditions at different storage temperatures. *Journal of Food Engineering*, 87(1): 116-123.

Bontempo, P., Mita, L., Miceli, M., Doto, A. & Nebbioso, A. 2007. Feijoa sellowiana derived natural Flavone exerts anti-cancer action displaying HDAC inhibitory activities. *The International Journal of Biochemistry & Cell Biology*, 39: 1902-1914.

Caleb, O.J., Mahajan, P.V., Opara, U.L. & Witthuhn, C., 2012. Modelling the respiration rates of pomegranate fruit and arils. *Postharvest Biology and Technology*, 64: 49-54.

Castellanos, D.A., Cerisuelo, J.P., Hernández-Muñoz, P., Herrera, A.O. & Gavara, R. 2016. Modelling the evolution of O_2 and CO_2 concentrations in MAP of a fresh product: application to tomato. *Journal of Food Engineering*, 168: 84-95.

Chen, J., Hu, Y., Wang, J., Yao, Y. & Hu, H. (2016), Respiration Rate Measurement and Chemical Kinetic Modelling for Mung Bean Sprouts. *Journal of Food Process Engineering*. Doi:10.1111/jfpe.12346

Chung, D., Papadakis, S.E. & Yam, K.L. 2003. Simple models for evaluating effects of smalls leaks on the gas barrier properties of food packages. *Packaging Technology and Science*, 16: 77-86.

Dos Santos, K.L., Peroni, N., Guries, R.P. & Nodari, R.O. 2009. Traditional knowledge and management of feijoa (*Acca sellowiana*) in Southern Brazil. *Economic Botany*, 63(2): 204-214.

East, A.R., Trejo-Araya, X.I., Hertog, M.L.A.T.M., Nicholson, S.E. & Mawson, A.J. 2009. The effect of controlled atmospheres on respiration and rate of quality change in 'Unique' feijoa fruit. *Postharvest Biology and Technology*, 53: 66-71.

Fonseca, S.C., Oliveira, F.A.O. & Brecht, J.K. 2002. Modelling respiration rate of fresh fruits and vegetables for modified atmosphere packages: a review. *Journal of Food Engineering*, 52: 99 -119.

Heydari, A., Shayesteh, K., Eghbalifam, N., Bordbar, H. & Falahatpisheh, S. 2010. Studies on the respiration rate of banana fruit based on enzyme kinetics. *International Journal of Agriculture & Biology*, 12(1): 145-149.

Mahajan, P. V., Oliveira, F. A. R., Montanez, J. C. & Frias, J., 2007. Development of user-friendly software for design of modified atmosphere packaging for fresh and fresh-cut produce. *Innovative Food Science and Emerging Technologies*, 8: 84-92.

Mangaraj, S. & Goswami, T.K., 2011. Modeling of Respiration Rate of Litchi Fruit under Aerobic Conditions. *Food and Bioprocess Technology*, 4: 272-281.

Mangaraj, S., Goswami, T.K. & Mahajan, P.V. 2015. Development and validation of a comprehensive model for map of fruits based on enzyme kinetics theory and arrhenius relation. *Journal of Food Science and Technology*, 52: 4286-4295.

Mendoza, R., Castellanos, D.A., García, J.C., Vargas, J.C. & Herrera, A.O. 2016. Ethylene production, respiration and gas exchange modelling in modified atmosphere packaging for banana fruits. *International Journal of Food Science and Technology*, 51(3), pp. 777-788.

Parra, A. & Fischer, G. 2014. Maduración y comportamiento poscosecha de la feijoa (*Acca sellowiana* (O. Berg) Burret). Una revisión. *Revista Colombiana de Ciencias Hortícolas*, 7(1): 98-110.

Sanders, M.G. & De Wild, H.P.J. 2003. The relation between in vivo ethylene production and oxygen partial pressure. *Postharvest Biology and Technology*, 30: 143-151.

Sandhya, K.V.K. 2010. Modified atmosphere packaging of fresh produce: current status and future needs. *LWT - Food Science and Technology*, 43: 381-392.

Velho, A.C., Do Amarante, C. V. T., Argenta, L.C. & Steffenls, C. 2011. Influência da temperatura de armazenamento na qualidade pós-colheita de goiabas serranas. *Revista Brasileira de Fruticultura*, 33(1): 14-20.

Wang, Z.W., Duan, H.W. & Hu, C.Y., 2009. Modelling the respiration rate of guava (*Psidium guajava* L.) fruit using enzyme kinetics, chemical kinetics and artificial neural network. *European Food Research and Technology*, 229: 495-503.

Xanthopoulos, G., Koronaki, E. & Boudouvis, A. 2012. Mass transport analysis in perforation-mediated modified atmosphere packaging of strawberries. *Journal of Food Engineering*, 111: 326-335.

Chapter 4. Representing water vapor transport, transpiration and weight loss in a perforated MAP system for feijoa fruits[4]

Abstract

In modified atmosphere packaging (MAP), the transpiration of the fresh product and the exchange of water through the packages are often not properly considered. In Chapters 2 and 3, a mathematical model to describe the evolution of O_2 and CO_2 concentration in a perforated MAP system was presented. In this chapter, the developed model is extended to describe the evolution of water vapor in the packaging headspace, the weight loss of the product and the condensation of water in the MAP system. Transpiration was considered as the sum of water evaporated due to the gain of energy by the product resulting from its respiration process and the difference in water activities between the product and the surrounding atmosphere. Respiration was represented using Michaelis-Menten enzyme kinetics. The gas transfer through the packaging and the perforations was described with Fick equations. The temperature influence on these processes was considered to follow the Arrhenius' law. To experimentally determine the model parameters, feijoa fruits were stored under different storage conditions: packaging, relative humidity and temperature. The completed model was subsequently validated in a MAP test by packaging fruits in perforated polypropylene (PP) and polylactic acid (PLA) bags for 13 days at 12 °C and 75% RH. Inside the PP bags, a saturated atmosphere (100% RH) was reached and 1.48% of the initial weight in the packed fruit was lost by day 7, while in the PLA bags, an equilibrium RH of 83% and a fruit weight loss of 3.29% were measured. The prediction capacity of the model was satisfactory, with coefficients of determination (R^2) between 0.88-0.99 for the different tests.

Keywords: transpiration, modelling, weight loss, water vapor exchange, respiratory heat

[4] This chapter (with minor modifications) was published as:
Castellanos, D.A., Herrera D.R. & Herrera A.O. 2016. Modelling water vapour transport, transpiration and weight loss in a perforated modified atmosphere packaging for feijoa fruits, *Biosystems Engineering*, 151: 218-230. http://dx.doi.org/10.1016/j.biosystemseng.2016.08.015

Nomenclature

a_w	water activity
A	effective exchange area of the packaging film (m^2)
A_h	cross sectional area of the perforations (cm^2)
D	diameter of the perforation (cm)
d_e	effective diameter of the perforations (cm)
D_i	diffusion coefficient of gas *i* in air ($cm^2\ d^{-1}$)
E_a	activation energy (kJ mol^{-1})
K	mass transfer coefficient (kg $kg^{-1}\ d^{-1}$)
K_{mO2}, K_{mCO2}	dissociation constants of the enzyme-substrate complex
K_{muCO2}, $K_{mu'CO2}$	constants of uncompetitive inhibition for consumption of O_2 and generation of CO_2, respectively
K_{Tri}	transmission rate of gas *i* through the perforations ($cm^3\ d^{-1}$)
L	film thickness (mm)
M_{H2O}	Molar mass of water (0.018 kg mol^{-1})
MMU	Michaelis-Menten Kinetics with uncompetitive inhibition
P	pressure (atm)
p_i	partial pressure of gas *i* inside the package (atm)
p_{iout}	partial pressure of gas *i* outside the package (atm)
p_p	water partial pressure in the produce (atm)
P_{sat}	saturation water vapor pressure at T (atm)
Q	effective respiration heat used for the moisture transfer (kJ $kg^{-1}\ d^{-1}$)
Q_i	film permeability coefficient for gas *i* ($cm^3\ mm\ m^2\ d^{-1}\ atm^{-1}$)
R	gas constant (0.008314 kJ $mol^{-1}\ K^{-1}$ or 82.057 atm $cm^3\ mol^{-1}\ K^{-1}$)
RH	relative humidity
r_{H2O}	transpiration rate (kg $kg^{-1}\ d^{-1}$)
r_{O2}, r_{CO2}	consumption of O_2 and generation of CO_2 rates ($cm^3\ kg^{-1}\ d^{-1}$)
r_{O2max}, r_{CO2max}	maximum consumption of O_2 and generation of CO_2 rates ($cm^3\ kg^{-1}\ d^{-1}$)
T	packaging/storage time (d)
T	temperature (°C, K)
V	free package volume - headspace (cm^3)
V_{cnd}	condensate water inside the package (cm^3)
W	fruit weight (kg)
Δw_{sg}	Weight change in the silica gel
y_{O2}, y_{CO2}, y_{H2O}, y_{N2}	O_2, CO_2, water vapor and N_2 concentrations inside the package
y_{O2out}, y_{CO2out}, y_{H2Oout}, y_{N2out}	O_2, CO_2, water vapor and N_2 concentrations outside the package

$y_{O2\ eq}$, $y_{CO2\ eq}$, $y_{H2O\ eq}$, $y_{N2\ eq}$	equilibrium O_2, CO_2, water vapor and N_2 concentrations inside the package
α	fraction of energy used from the respiration process
ε	Correction term for gas transmission through perforations (mm)
λ	latent heat of water evaporation (kJ kg^{-1})
ρ_{H2O}	liquid water density (kg cm^{-3})

4.1 Introduction

Modified atmosphere packaging (MAP) is a storage technology that has been widely used to extend the shelf-life of fruits, vegetables and other foods. In the case of fresh produce, it is required to reduce the rate of their metabolic processes and microbial counts by decreasing the O_2 concentration and maintaining moderate concentrations of CO_2 in the packaging headspace. This is achieved by balancing the produce respiration and the gas transfer through the packaging walls to favorable levels of O_2 and CO_2. A wide range of mathematical models to describe the evolution of these gases in MAPs has been developed (Castellanos, et al., 2016a; Del-Valle, et al., 2009; Kwon, et al., 2013; Mahajan, et al., 2008; Mangaraj, et al., 2014). These models have been used to successfully design packaging systems, allowing for the selection of packaging material and its configuration (surface area, thickness, perforations), which are necessary to achieve a favorable atmosphere for the packed product. However, the effect of the transport of water from the fresh produce to the surrounding atmosphere has not been widely considered. In the MAP system, fresh produce continually loses water through transpiration. The water is lost as vapor that goes to the packaging headspace and then the external atmosphere by passing through the packaging walls. If the permeability of the packaging material to water vapor is low, as with many of the most commonly used films, the packaging headspace will be saturated and part of the transpirated water will be condensed. In addition, if there are fluctuations in the storage temperature, the saturation pressure in turn will change and there will be condensation. Condensed water inside the package can lead to the growth of microorganisms and product deterioration, ruining the efforts made in the design of the modified atmosphere. On the other hand, if the permeability of the package is very high and there is a considerable difference between the water activity (a_w) of the product and the relative humidity of the external atmosphere, there will be a concentration differential that will lead to continuing loss of water from the product and, hence, undesirable weight loss.
Considering the above, an effective MAP system must consider water transport and its concentration (relative humidity) in the packaging headspace so that there is no

condensation inside the package, but also so that the flow of water lost from the product to the external atmosphere is minimal.

Several models have been developed to represent the evolution in the relative humidity and water exchange in MAP systems as linked to changing levels of O_2 and CO_2 (Guevara-Arauza, et al., 2006; Lu, et al., 2013; Rennie & Tavoularis, 2009; Sousa-Gallagher, et al., 2013; Techavises & Hikida, 2008). In these models, two major processes are considered: water generation by the packed product (transpiration) and transfer of water vapor through the package walls. As for transpiration, some authors (Lu, et al., 2013; Song, et al., 2002) believe that this process is a consequence of the energy transferred to and from the product in the form of heat due to the respiration process and to the temperature difference between the fruit itself and the surroundings (headspace, packaging system and external atmosphere). Other studies (Mahajan, et al., 2008; Montanaro, et al., 2012; Sousa-Gallagher, et al., 2013) have also considered the water loss in the product as a result of the difference in the vapor pressure (VPD) between the product surface and the surrounding atmosphere, in this case the packaging headspace. Considering the above, it can be suggested that the transpiration and water loss in the produce is a consequence of both, the heat transferred to and from the produce and the vapor pressure difference between the produce and the surrounding atmosphere.

When the vapor pressure in the atmosphere is less than the vapor pressure in the product, both processes will contribute to transpiration. When the vapor pressures become equal, transpiration only will be seen as a consequence of the heat exchange to and from the product. Likewise, if the vapor pressure in the atmosphere (in the packaging headspace) becomes equal to the saturation pressure at the storage temperature, the water lost by the product as vapor will be condensed inside the package.

This heat will be transferred to and from the product mainly by the temperature difference between it and the surrounding atmosphere in the process of cooling, the evaporation and condensation of water in the system and the respiration process where a number of substrates are oxidized to generate energy (Lu, et al., 2013). In case that the vapor pressure in the atmosphere (in the packaging headspace) becomes equal to the saturation pressure at the storage temperature, the water lost by the product as vapour will be condensed inside the package. On the other hand, as a result of transpiration and the water loss in this process, the weight of the packaged product will be decreasing over the storage time which can bring undesirable effects on its quality. This weight loss can be quite significant when the water activities between the product and the surrounding atmosphere are large or when

the storage time is long and for this reason, it should be considered in the modelling of the MAP system.

In this chapter, the MAP model developed in Chapters 2 and 3 is extended to include the evolution of water vapor (relative humidity) in the packaging headspace, weight loss of the packed produce and water condensation inside a flexible MAP system with perforations. In order to estimate the required model parameters, the respiration and transpiration rates of feijoa, gas permeability coefficients for polypropylene (PP) and polylactic acid (PLA) and gas transmission rates through perforations at several temperatures were adjusted to suitable equations. Thereafter, a validation experiment was conducted by packaging feijoa fruits in PP and PLA bags and comparing the results with those predicted by the model.

4.2 Materials and Methods

4.2.1 Fresh fruits

Feijoa fruits (cv. Quimba) used in the tests were obtained from commercial growers located in Tibasosa, in the department of Boyacá, Colombia in June 2015. These were harvested at the physiological maturity stage, 20 weeks after flowering (Parra & Fischer, 2014), and later transported to the Postharvest Laboratory, Faculty of Agricultural Sciences, Universidad Nacional de Colombia (Bogotá, Colombia) in the following days. After discarding those with evidence of damage, the fruits with homogeneous characteristics were selected and stored at 8 ºC. In the laboratory, the fruits were cleaned with fresh water, left to dry at room temperature and then arranged for the various storage tests

4.2.2 Packages

For the MAP tests, cast polypropylene bags (PP) with moderate permeability to water vapor and polylactic acid (PLA) with a biodegradable film with high permeability to water vapor were used to pack the fruits. The PP bags (Rediplast, Bogotá, Colombia) had a thickness of 0.025 ± 0.002 mm and the PLA bags (Q4 Packaging Systems S.L., Ribaroja - Valencia, Spain) had a thickness of 0.025 ± 0.001 mm. The thickness of the films was determined as the average of ten measurements with a Mitutoyo (Kawasaki, Japan) gauge. In the MAP tests, 25 x 20 cm bags (1000 cm^2) were used.

4.2.3 Packages permeability

The permeability coefficients of the PP and PLA packaging to O_2 and CO_2 were determined previously (Castellanos, et al., 2016b) with steady-state methods. A Mocon® Oxtran 2/21 (MOCON, Inc., Minneapolis, MN, USA) permeation instrument was used for O_2 and a temperature-controlled chamber with a parallel flow permeation cell connected to a gas chromatograph was used for CO_2. The N_2 permeability coefficient was estimated from information provided by the respective manufacturers and from other studies (Auras & Almenar, 2010; Hasbullah, et al., 2000; Techavises & Hikida, 2008). The dependence of permeability coefficients with respect to temperature was described using an Arrhenius equation (Eq. 4.2).

To determine the PP and PLA permeability coefficients for water vapor, an experiment was conducted at a steady state at 5, 14, 28 and 37 °C with the same principle proposed by Techavides & Hikida (2008). In this case, 7.00 ± 0.03 g of dry silica gel were placed in cylindrical metal capsules (2 cm height and 3 cm diameter) with an open face. A piece of film (PP or PLA) was placed on the open face, attached to the cylindrical capsule with a rubber ring and another metallic ring secured with screws. The capsules were then placed in a chamber that was kept at 100% RH throughout the experiment for each of the four temperatures. The capsules were weighed every 12 hours, measuring the water gain after the steady state was reached. The permeability coefficient of the film to water vapor was calculated as follows:

$$Q_{H_2O} = \frac{\Delta w_{sg}}{\Delta t} \frac{L}{A P_{sat}} \frac{RT}{M_{H_2O} P} \quad (4.1)$$

Where $\Delta w_{sg}/\Delta t$ is the weight gain of the silica gel over time in the steady-state region, P_{sat} is the saturation pressure of water at the test temperature and A is the surface area of the film. It was assumed that the relative humidity inside the capsule was zero, whereas the water vapor entering the capsule through the film was immediately absorbed by the silica gel.

The temperature influence was represented by replacing the Q_{H2O} data at each temperature in the linearized form of an Arrhenius-type equation (Eq. 4.2) and estimating the activation energy E_a and the reference permeability coefficient Q_{H2Oref} by linear regression. The reference temperature T_{ref} was 23 °C.

$$Q_{H_2O} = Q_{H_2Oref} e^{\frac{-E_a}{R}\left(\frac{1}{T}-\frac{1}{T_{ref}}\right)} \quad (4.2)$$

4.2.4 Gas transmission through perforations in the packaging

To determine the gas transfer through the perforation made in each bag, it was assumed that this process can be described by Fick's diffusion equation with a correction term (ε in Eq. 3) due to the resistance to diffusion at the perforation as described in Chapter 2 (Castellanos, et al., 2016a; Chung, et al., 2003). Thus, the gas *i* transmission rate through the perforation (K_{Tri}) can be defined as:

$$K_{TRi} = \frac{D_i A_h}{L+\varepsilon} \quad (2.7)$$

The correction factor ε can be between 0.5 and 1.1 times the effective diameter (d_e) of the perforations. The transfer rate of each gas through the perforation depends on the cross-sectional area and length (film thickness) of the perforation itself, the diffusivity of the gas in the air (gas mixture in the area to which the gas diffuses) and the concentration difference between the inside and the outside of the package.

For this study, the transmission rates for O_2, CO_2, N_2 and water vapor were estimated using the diffusivity of each gas in air at the test temperature and considering $\varepsilon = 0.5d_e$ and $d_e = N^{1/2}d$, where N is the number of perforations and d is the perforation diameter (Castellanos, et al., 2016a). The dependence of the diffusion coefficients with respect to temperature was described in the same way as the permeability coefficients using Arrhenius' law (Eq. 4.2).

4.2.5 Fruit respiration

The respiration rate of the feijoa fruits was determined in as mentioned in Chapter 3 from experimental data (Castellanos, et al., 2016b). The experimental respiration data were fitted to Michaelis-Menten enzyme kinetics with uncompetitive inhibition by CO_2 as previously described in Chapters 1 and 2 (Eqs. 1.8 and 2.1) in order to represent the O_2 consumption (r_{O2}) and the CO_2 production (r_{CO2}).

$$r_{O_2} = \frac{r_{O_{2max}} y_{O_2}}{K_{m_{O_2}} + y_{O_2}\left(1+\frac{y_{CO_2}}{K_{mu_{CO_2}}}\right)} \quad (1.8)$$

$$r_{CO_2} = \frac{r_{CO_{2max}} y_{O_2}}{K_{m_{CO_2}} + y_{O_2}\left(1 + \frac{y_{CO_2}}{K_{mu'_{CO_2}}}\right)} \quad (2.1)$$

It was considered that the influence of temperature on the respiration process could be described using the Arrhenius' Law (Eq. 4.3). The temperature dependence was determined by replacing the parameters of each equation in the linearized form of Eq. 4.3, calculating the pre-exponential factors and the activation energies for each parameter by linear regression.

$$P_m = P_{m\theta} e^{-Ea/RT} \quad (4.3)$$

P_m denotes each of the parameters of the MMU equation, $P_{m\theta}$ is the pre-exponential factor, E_a is the activation energy, R is the universal gas constant, and T is the storage temperature.

4.2.6 Determination of the fruit transpiration in the MAP

To estimate the transpiration rate in the fruits, the experimental weight loss under different storage conditions was measured. The transpiration rate in each storage condition was calculated with the following equation:

$$r_{H_2O}(t) = \frac{(W_{t-1} - W_{t+1})}{(W_t)\Delta t} \quad (4.4)$$

Where $r_{H2O}(t)$ is the transpiration rate at time t, Δt is the time elapsing between two consecutive measurements and W_t is the average fruit weight for Δt.

The feijoa fruits were stored in three packaging groups: 1) exposed without packaging, 2) packed in PP bags with one 0.225 mm macro-perforation and 3) packed in PP bags with two 0.225 mm macro-perforations. Each group was composed of two fruits with a total weight of 140 ± 10 g and the bags were filled with atmospheric air (P = 0.74 atm, 74.67 kPa). The bags had a total internal surface area of 1000 cm^2 and an effective transfer-area of 800 cm^2. A 200 cm^2 polystyrene support with a volume of 200 cm^3 was placed in each bag to hold the fruit in place and ease sample handling. A simple paper towel was used to collect the condensed water lost by the packed fruits after the storage time by carefully drying the inner walls of the packaging and the fruit surface before making the

measurement of fruit weight. In the packages, the macro-perforations were made to obtain two different internal atmospheres with equilibrium concentrations of O_2 and CO_2 (ensuring the level of O_2 was not close to 0-1% to prevent anaerobic fermentation), and also to have different transfer rates of water vapour in each MAP system to compare the evolution in transpiration and weight loss in each case.

After making groups and placing the fruits in the perforated bags, each group was stored in Sanyo-Panasonic MLR-352H-PE cabinets (SANYO Electric Co., Ltd, Osaka, Japan) with a controlled temperature and relative humidity, at 6, 12 and 18 ± 0.3 °C and 50 and 70±1 % RH for a period of 7 days (see table 4.5). For the packed fruits, the O_2 and CO_2 levels in the headspace were measured in the packages by daily taking a gas sample of 5 cm^3 through a rubber seal on the top of the container, which was then analyzed with an electronic analyzer, Oxybaby® 6i (Witt-Gasetechnik GmbH & Co. KG, Witten, Germany), previously calibrated with Gas Chromatography. Five cm^3 of air were introduced into the container to replace the withdrawn sample. For the fruits left without package, the O_2 and CO_2 concentrations were considered to be as those of atmospheric air. Daily weight measurements were made for the fruits left exposed without a bag using the same samples along the storage time, while for the fruits packed in perforated bags, weight measurements were taken on odd days (1, 3, 5 and 7) using different bags for each measurement. Furthermore, the paper towel was weighed after the storage time to record the condensate accumulated inside the package (V_{cnd}).

All measurements were performed in triplicate, reporting the average value.

4.2.7 Mathematical Approach

As presented in Chapter 1, several authors have described transpiration as a function of heat exchange between the stored produce and its surroundings (Kang & Lee, 1998; Lu, et al., 2013; Song, et al., 2002). The transpiration rate can be deduced from the energy balance in the packaging system containing the product (Kang & Lee, 1998):

$$qW + hA_p(T - T_p) = m_{H_2O,gen}\lambda + c_p W\frac{dT_p}{dt} \quad (1.17)$$

Where m_{H2Oevp} is the rate of water evaporated in the packed produce, q is the respiratory heat, W is the produce weight, h is the convective heat transfer coefficient, c_p is the specific

heat of the product, λ is the latent heat of moisture evaporation, A_p is the surface area of the produce, T is the headspace temperature and T_p is the produce temperature. The heat transferred through natural convection from ambient air and the heat generated from respiration inside the product both increase the temperature of a fruit, as sensible heat, and are converted to the latent heat of moisture evaporation in transpiration. This water loss in the produce was expressed as:

$$m_{H_2O,gen} = \frac{qW + hA_p(T_{at} - T_p) - c_p W\frac{dT_p}{dt}}{\lambda} \quad (1.18)$$

Assuming the produce is at a uniform temperature and it is in thermal equilibrium with the packaging headspace (Lu, et al., 2013), Eq. 1.18 can be simplified, resulting in:

$$m_{H_2O,gen} = \frac{qW}{\lambda} \quad (4.5)$$

The transpiration rate can be defined as the water lost per weight of product per unit time. For this, Eq. 10 is appropriately manipulated by dividing the weight on both sides and the transpiration rate is then:

$$r_{H_2O} = \frac{m_{H_2O,gen}}{W} \quad (1.21)$$

And replacing from Eq. 4.5:

$$r_{H_2O} = \frac{q}{\lambda} \quad (4.6)$$

Where r_{H2O} is defined as the kg of water lost per kg of fruit per day (kg kg^{-1} d^{-1}). The above can occur if the temperature control in the storage system is efficient with negligible temperature fluctuations, as in modern incubators and plant grow cabinets. Respiratory heat is expressed as the energy released by the complete oxidation of one molecule of hexose (Kang & Lee, 1998; Song, et al., 2002):

$$C_6H_{12}O_6(s) + 6O_2 \rightarrow 6CO_2 + 6H_2O + 2816\ (KJ/mol) \quad (4.7)$$

The respiration heat can be estimated from the respiration reaction (Eq. 4.7) and by considering the respiration rate as the average of the O_2 consumption and CO_2 production

rate (Eq. 4.8). The main function of the respiration process is to provide energy for the essential processes in the produce cells. However, this oxidation process is not efficient and a good part of the energy generated is not exploited. The fraction of energy effectively used, called α, is always less than one (Rennie & Tavoularis, 2009; Song, et al., 2002).

$$q = \alpha\left(\frac{2816\ \mathrm{kJ}}{6\ \mathrm{mol}}\right)\left(\frac{r_{O_2}+r_{CO_2}}{2}\right)\left(\frac{P}{RT}\right) \quad (4.8)$$

In Eq. 4.8, q is in kJ kg^{-1} d^{-1} and r_{O2} and r_{CO2} in cm^3 kg^{-1} d^{-1}. The gas constant R was 82.057 atm cm^3 mol^{-1} K^{-1} in this case. The latent heat of moisture evaporation λ in Eq. 4.8 can be obtained as a function of temperature from the equation developed by Brooker (Eq. 1.20; Brooker, 1967), where temperature is in Kelvin.

Other authors have considered transpiration to be the result of the difference between the partial pressures of water between the produce and the surrounding atmosphere. This pressure difference is the driving force that leads to this process. Thus, the transpiration rate can be obtained with the following equation (Becker & Fricke, 2001):

$$r_{H_2O} = k\left(p_p - p_{at}\right) \quad (1.14)$$

Where k is a mass transfer coefficient for this process, p_p is the water pressure in the produce and p_{at} is the water pressure at the headspace. The total mass coefficient is a function of the weight of the product, of the weight – surface area ratio and also of the type of mass transfer in the moisture loss that can be by diffusion or convection. The water concentrations in the produce and in the surrounding atmosphere can be expressed in terms of water activity (Mahajan, et al., 2008; Sousa-Gallagher, et al., 2013):

$$r_{H_2O} = k\left(a_{wp} - a_{wat}\right) \quad (4.9)$$

In Eq. 4.9, a_{wp} is the measured water activity in the produce and a_{wat} is the water activity in the surrounding atmosphere, RH/100. The relative humidity in the atmosphere surrounding the produce is given with:

$$RH\ (\%) = 100\frac{Py_{H2O}}{P_{sat}} \quad (4.10)$$

The mass transfer coefficient k should be considered to be dependent on the temperature and this dependency can be described using Arrhenius' law (similar to Eq. 4.3).

As mentioned above, considering that both processes, water loss in the produce due the gain of energy (by heat transfer) and due the concentration differences, contribute to the transpiration rate, the following equation can be stated, combining Eqs. 4.6 and 4.9:

$$r_{H_2O} = \frac{q}{\lambda} + k(a_{wp} - a_{wat}) \quad (4.11)$$

In Eq. 4.11, the rate of water vapor loss, r_{H2O}, is in kg kg^{-1} d^{-1}, q is in kJ kg^{-1} d^{-1}, λ is in kJ kg^{-1} and k in kg kg^{-1} d^{-1}. When the concentration of water vapor in the atmosphere is greater than the water activity in the produce, it is assumed that the produce does not regain the water, but the terms corresponding to the mass transfer become zero. The respiratory heat (q) should be effectively used for this process, as described in Eq. 4.7.

4.2.8 MAP modelling

In the headspace of the MAP system, the evolution of the O_2, CO_2 and N_2 concentrations with respect to storage time can be described using the system balance equations presented in Chapter 2 (Castellanos, et al., 2016a):

For O_2,

$$V\frac{dy_{O_2}}{dt} = K_{TRO_2}(y_{O_{2}Out} - y_{O_2}) + \frac{APQ_{O_2}}{L}(y_{O_{2}Out} - y_{O_2}) - r_{O_2}W - y_{O_2}\frac{dV}{dt} \quad (2.10)$$

For CO_2,

$$V\frac{dy_{CO_2}}{dt} = K_{TRCO_2}(y_{CO_{2}Out} - y_{CO_2}) + \frac{APQ_{CO_2}}{L}(y_{CO_{2}Out} - y_{CO_2}) + r_{CO_2}W - y_{CO_2}\frac{dV}{dt} \quad (2.11)$$

For N_2,

$$V\frac{dy_{N_2}}{dt} = K_{TRN_2}(y_{N_{2}Out} - y_{N_2}) + \frac{APQ_{N_2}}{L}(y_{N_{2}Out} - y_{N_2}) - y_{N_2}\frac{dV}{dt} \quad (2.12)$$

For the fruits exposed without a package, it was considered that the atmosphere levels of O_2, CO_2 and N_2 remained approximately constant.

As for the evolution of the water vapor, the concentration in the headspace will depend on whether the atmosphere inside the package is saturated or not. That is, when the relative humidity is less than 100 % in the headspace, there will be a change in the water vapor concentration over time; when the relative humidity is 100%, the change in the water vapor concentration in the headspace will be zero and the water emitted by the product will condense.

Then two situations arise:

1) Assuming the atmosphere inside the package is similar to that of the outside air: If $y_{H2O} < P_s/P$ (atmosphere not saturated) and if $RH/100 < a_w$, the change in the level of water vapor with the storage time is as follows:

$$V\frac{dy_{H_2O}}{dt} = K_{TRH_2O}\left(y_{H_2O_{out}} - y_{H_2O}\right) + \frac{APQ_{H_2O}}{L}\left(y_{H_2O_{out}} - y_{H_2O}\right) + r_{H_2O}W\left(\frac{RT}{PM_{H_2O}}\right) - y_{H_2O}\frac{dV}{dt} \quad (4.12)$$

In Eq. 21, r_{H2O} is in kg kg^{-1} d^{-1} and it must be multiplied by the ideal gas equation in order to obtain the water lost in units of volume (cm^3) to be consistent with the other equations. If $RH/100 \geq a_w$, the contribution of the water concentration differential to transpiration is zero and Eq. 4.11 is reduced to Eq. 4.6. The condensed water generated inside the packaging will be zero:

$$\frac{dV_{con}}{dt} = 0 \quad (4.13)$$

Furthermore, considering the sum of the mole fractions of O_2, CO_2, H_2O and N_2 in the headspace atmosphere can be regarded as 1:

$$y_{O_2} + y_{CO_2} + y_{H_2O} + y_{N_2} = 1 \quad (4.14)$$

The headspace volume change over time can be written as:

$$\frac{dV}{dt} = W\left(r_{CO_2} - r_{O_2} + r_{H_2O}\left(\frac{RT}{PM_{H_2O}}\right)\right) + \sum_{i=1}^{4}\left(\left(y_{iOut} - y_i\right)\left(K_{TRi} + \frac{APQ_i}{L}\right)\right) \quad (4.15)$$

Where *i* is O_2, CO_2, N_2 or water vapor.

2) If $y_{H2O} = P_s/P$ (atmosphere saturated), the change in the level of water vapor with the storage time in the headspace is zero (RH = 100%):

$$\frac{dy_{H_2O}}{dt} = 0 \quad (4.16)$$

The generated condensed water is given by:

$$\frac{dV_{con}}{dt} = r_{H_2O} W \left(\frac{1}{\rho_{H_2O}}\right) \quad (4.18)$$

The headspace volume change in this case can be written without considering the contribution of transpiration:

$$\frac{dV}{dt} = W\left(r_{CO_2} - r_{O_2}\right) + \sum_{i=1}^{4}\left((y_{iOut} - y_i)\left(K_{TRi} + \frac{APQ_i}{L}\right)\right) \quad (4.19)$$

Where *i* is again one of O_2, CO_2, N_2 or water vapor.

The water generated by transpiration is the same as Eq. 4.6 and will directly condense and not change the headspace volume inside the packaging. In the equations above, the saturation vapor pressure as a function of temperature can be calculated from an empirical equation as described in (ASABE, 2006). The liquid water density-depending temperature can be expressed as described by Kell (1975) or using another equation of water density as a function of temperature, expressing it in the appropriate units.

The weight change in the packed product over time is:

$$\frac{dW}{dt} = -W r_{H_2O} \quad (4.20)$$

For the model construction and use, it is necessary to consider the following assumptions:

- The produce is in thermal equilibrium with the surroundings.
- All temperature dependent processes can be modelled based on Arrhenius' law.
- Produce respiration and transpiration were not affected by ripening or senescence.
- There was no stratification of gases inside the package.
- The system pressure corresponded to atmospheric pressure.

- The produce did not regain the water lost through transpiration.

The equations for the MAP system were solved numerically using the same calculation routine mentioned in Chapters 2 and 3, which was built in the Matlab software (MathWorks, Inc., Natick, MA, USA) from the 'ode 15s' function, a multi-step implicit method based on numerical differentiation formulas, NDF (Castellanos, et al., 2016a; Castellanos, et al., 2016b). The change in the O_2, CO_2, and water vapor levels in the headspace, the weight loss and the condensated water inside the packages were calculated once the test conditions were defined in the calculation routine. The conditions defined in this case were: concentration of gases and relative humidity in the external atmosphere, atmospheric pressure, fruit weight, type of film, area and thickness of the bag used for packaging and initial gas levels and headspace volume in the package.

Finally, the data for the concentration of gases, fruit weight and condensed water generated in the calculation routine were compared with the experimental measurements in the bags to evaluate the predictive power of the developed model to describe changes in the MAP system. For this, the cumulative weight loss and condensed water inside the packaging system were calculated as follows:

$$\mathrm{CWL(t)\%} = 100\frac{(\mathrm{W_{ini}}-\mathrm{W_t})}{\mathrm{W_{ini}}} \quad (4.21)$$

$$\mathrm{CV_{cnd}(t)\%} = 100\frac{\mathrm{V_{cndt}}\rho_{\mathrm{H_2O}}}{\mathrm{W_{ini}}} \quad (4.22)$$

Where CWL(t)% is the percentage of weight loss in the packed product and $CV_{cnd}(t)\%$ is the percentage of condensed water accumulated within the packaging relative to the initial weight of the fruit at time t. W_{ini} is the initial product weight, W_t is the product weight at time t and V_{cndt} is the volume of condensate accumulated at time t.

4.2.9 Validation test

After obtaining the parameters for calculating the transpiration rate as a function of the storage temperature and for the numerical solution of the MAP model, a validation test for packing feijoa fruits (140 ± 20 g) in PP and PLA bags with the characteristics described above was performed. A perforation of 0.225 mm was made in each bag. Packed fruits were stored at 12 °C and 75 % RH for a period of 13 days, and the O_2 and CO_2 concentrations in the headspace, fruit weight and condensation inside the package were

measured in the storage time. In the PLA bags, a digital humidity/temperature meter CC-4096 Traceable® (Control Company, Friendswood, TX, USA) was introduced to record the relative humidity during the storage period. In the PP bags, 100 % RH was reached inside the bags (All measurements were made in triplicate). The results were compared with those predicted by the developed model in order to assess its predictive power.

4.3 Results and discussion

4.3.1 Gas permeation through the packages

The permeability parameters for the PP and PLA bags to O_2, CO_2 and N_2 are shown in Table 4.1. As mentioned above, PP bags were used to determine the transpiration rate of the fruits and in the validation test for the MAP, while PLA bags were only used in the validation test. The reference permeability coefficients and activation energies shown in Table 4.2 and required to calculate the permeability coefficients for each gas were obtained from several studies (Auras & Almenar, 2010; Castellanos, et al., 2016a; Hasbullah, et al., 2000; Techavises & Hikida, 2008).

Table 4.1. Reference permeability coefficients and Arrhenius activation energies of PP and PLA for water vapor, O_2, CO_2 and N_2

Film permeability coefficients	*PP*	*PLA*
H_2O		
Q_{ref}^* (cm^3 mm m^{-2} d^{-1} atm^{-1})	5499.06	404019.64
E_a (kJ mol^{-1})	72.22	55.56
R^2	0.991	0.995
O_2^{**}		
Q_{ref}^* (cm^3 mm m^{-2} d^{-1} atm^{-1})	115.04	73.05
E_a (kJ mol^{-1})	46.71	44.39
CO_2^{**}		
Q_{ref}^* (cm^3 mm m^{-2} d^{-1} atm^{-1})	340.25	201.07
E_a (kJ mol^{-1})	18.85	16.72
N_2^{***}		
Q_{ref}^* (cm^3 mm m^{-2} d^{-1} atm^{-1})	27.39	18.30
E_a (kJ mol^{-1})	41.70	11.20

*Reference permeability coefficients at T_{ref} = 296.15 K (23°C). ** Taken from Castellanos et al. (2016a). *** Estimated from Techavides & Hikida (2008), Auras & Almenar (2010), Hasbullah (2010) and manufacturers.

The transmission rates (K_{TR}) of O_2, CO_2 and N_2 through the perforations made in the bags were obtained using the diffusion coefficients of these gases in air reported by Burg (2004) and Xanthopoulos et al. (2012) and are shown in Table 4.2. These values were calculated using Fick's law (Eq. 2.7) and incorporating the correction term ε (Castellanos, et al., 2016a; Del-Valle, et al., 2009).

Table 4.2. Parameters of gas transmission through the perforations made in the packaging bags

	O_2	CO_2	H_2O	N_2
Coefficients of diffusion in air				
$D_{i/air\ ref}$ ($cm^2\ d^{-1}$)*	17477	12923	17692	17279
E_a ($kJ\ mol^{-1}$)*	4.20	4.31	4.63	4.22
Parameters of transmission through the perforations				
ε (mm)	$0.5d_e$**	$0.6d_e$**	$0.5d_e$	$0.5d_e$**
d_e (x1 perforation)	$1^{0.5}$ x 0.225 = 0.225 mm			
d_e (x2 perforations)	$2^{0.5}$ x 0.225 = 0.318 mm			

* Reference coefficients of diffusion (at T_{ref} = 296.15 °C) and activation energies adapted from Burg (2004), Xanthopoulos et al. (2012).

** Calculated in the same way as Castellanos et al. (2016a).

4.3.2 Permeation parameters to water vapor

To estimate the water exchange in the MAP system, it was first necessary to determine the permeation parameters of the packages that were used. The reference permeability coefficients and activation energies obtained experimentally for the PP and PLA films in the steady state test at different temperatures are shown in Table 4.1. The regression coefficients were 0.991 for PP and 0.995 for PLA, showing good correspondence of the Arrhenius parameters with experimental data of water permeability. The coefficients of permeability to water vapor experimentally obtained were in the same order but about 2 times higher than those reported by Kulchan et al. (2008) and Togashi & Hara (2011) for PP, and are nearly 15 % higher than the values reported by Auras & Almenar (2010) for PLA. The water vapor permeation through the perforations was calculated in the same way as for the other gases, using the modified Fick equation (Eq. 2.7) with a correction factor equal to $0.5d_e$ and using the parameters shown in Table 4.2 from data reported by several

authors (Burg, 2004; Castellanos, et al., 2016a; Xanthopoulos, et al., 2012) and packaging manufacturers.

4.3.3 Respiration and O_2 and CO_2 evolution

O_2 consumption and CO_2 production rates for the fruits packed in the three storage conditions described above were calculated using the respiration parameters for the MMU equation (Castellanos, et al., 2016b) shown in Table 4.3. For the fruits stored without packaging, the O_2 and CO_2 concentrations were kept at a constant 0.202 ± 0.003 mole fraction of O_2 and 0.004 ± 0.002 mole fraction of CO_2 throughout the storage time. In Figure 4.1, the headspace O_2 and CO_2 evolution for the fruits packed in PP bags with perforations are shown.

Table 4.3. Estimated parameters of O_2 consumption and CO_2 production rates of the Michaelis-Menten Uncompetitive (MMU) equation for feijoa fruits

*MMU parameters**	*O_2*	*CO_2*
r_{max} (cm^3 kg^{-1} d^{-1})		
$r_{max\theta}$ (cm^3 kg^{-1} d^{-1})**	9.60 ± 0.42 x 10^{15}	3.59 ± 0.24 x 10^{14}
E_a (kJ mol^{-1})	68.51 ± 3.12	60.43 ± 4.09
K_m		
$K_{m\theta}$**	7.09 ± 0.33 x 10^{10}	2.99 ± 0.20 x 10^{7}
E_a (kJ mol^{-1})	65.07 ± 3.00	46.76 ± 3.16
K_{mu}		
$K_{mu\theta}$**	5.27 ± 0.24 x 10^{11}	7.60 ± 0.51 x 10^{14}
E_a (kJ mol^{-1})	70.92 ± 3.24	88.15 ± 5.96

*Taken from Castellanos et al. (2016b). For each parameter, standard deviation is included

** Pre-exponential factor of each parameter.

For the different storage conditions, equilibrium O_2 and CO_2 levels were reached inside the packages. O_2 consumption and CO_2 production by the fruit were greater at higher temperatures, decreasing the O_2 concentration and increasing the CO_2 concentration to reach the steady state. Moreover, for the PP bags with two 0.225 mm perforations, the O_2 equilibrium levels were greater and the CO_2 levels were lower as compared with the PP bags with one perforation. This was due to the greater gas permeation rate resulting from having one additional perforation. At 18 °C, equilibrium concentrations of 4% O_2 and 14% CO_2 for the PP bags with 1 perforation and 7% O_2 and 13% CO_2 for bags with two

perforation were reached. At 6 °C, equilibrium concentrations of 15% O_2 and 6% CO_2 for bags with 1 perforation and 14% O_2 and 7% CO_2 for bags with two perforations were reached after 7 days of storage. There were no significant differences in the equilibrium of the O_2 and CO_2 levels due to the external relative humidity in the storage cabinets, as can be seen for bags stored at 50% RH and 70% RH at the same temperature and number of perforations in the packaging. The lines in Figure 4.1 show the O_2 and CO_2 concentrations predicted by the developed model for inside the PP bags, using MMU kinetics (Eqs. 1.8 and 2.1) to calculate the respiration rates. The transfer of these gases through the package walls and perforations was calculated in the model using the parameters shown in Table 4.1 (PP permeability coefficients) and Table 2 (transmission rate through the perforations), respectively. The predicted values satisfactorily represented the experimental evolution of gases, as shown in Figure 4.1, under the different conditions of temperature, RH and perforations.

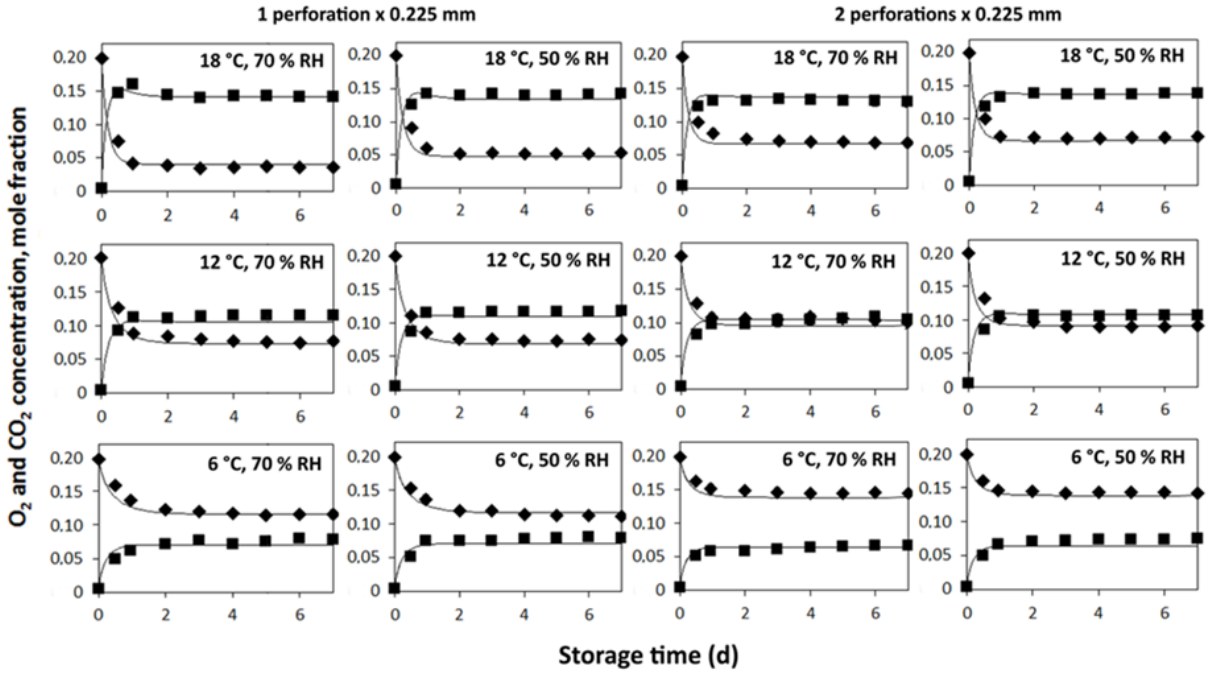

Figure 4.1. O_2 (♦) and CO_2 (■) evolution inside PP bags with one and two perforations of 0.225 mm at 6 °C, 12 °C and 18 °C, and 50 and 70 % RH for feijoa fruits. Lines represent O_2 and CO_2 concentrations predicted by the model.

4.3.4 Determination of the fruit transpiration in the MAP

The transpiration rate of the feijoa fruits was determined from the weight loss data obtained for the fruit stored without packaging and packed in PP bags with perforations. In all the studied storage conditions, the fruits lost weight linearly throughout the storage period as

shown in Figures 4.2 (18 °C), 4.3 (12 °C) and 4.4 (6 °C). By increasing the storage temperature, fruit weight loss was greater, being highest at 18 ° C. By day 7 of storage, the weight loss in the fruit stored at 18 °C was between 2 and 3 times higher than for the fruit stored at 6 °C, considering all of the conditions of the packaging and relative humidity (see also Table 4.4). In addition, as the relative humidity in the atmosphere surrounding the product was lower, the weight loss was greater. For the fruits stored without packaging, the weight loss was greater at 50% RH than at 70% RH at the three test temperatures. Similarly, the fruits stored without packaging lost far more weight compared to the fruits stored in perforated PP bags as shown in Figures 4.2-4.4.

In the fruits packed in PP with one and two perforations, a saturated atmosphere (100% RH) in the headspace was quickly reached, about 1-2 hours after packing in all cases. By day 7 of storage, the weight loss in the fruits stored without packaging at 50% RH was 5 to 7 times greater than for the fruits packed in PP bags at 100% RH in the headspace. Weight losses were higher as the concentration differential (water activity) between the fruits and the surrounding atmosphere increased.

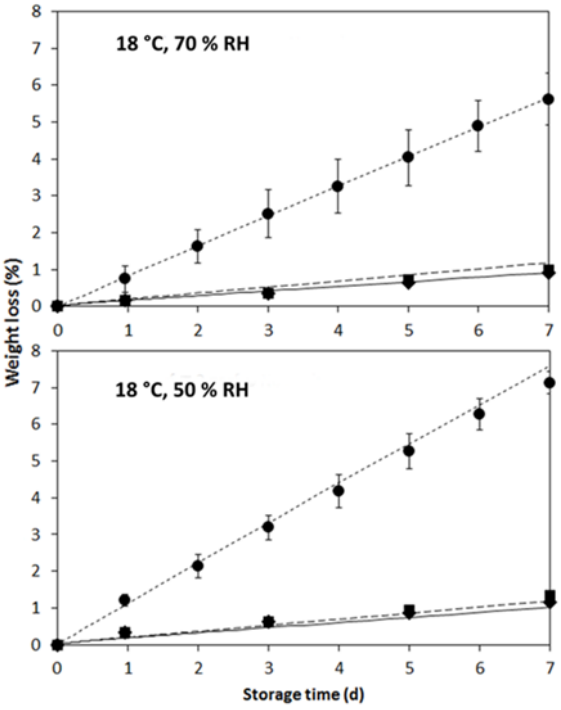

Figure 4.2. Cumulative weight loss for the feijoa fruits stored without packaging (●) and packed in PP bags with one perforation (♦) and two perforations (■) of 0.225 mm at 18 °C and 50 and 70 % RH. Lines represent weight loss predicted by the model. Bars represent standard deviation (SD).

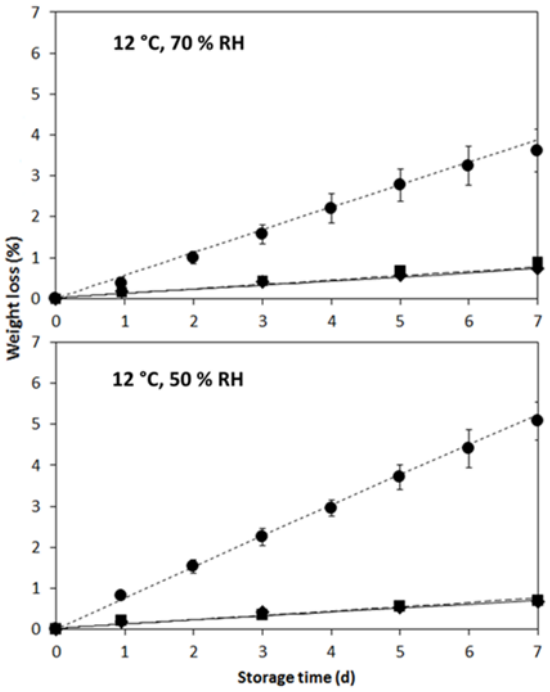

Figure 4.3. Cumulative weight loss for the feijoa fruits stored without packaging (●) and packed in PP bags with one perforation (♦) and two perforations (■) of 0.225 mm at 12 °C and 50 and 70 % RH. Lines represent weight loss predicted by the model. Bars represent SD.

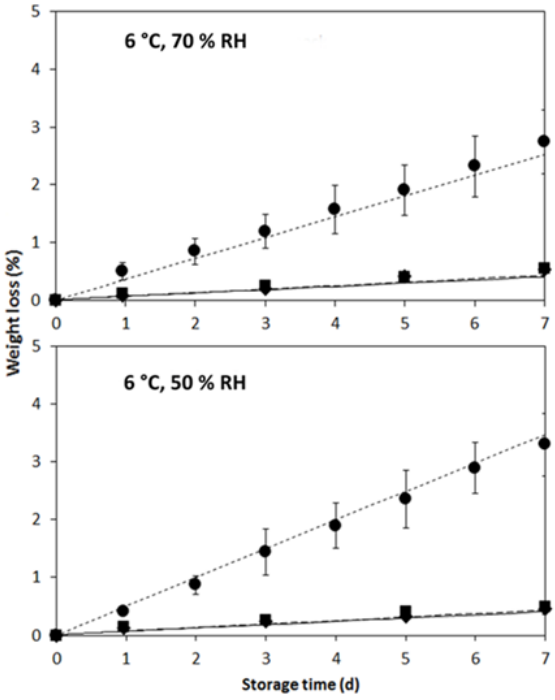

Figure 4.4. Cumulative weight loss for the feijoa fruits stored without packaging (●) and packed in PP bags with one perforation (♦) and two perforations (■) of 0.225 mm at 6 °C and 50 and 70 % RH. Lines represent weight loss predicted by the model. Bars represent SD.

The greatest weight loss for the 7 days of storage corresponded to the fruits stored without packaging at 18 °C and 50% RH, at 7.13% (Table 4.4). The differences in weight loss between the fruits packed in PP with one and two perforations at 6 and 12 °C were negligible and, at 18 °C, a slightly greater loss for the fruits stored in bags with two perforations was observed. This was due to that in both packaging configurations water vapor saturation in the headspace was quickly reached.

Eq. 4.11 was used to calculate the transpiration rate of the fruits to the different conditions. In this equation, as mentioned above, it was assumed that two processes contributed to the transpiration. On one hand, the transfer of water vapor due to the difference in water activity between the product and the surrounding atmosphere and, on the other hand, the product water loss due to the heat transfer and, assuming there was a thermal equilibrium in the system, specifically, to respiratory heat.

In Figures 4.2-4.4, it can be seen that for the PP perforated bags, there was a continuous loss of water although, as discussed earlier, 100 % RH was achieved 1-2 hours after initiating storage. This water lost by the product was not transferred to the headspace atmosphere because it was saturated and was condensed inside the packaging (Table 4.4). In this case, Eq. 4.11 was simplified to Eq. 4.6 considering there was no actual transfer of water between the product and the surrounding atmosphere. Numerically, the difference between the water activity of the headspace atmosphere (equal to 1) and the water activity of the product (estimated to be 0.97) was negative; however, it was assumed that, at this point, the water lost by the product due to transpiration was not regained. With Eq. 4.6 and considering the fact that saturation inside the packages is reached in a short time compared to the total storage time, the respiratory heat was calculated depending on the respiration rates (Eq. 4.8) and then term α; the fraction of energy used from the respiration process in the transpiration rate was found by iteration. The value of α was found by replacing the experimental transpiration rate calculated using Eq. 4.4 for packed fruits and then finding the respiratory heat required to generate that transpiration rate in Eq. 4.6. As shown in Table 4.5, α was equal to 0.25. This value was less than that estimated in other studies (Rennie & Tavoularis, 2009; Song, et al., 2002), who gave an alpha value of 0.8-0.95. However, it is necessary to say that of the energy resulting from the oxidation of substrates in respiration process, a good part is used in metabolic cycles of the product (about 50-60 %) and the rest is dissipated as heat (Mir & Beaudry, 2002). Of the respiratory heat that is dissipated, a part is exchanged with the surroundings and the other part will be used to transfer out moisture from the product.

Table 4.4. Experimental and predicted cumulative fruit weight loss and condensate water inside the bags at day 7 of storage

T (°C)	External RH	Packaging	Internal RH	C-WL % (exp)	C-WL % (pre)	R^2	C-V_{cnd} % (exp)	C-V_{cnd} % (pre)	R^2
18	70	Bag + 1 perf	100	0.92 ± 0.07	0.92	0.988	0.87 ± 0.05	0.90	0.994
18	70	Bag + 2 perf	100	1.01 ± 0.13	1.19	0.876	1.06 ± 0.06	1.16	0.987
18	70	No pack	..	5.62 ± 0.71	5.66	0.998	..	..	..
18	50	Bag + 1 perf	100	1.16 ± 0.11	0.91	0.900	0.89 ± 0.03	0.90	0.986
18	50	Bag + 2 perf	100	1.35 ± 0.08	1.19	0.944	1.23 ± 0.04	1.17	0.987
18	50	No pack	..	7.13 ± 0.30	7.59	0.990	..	..	..
12	70	Bag + 1 perf	100	0.74 ± 0.06	0.73	0.974	0.66 ± 0.04	0.71	0.986
12	70	Bag + 2 perf	100	0.90 ± 0.13	0.77	0.937	0.80 ± 0.03	0.75	0.974
12	70	No pack	..	3.61 ± 0.52	3.88	0.988	..	..	..
12	50	Bag + 1 perf	100	0.67 ± 0.05	0.70	0.955	0.64 ± 0.02	0.68	0.987
12	50	Bag + 2 perf	100	0.69 ± 0.05	0.75	0.966	0.65 ± 0.02	0.73	0.989
12	50	No pack	..	5.09 ± 0.46	5.25	0.996	..	..	..
6	70	Bag + 1 perf	100	0.53 ± 0.09	0.41	0.855	0.42 ± 0.05	0.38	0.974
6	70	Bag + 2 perf	100	0.55 ± 0.06	0.44	0.863	0.47 ± 0.04	0.43	0.971
6	70	No pack	..	2.75 ± 0.35	2.52	0.981	..	..	..
6	50	Bag + 1 perf	100	0.47 ± 0.09	0.41	0.916	0.39 ± 0.02	0.40	0.976
6	50	Bag + 2 perf	100	0.49 ± 0.06	0.44	0.858	0.42 ± 0.02	0.43	0.985
6	50	No pack	..	3.29 ± 0.44	3.46	0.992	..	..	..

C-WL: percentage of cumulative weight loss, experimental (exp) and predicted (pre). C-V_{cnd}: percentage of cumulative condensate water related to the initial fruit weight. R^2: coefficient of determination. Test in bags with one perforation (Bag + 1 perf x 0.225 mm), two perforations (Bag + 2 perf x 0.225 mm) and fruits without bag (No pack). Standard deviation is included.

After determining the value of α, the coefficients of mass transfer (k in Eq. 4.11) were estimated using the experimental data from weight loss corresponding to the fruits stored without packaging (where the RH remained constant at 50% or 70%). The k coefficients were found to be similar to the term α, replacing the experimental transpiration rates of the fruit stored without packaging in Eq. 4.11 and iteratively finding the values required to meet this transpiration rate. With the k coefficients estimated at each temperature, the Arrhenius equation (Eq. 4.2) was used to find the reference coefficient of mass transfer (T_{ref} = 23 °C) and the activation energy. These values are shown in Table 4.5 and correlate well with the experimental data with an R^2 = 0.943. Once the required parameters in Eq. 4.11 were found, the experimental cumulative percentages of weight loss by the fruits and condensed water within the packaging during the storage time and the corresponding values predicted by the model were calculated with Eqs. 4.21 and 4.22. These values are shown in Table 4.4 together with the corresponding R^2. Of course, there was no condensed water for the fruits

stored without packaging. The values predicted by the model had a good fit to the experimental values as shown in Figures 4.2-4.4 and in Table 4.4. With the model, it was possible to adequately predict the evolution in the weight loss of the fruits and the accumulation of condensation within the perforated PP bags.

Table 4.5. Parameters for the calculation of the transpiration rate due the respiration heat and the water partial pressure difference between the fruit and the surrounding atmosphere (Eq. 4.11)

Respiration heat (Eq. 4.8)	
α	0.25 ± 0.02
Mass transfer due the water partial pressure difference	
k (kg kg^{-1} d^{-1})	
k_{ref} (kg kg^{-1} d^{-1})*	3.65 ± 0.28 x 10^{-2}
E_a (kJ mol^{-1})	44.93 ± 2.77
R^2	0.943

*Reference mass transfer coefficient at T = 296.15 K (23 °C). Standard deviation is included.

4.3.5 Validation packaging test with PP and PLA

As in the initial tests, for the perforated bags of PP and PLA, the O_2 concentration decreased and the CO_2 concentration increased until equilibrium levels for both gases were reached in the headspace, as shown in Figure 4.5. In the PLA bags, equilibrium O_2 and CO_2 concentrations of 7.8 % and 13.5 % were reached, while, for the PP bags, 8.3 % O_2 and 10.5 % CO_2 were reached. This difference was due solely to the lower PLA permeability to these gases regarding PP (Table 4.2) since, for both bags, one perforation of the same effective diameter was made. As shown in Figure 4.5, the O_2 and CO_2 concentrations predicted by the model were satisfactorily closer to the experimentally measured values for both packaging types.

In both types of packaging, the fruits lost weight throughout the storage time, with a greater weight loss for the PLA bags, as shown in Figure 4.6 and Table 4.6. By the day 13 of storage, the fruits packed in PLA lost 3.29% of their initial weight, while the fruits packed in PP lost 1.48% of their initial weight. In the PP bags, a RH of 100 % was quickly reached in the atmosphere headspace, while, in the PLA bags, there was no saturation in the headspace and an equilibrium RH of 84% was reached. Furthermore, there was water condensation inside the PP bags (1.39 % compared to the initial weight of the fruits), while, in the PLA bags, the condensation was negligible (Table 4.6). This was due to the large difference in the permeability to water vapor between the two packaging materials. The PLA

permeability to water vapor was close to 100 times greater than that of PP. The values predicted by the model developed for the relative humidity in the packaging headspace, the weight lost by the fruits and the accumulated condensate satisfactorily fit to the experimental measurements. The coefficients of determination of the model for these values were between 0.91 and 0.99, showing its good predictive power.

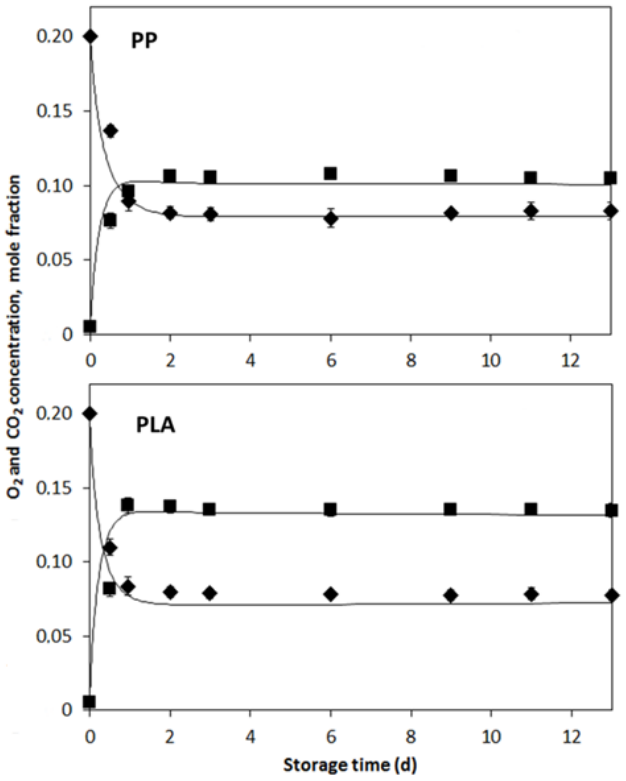

Figure 4.5. O_2 (♦) and CO_2 (■) evolution inside PP and PLA with one of 0.225 mm at 12 °C and 75 % RH for feijoa fruits. Lines represent O_2 and CO_2 concentrations predicted by the model. Bars represent SD.

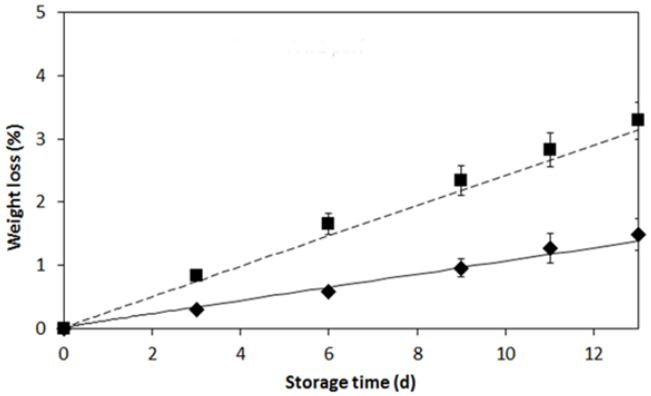

Figure 4.6. Cumulative weight loss for the feijoa fruits packed in PP (♦) and PLA bags (■) with 1 perforation of 0.225 mm at 12 °C and 75 % RH. Lines represent weight loss predicted by the model. Bars represent SD.

Table 4.6. Experimental and predicted equilibrium relative humidity, cumulative weight loss and condensate water inside the perforated PP and PLA bags for the validation test at 12 °C and 75 % RH

Packaging	Internal RH_{eq} (exp)	Internal RH_{eq} (pre)	R^2	C-WL % (exp)	C-WL % (pre)	R^2	C-V_{cnd} % (exp)	C-V_{cnd} % (pre)	R^2
PP + 1 perf	99 ± 1	100	0.991	1.48 ± 0.15	1.38	0.984	1.39 ± 0.09	1.36	0.977
PLA + 1 perf	84 ± 2	83	0.933	3.29 ± 0.29	3.14	0.985	0.03 ± 0.01	0.00	0.913

Internal RH_{eq}: Equilibrium relative humidity inside the package, experimental (exp) and predicted (pre). C-WL: percentage of cumulative weight loss. C-V_{cnd}: percentage of cumulative condensate water related to the initial fruit weight. R^2: coefficient of determination of the model.

4.4 Conclusions

A mathematical model to describe the transpiration rate by a product packed in a MAP and the water transport through the system was successfully developed. The model considered the storage temperature, the difference in water activity between the packed product and the atmosphere that surrounded it and the respiratory heat influence for the transpiration of the fruits. The respiration rate (O_2 consumption and CO_2 production), the gas exchange through the packaging system and the perforations made in the package, and the change in volume of the headspace were properly integrated in the model.

The developed model was validated in a MAP test by packing feijoa fruits in PP and PLA bags and showed good predictability for the evolution of product weight loss, accumulation of condensed water and changes in relative humidity in packaging headspace.

4.5 References

ASABE, S., 2006. Psychrometric Data. In: *ASAE D271.2 APR1979*, R2005. St. Joseph, MI.

Auras, R. & Almenar, E. 2010. Permeation, sorption and diffusion in poly(lactic acid). In: R. Auras, L.T. Lim, S.E.M. Selke & H. Tsuji (Eds.), *Poly(Lactic Acid): synthesis, structures, properties, processing and application*. New York: Wiley & Sons, pp. 164-170.

Becker, B.R. & Fricke, B.A., 2001. A numerical model of commodity loss and temperature distribution during refrigerated storage. *Acta Horticulturae*, 566: 431-436.

Brooker, D.B. 1967. Mathematical model of the psychrometric chart. *Transactions of the ASAE*, 10(4): 558-560.

Burg, S.P. 2004. *Postharvest Physiology and Hypobaric Storage of Fresh Produce*. Wallingford: CABI Publishing.

Castellanos, D.A., Cerisuelo, P., Hernández-Muñoz, P., Herrera, A.O. & Gavara, R. 2016a. Modelling the evolution of O_2 and CO_2 in MAP of a fresh product: Application to tomato. *Journal of Food Engineering*, 168: 84-95.

Castellanos, D., Mendoza, R., Gavara, R. & Herrera, A. 2016b. Respiration and Ethylene Generation Modeling of 'Hass' Avocado and Feijoa Fruits and Modified Atmosphere Packaging Application. *International Journal of Food Properties*,
doi: 10.1080/10942912.2016.1160921

Chung, D., Papadakis, S.E. & Yam, K.L. 2003. Simple models for evaluating effects of smalls leaks on the gas barrier properties of food packages. *Packaging Technology and Science*, 16: 77-86.

Del-Valle, V., Hernández-Muñoz, P., Catalá, R. & Gavara, R. 2009. Optimization of an equilibrium modified atmosphere packaging (EMAP) for minimally processed mandarin segments. *Journal of Food Engineering*, 91: 474-481.

Guevara-Arauza, J., Yahia, E. M., Cedeño, L. & Tijskens, L. M. M., 2006. Modeling the effects of temperature and relative humidity on gas exchange of prickly pear cactus (Opuntia spp.) stems. *LWT - Food Science and Technology*, 39: 796-805.

Hasbullah, R., Gardjito, Syarief, A.M. & Akinaga, T. 2000. Gas permeability characteristics of plastic films for packaging of fresh produce. *Journal of the Society of Agricultural Structures, Japan*, 31(2): 5-11.

Kang, J.S. & Lee, D.S. 1998. A kinetic model for transpiration of fresh produce in a controlled atmosphere. *Journal of Food Engineering*, 35: 65-73.

Kell, G.S. 1975. Density, Thermal Expansivity, and Compressibility of Liquid Water from 0" to 150°C: Correlations and Tables for Atmospheric Pressure and Saturation Reviewed and Expressed on 1968 Temperature Scale. *Journal of Chemical Engineering Data*, 20(1): 97-105.

Kulchan, R., Boonsupthip, W. & Suppakul, P. 2008. Determination of activation energy for water vapor permeability of polyolefin films and application to predict shelf life of moisture-

sensitive Thai cookies. *The Proceedings of 16th IAPRI World Conference on Packaging*, Bankok, Thailand, June 8-12.

Kwon, M.J., Jo, Y.H., An, D.S. & Lee, D.S. 2013. Applicability of simplified simulation models for perforation-mediated modified atmosphere packaging of fresh produce. *Mathematical Problems in Engineering*, doi: 10.1155/2013/267629

Lu, L., Tang, Y. & Lu, S., 2013. A Kinetic Model for Predicting the Relative Humidity in Modified Atmosphere Packaging and Its Application in Lentinula edodes Packages. *Mathematical Problems in Engineering*, doi: 10.1155/2013/304016

Mahajan, P.V., Oliveira, F.A.R., Montañez, J.C. & Frias, J. 2008. Effect of temperature and humidity on the transpiration rate of the whole mushrooms. *Journal of Food Engineering*, 84: 281-288.

Mangaraj, S., Goswami, T.K. & Mahajan, P.V. 2014. Development and validation of a comprehensive model for MAP of fruits based on enzyme kinetics theory and Arrhenius relation. *Journal of Food Science and Tecnology*, 52(7): 4286-4295.

Montanaro, G., Dichio, B., Xiloyannis, C. & Lang, A. 2012. Fruit transpiration in kiwifruit: environmental drivers and predictive model. *AoB Plants*, doi: 10.1093/aobpla/pls036

Parra, A. & Fischer, G. 2014. Maduración y comportamiento poscosecha de la feijoa (*Acca sellowiana* (O. Berg) Burret). Una revisión. *Revista Colombiana de Ciencias Hortícolas*, 7(1): 98-110.

Mir, N. & Beaudry, R. 2002. Atmosphere control using oxygen and carbon dioxide. In: Knee, M. (Ed.), *Fruit quality and its biological basis*. Columbus: Sheffield Academic, pp.122-149.

Rennie, T. & Tavoularis, S. 2009. Perforation-mediated modified atmosphere packaging Part I. Development of a mathematical model. *Postharvest Biology and Technology*, 51: 1-9.

Song, Y., Vorsa, N. & Yam, K. L., 2002. Modeling respiration–transpiration in a modified atmosphere packaging system containing blueberry. *Journal of Food Engineering*, 53: 103-109.

Sousa-Gallagher, M., Mahajan, P.V. & Mezdad, T. 2013. Engineering packaging design accounting for transpiration rate: Model development and validation with strawberries. *Journal of Food Engineering*, 119: 370-376.

Techavises, N. & Hikida, Y. 2008. Development of a mathematical model for simulating gas and water vapor exchanges in modified atmosphere packaging with macroscopic perforations. *Journal of Food Engineering*, 85: 94-104.

Togashi, Y. & Hara, M. 2011. Tritiated water permeation and sorption in polyimide film. *Fusion Science and Technology*, 60: 1471-1474.

Xanthopoulos, G., Koronaki, E. & Boudouvis, A. 2012. Mass transport analysis in perforation-mediated modified atmosphere packaging of strawberries. *Journal of Food Engineering*, 111: 326-335.

Chapter 5. Development of an suitable EMAP system for feijoa fruits and modelling firmness and color evolution[5]

Abstract

Equilibrium modified atmosphere packaging (EMAP) improve the preservation of fresh produce by using favorable levels of gases that remain constant for most of the packaging time. An experiment was conducted to obtain a suitable EMAP system for feijoa fruits (*Acca sellowiana* Berg), storing samples without packaging and packed in PP bags (unperforated and with 1-3 perforations of 0.225 mm) at 6, 12 and 17 °C and 85% RH. The equilibrium concentration of the gases in the packaging headspace for each EMAP was estimated in advance, using the MAP model developed in Chapters 2-4. The effect of different storage conditions on the fruits was determined by evaluating the change in the deterioration index, weight, firmness, color and organic acids. In the different EMAP systems, the storage time of the fruits was significantly increased as compared to those stored without packaging at 17 °C, from 17 to 25-31 days for the EMAP at 12 and 17 °C, and 35-38 days for the EMAP at 6 °C. Based on the evolution of the measured properties, the most favorable EMAP configuration was 6 °C and 8.2 kPa of O_2 – 5.8 kPa of CO_2 (PP bags with one perforation). With the obtained data, mathematical models were also developed to describe the evolution in firmness and flesh color of the stored fruits depending on the temperature and O_2 and CO_2 concentrations. The models adequately represented the behavior of these properties, obtaining R^2_{adj} values of 0.948 for firmness and 0.94-0.95 for the color coordinates L*, *a** and *b**.

Keywords: EMAP, storage life, quality properties, simulation, modelling

[5] This chapter (with minor modifications) was published as:
Castellanos, D.A., Polanía, W. & Herrera A.O. 2016. Development of an equilibrium modified atmosphere packaging for feijoa fruits and modeling color and firmness evolution, *Postharvest Biology and Technology*, 120: 193-203. http://dx.doi.org /10.1016/j.postharvbio.2016.06.012

Nomenclature

a, b	apparent reaction orders
A	effective exchange area of the bag (m^2)
*a**	CIELAB red(+)/green(−) color coordinate
a_0*	CIELAB red(+)/green(−) color coordinate on day zero of storage
*b**	CIELAB yellow(+)/blue(−) color coordinate
b_0*	CIELAB yellow(+)/blue(−) color coordinate on day zero of storage
E_a	activation energy (kJ mol^{-1})
F	firmness (N)
F_0	firmness on day zero of storage (N)
F_{fix}	fixed firmness in the produce (N)
K_{mO2}	dissociation constant of the enzyme-substrate complex for firmness and respiration
K_{muCO2}	constant of uncompetitive inhibition by CO_2 for firmness and respiration
K_{TRO2}, K_{TRCO2}, K_{TRN2}	transmission rate of O_2, CO_2 and N_2 through the perforations (cm^3 d^{-1})
k	firmness, L* or *a** parameter of change as a function of the O_2 and CO_2 levels in the headspace (d^{-1})
ko^{max}	maximum oxidative rate of firmness loss (d^{-1})
k_T	L*, *a** or *b** parameter of change as a function of the storage temperature
k_1, k_2, k_3	b* parameters of change as a function of the O_2 and CO_2 levels
L	film thickness (mm)
L*	CIELAB lightness coordinate
L_0*	CIELAB lightness coordinate on day zero of storage
L_{fix}*	minimum CIELAB lightness coordinate
P	system pressure (kPa)
P_m	firmness or color parameter depending on temperature
P_{mref}	firmness or color parameter at T_{ref}
Q_{O2}, Q_{CO2}, Q_{N2}	packaging permeability coefficient to O_2, CO_2 and N_2 (cm^3 mm m^2 d^{-1} atm^{-1})
R	universal gas constant (0.008314 kJ mol^{-1} K^{-1} or 8314 kPa cm^3 mol^{-1} K^{-1})
r_{O2}, r_{CO2}	rates of O_2 consumption and CO_2 generation (cm^3 kg^{-1} d^{-1})
t	storage time (d)
T	temperature (°C, K)
T_{ref}	reference temperature (°C, K)
V	packaging headspace (cm^3)
W	fruit weight (kg)
y_{O2}, y_{CO2}, y_{N2}	O_2, CO_2 and N_2 concentrations inside the packaging
y_{O2out}, y_{CO2out}, y_{N2out}	O_2, CO_2 and N_2 concentrations outside the packaging

5.1 Introduction

In a modified atmosphere packaging system, there is a dynamic interaction between the product metabolism (O_2 consumption and CO_2 generation) and the transfer of gases through the package (O_2 input and CO_2 output). A balance in these two processes is desirable to obtain an equilibrium modified atmosphere packaging (EMAP) specifically favorable for increasing the storage life of the packed product (Del-Valle, et al., 2009; Mistriotis, et al., 2016).

In order to obtain a satisfactory EMAP system, it is necessary to know the type of product to be packed, the weight and the rates of respiration and transpiration at the storage temperature. It is also necessary to know the permeability of the package, which is defined by the type of packaging material, the thickness, the effective area of gas exchange and whether or not it is perforated. From these data, it is possible to construct models to describe the behavior of the system and thus predict the concentrations of the gases in the equilibrium period (Castellanos, et al., 2016; Mangaraj, et al., 2011). However, each particular product has a specific reaction to a particular MA and, therefore, the most appropriate gas concentrations and temperature that extend the shelf-life of the product are required. This aspect is critical for implementing the system since not every AM will be suitable for a fresh product and, if the favorable gas concentrations are not known, in the best-case scenario, the best product preservation is not achieved and, in the worst-case, it may induce damage and decrease the shelf-life, the opposite of what is intended.

The EMAP effectiveness in a packed product is related to the change in quality properties, considering that these properties are influenced by storage conditions, such as temperature and gas concentrations in the packaging headspace (Gwanpua, et al., 2012; Selcuk & Erkan, 2015). As previously mentioned, in a MAP system, the ripening and deterioration will be influenced and, if the system is suitable, these processes will be delayed since the enzyme activity is reduced due to a decrease in temperature and O_2 and an increase in CO_2 concentration in the headspace surrounding the product (Castellanos & Algecira, 2012). This results in a reduction of metabolic activity and a decrease in the rate of degradation of organic acids, carbohydrates, chlorophylls, pigments, volatile and sugars production and moisture loss and hence, the evolution of physicochemical and quality properties such as color, firmness, weight, acidity, soluble solids and shelf-life (Banda, et al., 2015; Gwanpua, et al., 2012; Hertog, et al., 2004).

When, through the evolution in quality properties, the most satisfactory EMAP for a given product has been defined, available mathematical models can be used to determine a suitable packaging system (the required permeability) to reach these equilibrium concentrations. However, in many cases it may not be feasible or practical to obtain a packaging system with the permeability necessary for achieving the desired EMAP. The appropriate packing material may not be available, the available package size may be different from that required or the equipment necessary to make the needed perforations to achieve the target permeability may not be available; or the conditions may change during the storage period uncontrollably (mainly refrigeration temperature). In these situations, it may be very useful to know in advance how to evolve the product quality properties considering the current storage conditions to determine how its shelf-life is modified.

As there is a direct relationship between the packaging conditions and the change in quality properties, it is also possible to develop and use mathematical models to describe the evolution of these properties in the same way as have been used to describe the evolution in the concentration of gases in the MAP system. Some authors have shown changes in properties such as color, firmness (texture) and weight loss due to the ease of measurement and its direct relationship with the product shelf-life (Hertog, et al., 2003; Mangaraj & Goswami, 2011; Pathare, et al., 2013; Tijskens & Schouten, 2009). However, the evolution of these properties has been generally considered only as a function of temperature and only a few studies have considered the influence of the O_2 or CO_2 levels on the firmness or color of a product (Castellanos & Algecira, 2012; Hertog, et al., 2003; Hertog, et al., 2004). In the end, it is desired to use properties that are indicative of quality, such as color or firmness, which are easy to measure and representative throughout the product storage life.

In the case of feijoa fruits (*Acca sellowiana* Berg) there is not much information available on the use of modified atmospheres for conservation and the existing information is contradictory (Parra & Fischer, 2013). Galvis et al. (2003) packed feijoa fruits in PE bags with 8% O_2 and 5% CO_2 (at 0.74 atm) for 3 weeks at 6 °C with some damage in the quality properties. East et al. (2009) reported that O_2 concentrations between 1-3% and CO_2 concentrations less than 1% (at 1 atm) contributed to the conservation of 'Unique' feijoa for 56 days at 5 °C without harming the quality properties. As for the modelling of the evolution of the feijoa quality properties, we have not found any available literature.

In this Chapter, EMAP systems for feijoa fruits are developed, identifying the most suitable conditions of preservation in their quality properties and a model to represent the evolution

in firmness and color of the fruits as a function of the packaging conditions is also presented. The fruits were packed in polypropylene bags with different numbers of micro-perforations and stored at various temperatures, determining the effects of the different equilibrium atmospheres on the evolution of the product quality. The concentration of the gases in each EMAP was previously estimated by simulation using the MAP model described in Chapters 2-4 to ensure that the samples would not be stored under inappropriate conditions and that the equilibrium concentrations in each system were different.

5.2 Materials and Methods

5.2.1 Fresh samples

The fruits used in the tests were obtained from commercial growers located in Tibasosa, in the department of Boyacá, Colombia in November-December, 2015. They were harvested at the physiological maturity stage, 20 weeks after flowering (Galvis, 2003; Parra & Fischer, 2014), and transported to the Postharvest Laboratory, Faculty of Agricultural Sciences, Universidad Nacional de Colombia (Bogotá, Colombia) in the following days. After discarding those with evidence of damage, the fruits with homogeneous characteristics were selected to ensure uniformity in the size, weight and color of the sample group and stored at 8 ºC. In the laboratory, the fruits were randomly arranged for the different MAP tests. The initial properties of the fruits are shown in Table 5.1.

5.2.2 Packaging material

For the MAP tests, cast polypropylene bags (PP) with moderate permeability to water vapor and CO_2 and low permeability to O_2 were used (Table 5.2). The PP bags (Rediplast, Bogotá, Colombia) had a thickness of 0.025 ± 0.002 mm and a size of 25 x 20 cm. The thickness of the films was determined as the average of ten measurements with a Mitutoyo (Kawasaki, Japan) gauge. The permeability coefficients of the PP packaging to O_2 and CO_2 were determined as described in Chapter 2 with steady-state methods (Castellanos, et al., 2016). A Mocon® Oxtran 2/21 (MOCON, Inc., Minneapolis, MN, USA) permeation instrument was used for the O_2 and a temperature-controlled chamber with a parallel flow permeation cell connected to a gas chromatograph was used for the CO_2. The N_2 permeability coefficient was estimated from information provided by the respective manufacturers and from other studies (Hasbullah, et al., 2000; Techavises & Hikida, 2008). Perforations were made in some of the PP bags to increase their permeability. The permeation rate of gases through

these perforations was estimated from a modified Fick equation, Eq. 2.7. The transmission rates of O_2, CO_2 and N_2 through the perforations made in the bags at the different storage temperatures are shown in Table 5.2.

5.2.3 Making the EMAP systems and storage

Groups of two fruits with a total weight of 125 ± 7 g were placed in each PP bag and the bags were filled with atmospheric air (P = 74.7 kPa). The bags had a total internal surface area of 1000 cm^2, an effective transfer-area of 800 cm^2 and an initial headspace volume of 410 ± 12 cm^3. A 200 cm^2 polystyrene (PS) support with a volume of 200 cm^3 was placed in each bag to hold the fruit in place and ease the sample handling. A paper towel of the same surface area was placed on the PS support to collect the condensed water lost by the packed fruits. The packed fruits were stored at 6, 12 and 17 °C and 85% RH between 28-35 days, depending on the evolution of the quality properties. At 6 °C, bags without perforations and with 1 and 2 perforations with an effective diameter of 0.225 mm were used. At 12 and 17 °C, bags with 1, 2 and 3 perforations of 0.225 mm were used (Table 5.3). In all of the packaging systems, an equilibrium gas concentration was reached in the packaging headspace and the O_2 level did not reach 0% by previously simulating the evolution of the system using the MAP model developed in Chapters 2-4 (see modelling MAP). The evolution of the O_2 and CO_2 concentrations in the headspace of each bag was followed by taking a gas sample of 5 cm^3 through an adhesive septa on the package surface, which was analyzed with an electronic analyzer Oxybaby® 6i (Witt-Gasetechnik GmbH & Co. KG, Witten, Germany), previously calibrated with Gas Chromatography. A sample of 5 cm^3 of air were introduced into the bag to replace the withdrawn one.

Besides packed fruits (9 combinations of temperature and packaging), a group of fruits was stored at 17 °C without packaging to serve as a control. The fruits in the different packaging systems and the control fruits were compared with an analysis of variance (ANOVA) and evaluating the significant differences between mean of a number of response variables in the stored fruits at $p \leq 0.05$ with a Tukey's test. The response variables measured in the fruits during the storage time were weight loss, peel firmness to penetration, flesh color and content of citric, malic and oxalic acids.

5.2.4 Simulation of gas evolution in the EMAP systems

Prior to the packaging test, the evolution in the O_2 and CO_2 concentrations inside the package was simulated for each EMAP system. In this way, it was possible to define in

advance the approximate O_2 and CO_2 concentrations in the equilibrium time of the system as shown in Table 5.4 and it was possible to predict how fast the equilibrium gas levels were reached in each packaging headspace. For the simulation, the parameters of the MAP model were used to represent the gas exchange through the PP bags and the respiration of the feijoa fruits. As described in Chapters 2 and 3, the evolution of O_2, CO_2 and N_2 in the packaging headspace during the storage time can be predicted by using the differential mass balance, which considers the gas exchange through the package walls and perforations and the O_2 consumption and CO_2 production of the packed produce:

For O_2,

$$V\frac{dy_{O_2}}{dt} = K_{TRO_2}\left(y_{O_{2}Out} - y_{O_2}\right) + \frac{APQ_{O_2}}{L}\left(y_{O_{2}Out} - y_{O_2}\right) - r_{O_2}W - y_{O_2}\frac{dV}{dt} \quad (2.10)$$

For CO_2,

$$V\frac{dy_{CO_2}}{dt} = K_{TRCO_2}\left(y_{CO_{2}Out} - y_{CO_2}\right) + \frac{APQ_{CO_2}}{L}\left(y_{CO_{2}Out} - y_{CO_2}\right) + r_{CO_2}W - y_{CO_2}\frac{dV}{dt} \quad (2.11)$$

For N_2,

$$V\frac{dy_{N_2}}{dt} = K_{TRN_2}\left(y_{N_{2}Out} - y_{N_2}\right) + \frac{APQ_{N_2}}{L}\left(y_{N_{2}Out} - y_{N_2}\right) - y_{N_2}\frac{dV}{dt} \quad (2.12)$$

The headspace volume change over time can be written as:

$$\frac{dV}{dt} = W\left(r_{CO_2} - r_{O_2}\right) + \sum_{i=1}^{3}\left(\left(y_{iOut} - y_i\right)\left(K_{TRi} + \frac{APQ_i}{L}\right)\right) \quad (2.14)$$

Where *i* could be O_2, CO_2 or N_2.

The permeability of the packaging film to O_2, CO_2 and N_2 is temperature-dependent and this dependence was described using an Arrhenius-type equation similar to Eq. 5.3 (Mangaraj, et al., 2009; Techavises & Hikida, 2008). The mass transfer of each gas through the perforation (K_{TR}) made in the packaging system was estimated using a modified Fick's diffusion equation with a correction term due to the resistance to diffusion at the perforation (Castellanos et al., 2016; Chung, et al., 2003; Del-Valle, et al., 2003).

The respiration rate of the packed product, O_2 consumption (r_{O2}) and the CO_2 production (r_{CO2}) rates were described using a Michaelis-Menten enzyme kinetics with uncompetitive type inhibition by CO_2 as mentioned in Chapter 3. For the O_2 consumption, the Eq. 1.8 is again used:

$$r_{O_2} = \frac{r_{O_{2max}} y_{O_2}}{K_{m_{O_2}} + y_{O_2}\left(1 + \frac{y_{CO_2}}{K_{mu_{CO_2}}}\right)} \quad (1.8)$$

To describe the CO_2 production (r_{CO2}) the Eq. 2.1 is used as described in Chapters 2 and 3, with the corresponding r_{CO2max}, K_{mCO2} and $K_{mu'CO2}$ values. Parameters for the O_2 consumption or CO_2 production kinetics are dependent on temperature and this relationship is expressed through Arrhenius' Law (Eq. 5.3).

The equations for the simulation of the MAP system were solved numerically using the calculation routine built in the Matlab software (MathWorks, Inc., Natick, MA, USA) as described in previous Chapters. The evolution in the O_2, CO_2, and N_2 levels in each packaging headspace was calculated with the different packaging conditions: in this case, the fruits with or without packaging, number of perforations in the PP bags and storage temperature.

5.2.5 Fruit quality properties

First, an index of deterioration was estimated for the stored fruits with a scale of 1 to 5 based on the amount of decay and injury evidenced in the surface and flesh of the stored fruits, in a similar way to the estimation of Nguyen et al. (2004). For the index of deterioration, 1 denotes fruits without evidence of deterioration (affected area, AA = 0 %), 2 very light deterioration (AA = 1-5 %), 3 moderate deterioration (AA = 5-15 %), 4 severe deterioration (AA = 15-30 %) and 5 very severe deterioration (AA > 30 %). When the fruits reached condition 4, they were withdrawn from the test. The index was reported as the average value of all the measured fruits and rounded as an integer.

The fruit weight was measured using a PG503-S Mettler-Toledo scale (Ohio, USA), with an accuracy of ±0.001 g. The weight loss was calculated as follows:

$$WL(t)\% = \frac{100(W_{ini} - W_t)}{W_{ini}} \quad (5.1)$$

Where W_{ini} is the initial weight and W_t is the fruit weight at day t.

The firmness was measured at the middle region of each fruit (subjected to axial puncture) using a Universal Testing Machine with a 6 mm Magness-Taylor probe at a test speed of 2 mm s^{-1}. The firmness was taken as the maximum force (N) needed for the probe to penetrate the fruit to a depth of 10 mm.

The flesh color was measured using a Minolta ChromaMeter (Model CR-331, Minolta Camera Co., Osaka, Japan), and reporting the L*, *a** and *b** coordinates of the CIELAB color space. A standard illuminant, 'Daylight 65', was considered. Each measurement was taken by making a transverse cut in the middle of the fruits and recording the color in the central part of the cut section.

The acid content was determined by extracting a sample of the fruits and analyzing it in a Thermo Dionex Ultimate 3000 UHPLC using the Chromeleon® 7.2 software, a LPG-3400SD pump and a UV-Vis detector DAD 3000 (Waltham, MA, USA). The separation was carried out on a Hypersil gold column (150 mm x 4.6 mm, 5 µm). The detection was performed at 210 nm for all of the acids. The optimum efficiency of separation was obtained using 10 mM phosphate buffer, pH 2.2. Other chromatographic parameters included: injection volume, 0.02 cm^3; column temperature, 35 °C and flow rate, 0.8 cm^3 min^{-1}. For extracting the samples, 5 g of fruit were diluted in 25 cm^3 of type I water; the samples were put in Falcon® tubes and homogenized for 45 minutes on a Vortex Mixer. The homogenate was centrifuged at 2200g for 20 min. The supernatants were filtered through a 0.45 µm membrane filter (Iwaki Glass) before the HPLC analysis, and the mobile phase solvents were degassed before use. The samples were analyzed immediately upon completion of the extraction. The contents of citric, malic and oxalic acids were reported in g per kg of fruit (g kg^{-1}). All the measurements were made in triplicate, reporting the mean values of each property.

Total soluble solids (TSS) were measured only for the fruits in physiological maturity (initial day of storage) and ripe using an Atago® digital refractometer (Model PAL-1, Atago Co. Ltd, Tokyo, Japan) and expressed as percent.

The experiments were conducted using randomized factorial experimental design being the factors the different EMAP configurations. The fruits in the different packaging systems and the control fruits were compared with an analysis of variance (ANOVA) and the significant differences between mean of the measured properties in the stored fruits were determined at $p \leq 0.05$ with a Tukey's HSD test. The SAS® software (version 9.2, SAS Institute, Cary, NC, USA) was used to perform the statistical analysis.

After evaluating the experimental evolution of the fruits for the different EMAP systems, the changes in firmness and flesh color were modeled as a function of the O_2 and CO_2 concentrations in the packaging headspace and the storage temperature.

5.2.6 Modelling firmness and color

Firmness declines as ripening continues to a minimum level when produce senescence is reached. Firmness loss can be attributed to various factors, including disassembly of polysaccharide networks, pectin degradation, hydrolysis of starch, celluloses and hemicellulose in cellular walls and water loss by transpiration (Biswas, et al., 2014; Paliyath & Murr, 2008). During postharvest storage, some compounds are affected while others are not. Thus, firmness can be considered to have a fixed (F_{fix}) and a variable (F_{var}) component:

$$F = F_{fix} + F_{var} \quad (1.23)$$

The compounds that do not undergo degradation or that are broken down slowly, such as celluloses and hemicelluloses, contribute to the fixed firmness. The compounds that undergo degradation, such as pectins, or that are lost, such as moisture, contribute to the variable firmness (Biswas, et al., 2014). For this study, fruit firmness was represented as a function of storage time through a first order model of fractional conversion (Eq. 1.23), which has been used by several authors (Hertog, et al., 2004; Lana, et al., 2005; Tijskens & Schouten, 2009). In this model, a k parameter represents the influence of respiration and O_2 and CO_2 concentrations on the firmness loss rate. The change of k can be described using an integrated Michaelis-Menten kinetics as shown in Eq. 5.2 (Hertog, et al., 2004; Castellanos & Algecira, 2012). Furthermore, parameters for Eq. 5.3 are temperature-dependent and this dependence can be represented by an Arrhenius relationship, as shown in Eq. 10 (Sila, et al., 2004).

$$F = F_{fix} + (F_0 - F_{fix})e^{-kt} \quad (1.31)$$

$$k = \frac{k_O^{max} r_{O_2}^{max} y_{O_2}}{K_{mO_2} + y_{O_2}\left(1 + {y_{CO_2}}/{K_{mu_{CO_2}}}\right)} \quad (5.2)$$

$$P_m = P_{mref} e^{\frac{-E_a}{R}\left(\frac{1}{T} - \frac{1}{T_{ref}}\right)} \quad (5.3)$$

In Eq. 5.3, P_m is parameter dependent on T, P_{mref} is the parameter value to T_{ref}, E_a is the activation energy and R is the gas constant.

Color change in fruits occurs when chlorophyll (Chl) is degraded by enzyme action and revealing carotenoids, such as lycopene and carotene, that are present in the peel or flesh (Hörtensteiner, 2006). In some fruits, there are other compounds developed in the ripening, such as anthocyanins, that are responsible for the color evolution (Paliyath & Murr, 2008). Several authors have represented the change in color of the product as a function of storage conditions. In these models, the color is usually represented using color spaces such as CIELAB or HunterLab, where there are three coordinates to define the color at a particular point of the product (Pathare, et al., 2013). In the CIELAB space, color is defined through the coordinates of lightness, L*, and chromaticity, *a**, *b**, and is presented in a three-dimensional space. L* represents the lightness or clarity and is the vertical axis with values ranging between 100, for white, and zero, for black. The axes for *a** and *b** have no specific numeric limits. Positive values for *a** represent red/magenta and negative values represent green. Similarly, positive values for *b** represent yellow and negative values represent blue (Pathare, et al., 2013; Tijskens & Schouten, 2009).

A number of equations have been proposed to represent individual change of the CIELAB coordinates L*, *a** and *b** in the flesh color of the packed feijoa fruits, considering models developed in previous studies (Chen & Ramaswamy, 2002; Castellanos & Algecira, 2012; Pathare, et al., 2013; Ren, et al., 2006). According with the experimental behavior described below, the evolution in lightness (L*) in the fruit flesh was described using a first-order model, as shown in Eq. 5.4, similar to the one used for firmness (Eq. 1.31), where L* is varying over time between an initial L_0* value and an equilibrium L_{fix}* value that is the minimum that can be reached. The change of *a** throughout the storage time (green/red) was represented using a zero-order equation (Eq. 5.5) with an initial a_0* value (similar to Eq. 1.38). A modified kinetic model (Eq. 5.6) was used to represent the evolution in coordinate *b**, also incorporating an initial b_0* value (see results and discussion).

$$L^* = L^*_{Fix} + (L^*_0 - L^*_{Fix})e^{-kt} \quad (5.4)$$

$$a^* = a^*_0 + kt \quad (5.5)$$

$$b^* = b^*_0 + \frac{t}{k_1 + k_2 t + k_3 t^2} \quad (5.6)$$

In Eqs. 5.4-5.6, k parameters represent the influence of the O_2 and CO_2 concentrations on the rate of change of each color coordinate. This dependence was represented using chemical kinetic equations, as shown in Eq. 5.7.

$$\mathrm{k} = k_{\mathrm{T}} \mathrm{y}_{\mathrm{O}_2}^{a} \mathrm{y}_{\mathrm{CO}_2}^{\mathrm{b}} \quad (5.7)$$

The temperature dependence in the change of k parameters, specifically k_T parameters in Eq. 5.7, was described using the Arrhenius' law (Eq. 5.3).

5.2.7 Parameter estimation for the color and firmness models

The equations of firmness and color (L*, *a**, *b**) were fitted to the experimental data measured in the various EMAP conditions and from this, the parameters of each model were estimated by regression to determine the combined influence of the O_2 and CO_2 concentrations and the storage temperature. First, the k values in Eqs. 1.31 (firmness) and 5.4-5.6 (color coordinates) were estimated by linear regression of these equations replacing the experimental measurements of each property at the different measurement times. Then, k values were obtained for each of the combinations of T and O_2 and CO_2 (Table 5.2). To determine the dependence of the k values of each property with respect to the O_2 and CO_2 levels in the packaging headspace, the respective parameters were estimated by linear regression of Eqs. 5.2 (firmness) and 5.7 (for each color coordinate). Finally, the dependence with respect of the storage temperature in the parameters of the Michaelis-Menten kinetics for firmness and the k_T values in chemical kinetics for the color coordinates were also obtained with the linear regression of the Arrhenius' equation (Eq. 5.3), replacing the values of each parameter estimated at each temperature. That is, the k_o^{max}, K_{mO2}, and K_{mCO2} values in Eq. 5.2 and k_T in Eq. 5.7. In Eq. 5.2 for firmness, r_{O2max} corresponds to the maximum rate of O_2 consumption and was estimated from Castellanos et al. (2016). In all of the linear regressions, a method of least squares was used to determine the different parameters.

In order to determine the degree of fit of the model to the experimental data, the R^2_{adj} coefficients were calculated for each property. This allows for the comparison between non-linear models and compensates for possible bias due to a different number of parameters (Spiess & Neumeyer, 2010). In this case, although the equations for the firmness and color models are linear, the complete model of the property is not linear.

5.3 Results and discussion

Table 5.1 shows the properties of physiological maturity (beginning of the storage period) and ripe feijoa fruits. During the ripening time, the produce weight, firmness to penetration,

content of organic acids and lightness (L*) decreased, and the soluble solids and color coordinates *a** (green to red) and *b** (blue to yellow) increased. These values were used subsequently for comparison purposes and as initial and equilibrium values in the firmness and color models.

Table 5.1. Physico-chemical properties of the feijoa fruits

Parameter	Physiological maturity[a]	Ripe fruits
Weight per fruit (g)	58.61 ± 3.25	…
Firmness (N)	76.60 ± 3.93	23.40 ± 4.08
Color parameters (CIELAB)		
L*	79.94 ± 1.99	60.01 ± 3.11
*a**	-2.93 ± 0.11	1.56 ± 0.34
*b**	12.46 ± 1.30	21.74 ± 1.72
Total soluble solids (°Brix)	10.73 ± 0.43	12.53 ± 0.77
Organic acids (g/kg)		
Citric	39.80 ± 6.47	13.65 ± 1.56
Malic	1.55 ± 0.24	0.55 ± 0.18
Oxalic	0.81 ± 0.18	0.39 ± 0.12

[a] Day zero of storage.

The standard deviation of each value is included.

5.3.1 EMAP simulation

From the simulations performed for the different EMAP configurations, it was decided to perform the packaging tests with perforated bags (1, 2 and 3 perforations) at 12 and 17 °C and with bags without perforations and with 1 and 2 perforations at 6 °C. Through the simulations, it was estimated that the equilibrium O_2 and CO_2 concentrations in each EMAP of the experimental design were different from each other to compare the individual effect of these levels of gases on the properties of the packed fruit. The experimental evolution of the O_2 and CO_2 levels in each EMAP system can be seen in Fig. 5.1 (symbols). In all of the PP bags, steady gas levels were reached between the 1st and 4th day of storage. Previous estimates done with the MAP model proved to be successful, as shown in Fig. 5.1 (lines), except for the unperforated PP bags at 6 °C, where the CO_2 concentration was somewhat higher than expected, 5.60 % versus 4.01 % predicted by the model. The coefficients of determination (R^2) obtained for the simulation with respect to the experimental data were 0.93 and 0.86 for O_2 and CO_2, respectively. This is consistent with the results obtained in Castellanos et al. (2016). The deviation for CO_2 in the PP bags without perforations can be

attributed to the fact that the O_2 level remained close to 1 % resulting in the development of some anaerobic processes that are not taken into account in the Michaelis-Menten kinetics (Eq. 1.8) to describe respiration (Castellanos et al., 2016; Mangaraj & Goswami, 2011).

Table 5.2. Parameters of feijoa respiration and gas exchange in the PP bags used for the simulation of the O_2 and CO_2 evolution in the EMAP system

Respiration parameters[a]	r_{O2} ($cm^3\ kg^{-1}\ d^{-1}$)	r_{CO2} ($cm^3\ kg^{-1}\ d^{-1}$)	
6 °C			
$r_{max\ (cm^3\ kg^{-1}\ d^{-1})}$	1452.76	1766.06	
K_m	0.05	0.05	
K_{muCO2}	0.03	0.02	
12 °C			
$r_{max\ (cm^3\ kg^{-1}\ d^{-1})}$	2703.64	3054.53	
K_m	0.09	0.08	
K_{muCO2}	0.05	0.05	
17 °C			
$r_{max\ (cm^3\ kg^{-1}\ d^{-1})}$	4448.58	4739.26	
K_m	0.14	0.11	
K_{muCO2}	0.09	0.10	
Gas exchange parameters[a]	O_2	CO_2	N_2
PP permeability coefficients, Q ($cm^3\ mm\ m^{-2}\ d^{-1}\ atm^{-1}$)			
6 °C	31.89	192.08	29.31
12 °C	48.70	227.91	42.90
17 °C	68.44	261.42	61.53
Transmission rates through the perforations, K_{TR} ($cm^3\ d^{-1}$)			
6 °C			
1 perf.	455.52	288.74	450.35
2 perf.	680.43	427.93	672.72
3 perf.	854.65	535.48	844.97
12 °C			
1 perf.	473.20	300.22	467.83
2 perf.	706.84	444.94	698.83
3 perf.	887.82	556.76	877.77
17 °C			
1 perf.	487.86	309.75	482.33
2 perf.	728.75	459.06	720.50
3 perf.	915.35	574.44	904.97

[a] Estimated from Castellanos et al. (2016).

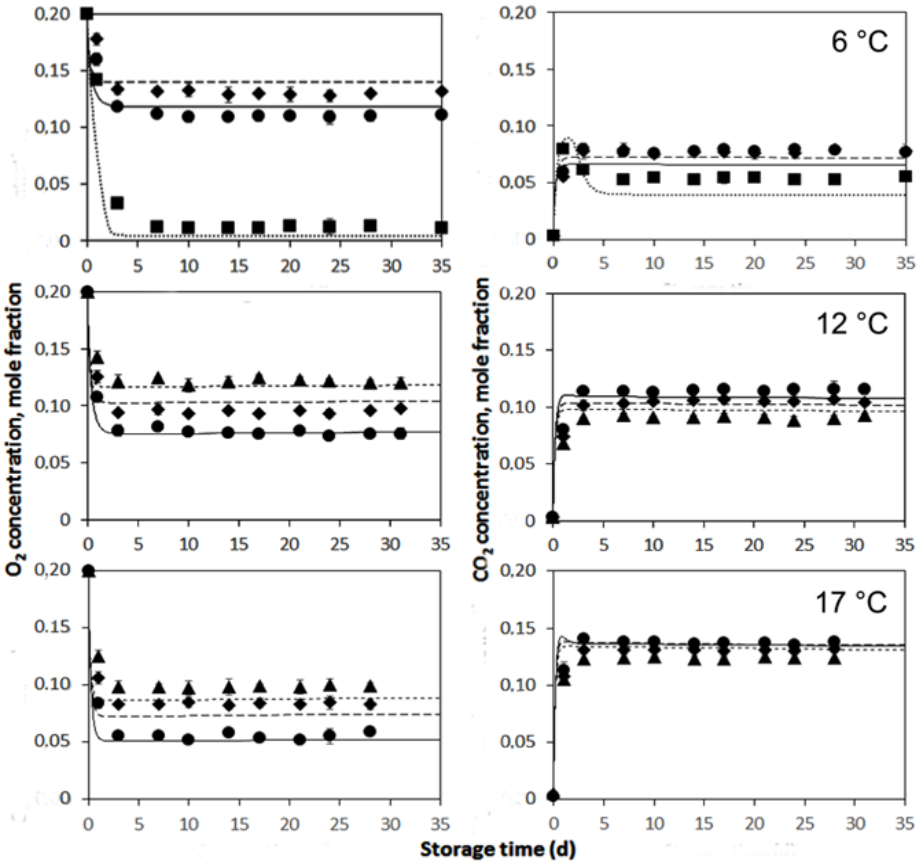

Figure 5.1. O_2 and CO_2 evolution inside the PP bags without perforations (■) and with one (●), two (♦) or three (▲) 0.225 mm perforations at 6, 12 and 17 °C for feijoa fruits. Lines represent predicted O_2 and CO_2 concentrations using the MAP model.

5.3.2 Packaging tests

With the simulation results, the feijoa fruits were packed in nine packaging combinations at the three evaluated temperatures, while others were left unpacked at 17 °C as control samples (Table 5.3). As mentioned before, in all of the bags, steady levels of O_2 and CO_2 were reached plus a relative humidity of 100% as a few condensed water droplets were observed on the internal surface of the packages.

5.3.3 Deterioration Index

According to the evidence of deterioration, which gradually increased with storage time (Table 5.4), the fruits packed in different configurations were removed from the test after reaching condition 4 (significant deterioration). The fruits stored at 17 °C without packaging were removed after 17 days of storage, those packed at 17 °C at 28 days, those packed at 12 °C at 33 days and the ones packed at 6 °C between 35 and 38 days after the start of

the storage. At 12 °C, the fruits packed in bags with one perforation had further deterioration, as compared to those packed with 2-3 perforations. At 17 °C, the evidence of deterioration was similar for all three combinations of packaging. For 'Unique' feijoa fruits, East et al. (2009) reported deterioration evidence at 4 °C and ca. 1 % of O_2 and 0.1 % of CO_2 after 6 weeks of storage, something similar to the fruits packed in bags without perforations but with a longer storage time. On the other hand, Galvis (2003) reported deterioration evidence at 6 °C and 6 % of O_2 and 3.7 % of CO_2 after 3 weeks; for the fruits packed in bags with one perforation (11 % of O_2 and 7.8 % of CO_2), a longer storage time (38 days) was obtained instead.

Table 5.3. Experimental design and level of gases in each packaging system

T (°C)	Packaging	External RH (%)	Eq. yO_2[b]	Eq. yCO_2[b]	Internal RH (%)
6	PP Bag[a]	85±2	0.012 (0.90 kPa)	0.056 (4.18 kPa)	100
6	Bag + 1 perf.	85±2	0.110 (8.21)	0.078 (5.82)	100
6	Bag + 2 perf.	85±2	0.130 (9.71)	0.076 (5.67)	100
12	Bag + 1 perf.	85±2	0.076 (5.67)	0.115 (8.59)	100
12	Bag + 2 perf.	85±2	0.095 (7.09)	0.105 (7.84)	100
12	Bag + 3 perf.	85±2	0.121 (9.03)	0.091 (6.79)	100
17	Bag + 1 perf.	85±2	0.055 (4.11)	0.138 (10.30)	100
17	Bag + 2 perf.	85±2	0.083 (6.20)	0.131 (9.78)	100
17	Bag + 3 perf.	85±2	0.098 (7.32)	0.124 (9.26)	100
17	No Pack[c]	68±2	0.202 (15.08)	0.005 (0.37)	…

[a] PP bags without perforations and with one, two or three perforations of 0.225 mm.

[b] Equilibrium O_2 and CO_2 concentrations in the packaging system (P = 74.7 kPa).

[c] Control fruits.

5.3.4 Weight loss

The weight loss in the fruits stored without packaging at 17 °C was considerable, 6.82% for day 14, while that corresponding to the fruits packed in PP bags was significantly lower as shown at the top of Table 5.4. Temperature had the greatest effect on weight loss, being greater at 17 °C than at 12 °C and 6 °C. In addition, the O_2 concentration in the EMAP influenced the weight loss in the packed fruits with lower values corresponding to fewer perforations (lower O_2 levels). For bags without perforations at 6 °C, the weight loss was 0.64% on day 35, followed by 1.64% for bags with one perforation, while the fruits packed in bags with three perforations at 17 °C lost 4.08% of their initial weight after 28 days of storage. This loss occurs mainly via transpiration, which in turn is influenced by the difference of partial pressures of water between the surface of the fruit and the headspace

surrounding it, and its metabolic processes of respiration and the breaking down of substrates (East, et al., 2009; Sousa-Gallagher et al., 2013).

Table 5.4. Weight loss, firmness and deterioration index of the feijoa fruits during the storage time in the EMAP systems.

Parameter	EMAP	Day 0	Day 14	Day 21	Day 28	Day 35
Weight loss (%)	6 °C, bag + no perf.	..	0.35 ± 0.06^{a}	0.42 ± 0.06^{ab}	0.57 ± 0.03^{bc}	0.64 ± 0.06^{c}
	6 °C, bag + 1 perf.	..	0.67 ± 0.08^{c}	0.90 ± 0.06^{d}	1.32 ± 0.08^{fg}	1.64 ± 0.11^{hi}
	6 °C, bag + 2 perf.	..	0.67 ± 0.04^{c}	1.00 ± 0.12^{de}	1.41 ± 0.13^{g}	1.81 ± 0.08^{ij}
	12 °C, bag + 1 perf.	..	1.16 ± 0.14^{ef}	1.78 ± 0.04^{ij}	2.29 ± 0.11^{l}	..
	12 °C, bag + 2 perf.	..	1.35 ± 0.09^{fg}	1.95 ± 0.09^{jk}	2.59 ± 0.12^{mn}	..
	12 °C, bag + 3 perf.	..	1.46 ± 0.04^{gh}	2.12 ± 0.09^{kl}	2.76 ± 0.08^{no}	..
	17 °C, bag + 1 perf.	..	1.67 ± 0.12^{i}	2.48 ± 0.19^{m}	3.19 ± 0.15^{p}	..
	17 °C, bag + 2 perf.	..	1.71 ± 0.20^{i}	2.67 ± 0.06^{mn}	3.67 ± 0.15^{q}	..
	17 °C, bag + 3 perf.	..	1.81 ± 0.24^{ij}	2.89 ± 0.19^{o}	4.08 ± 0.21^{r}	..
	17 °C, No pack	..	9.82 ± 0.15^{s}	..	..	..
Firmness (N)	6 °C, bag + no perf.	76.60 ± 3.93^{a}	47.80 ± 2.33^{b}	41.30 ± 2.98^{cd}	31.40 ± 3.96^{gh}	23.53 ± 2.42^{kl}
	6 °C, bag + 1 perf.	"	41.50 ± 4.97^{c}	31.40 ± 3.03^{gh}	22.34 ± 2.55^{lm}	20.43 ± 3.35^{lmno}
	6 °C, bag + 2 perf.	"	38.30 ± 2.66^{de}	28.40 ± 4.00^{hij}	21.65 ± 2.95^{lmo}	19.97 ± 3.79^{mnop}
	12 °C, bag + 1 perf.	"	36.67 ± 1.81b^{ef}	25.55 ± 4.17^{jk}	18.81 ± 1.56^{nopq}	..
	12 °C, bag + 2 perf.	"	34.20 ± 3.39^{fg}	20.53 ± 4.83^{lmno}	16.60 ± 1.28^{qr}	..
	12 °C, bag + 3 perf.	"	30.77 ± 3.85^{hi}	21.21 ± 4.55^{lm}	15.77 ± 2.15^{qr}	..
	17 °C, bag + 1 perf.	"	34.09 ± 3.31^{fg}	25.50 ± 2.93^{jk}	20.48 ± 3.83^{lmno}	..
	17 °C, bag + 2 perf.	"	30.10 ± 4.82^{hi}	21.49 ± 2.48^{lmno}	16.90 ± 3.42^{pqr}	..
	17 °C, bag + 3 perf.	"	28.00 ± 4.36^{ij}	18.42 ± 0.78^{opqr}	15.39 ± 1.62^{r}	..
	17 °C, No pack	"	19.86 ± 2.81^{mnop}	..	..	..
Deterioration Index[a]	6 °C, bag + no perf.	1	1	2	2	3
	6 °C, bag + 1 perf.	"	1	1	1	2
	6 °C, bag + 2 perf.	"	1	1	1	2
	12 °C, bag + 1 perf.	"	1	1	3	..
	12 °C, bag + 2 perf.	"	2	2	2	..
	12 °C, bag + 3 perf.	"	1	1	2	..
	17 °C, bag + 1 perf.	"	1	2	4	..
	17 °C, bag + 2 perf.	"	1	3	3	..
	17 °C, bag + 3 perf.	"	1	2	4	..
	17 °C, No pack	"	2	..	..	..

Means with different letters across each column and row are significantly different at P≤ 0.05 by the Tukey's HSD test. The standard deviation (SD) is included.

[a] 1 = no deterioration evidence, 2 = very light deterioration, 3 = moderate deterioration, 4 = considerable deterioration.

For the fruits without packaging, the transpiration was greater due to the higher constant difference between the partial pressure of water in the fruits and in the storage chamber

(68% RH). For the packed fruits, the difference between the partial pressure of water and the headspace (initially 85% RH) was lower and it became even smaller when the headspace was saturated (small drops of condensed water were observed in the internal package walls) after 1-3 days of storage for all the EMAP. The difference in weight loss for the different EMAP systems was in the elapsed time for the headspace saturation, which was higher for the packages with more perforations (more mass transfer area) and at higher temperatures as a result of the higher exchange rates of water vapor towards the outside (Sousa-Gallagher et al., 2013; Techavises & Hikida, 2008).

5.3.5 Firmness

The fruit firmness decreased significantly for all the packaging systems throughout the storage time; from 76.6 N on day zero to 15.39 N on day 28 for the fruits packed in bags with three perforations at 17 °C, as shown in Table 5.4. Also, on day 14, there was a significant difference between the fruits stored without packaging (19.86 N) and those packed in different EMAP combinations (47.80-28.00 N).

As with the weight loss, temperature had a significant effect on the loss of firmness of the fruits, as can be seen by comparing the packaging systems with the same number of perforations at different storage temperatures on each measurement day. At higher temperatures, the firmness loss was higher. At the same temperature, the fruits packed with a higher O_2 level had greater firmness loss, as shown in Table 5.4. The combined effect of temperature and level of gases was more relevant for the firmness than for the weight loss. In the case of weight, there were significant differences between the fruits packed at different temperatures and different number of perforations (e.g. 6 °C and 3 perforations and on the other hand 12 °C and 1 perforation), whereas, in the case of firmness, this difference was not significant although higher firmness values were measured at the lower temperature. At a lower temperature, the rate of degradation of structural compounds in the cell wall, such as pectins and hemi-celluloses, and the water retention capacity become lower and, therefore, the loss of firmness becomes lower in turn (Biswas, et al., 2014; Paliyath & Murr, 2008; Parra & Fischer, 2014). Likewise, in the metabolic oxidation reactions of substrates, the reduced availability of O_2 slows down these processes, delaying the firmness loss (Gwanpua, et al., 2012; Hertog, et al., 2004). By day 21, the fruits packed at 12 and 17 °C with 2 and 3 perforations had reached the firmness corresponding to the ripeness stage (23.80 N). By day 28, the ripeness firmness was

reached in all of the EMAP systems, except the samples packed at 6 °C without perforations (31.40 N), coming close the fruits packed at 6 °C and 1 perforation (22.34 N).

5.3.6 Color

It was decided to measure the change in color of the fruit flesh because the peel maintains a green hue independent of its degree of ripeness. The color coordinates of the fruit flesh significantly changed relative to the initial day measurements as shown in Table 5.5. Flesh lightness L* decreased in all cases, while the coordinate *a** values increased from green (-) to red (+), as shown in Table 5.5 and Figures 5.3 and 5.4, L* from 79.94 to 58.48 and *a** from -2.93 to 4.67. With respect to *b**, it increased to approximately the value corresponding to ripe fruits (21-22) and then progressively decreased from 12.46 to 18.60, with a maximum value of 22.98 for fruits packed at 17 °C and 1 perforation. On day 14, the L* and *a** values for the fruits stored at 17 °C without packaging were significantly different with respect to the packed fruits, while for *b**, the measured values were higher for the fruits without packaging than for the packed fruits. However, this difference was not significant with respect to the samples packed at 17 °C with 2 and 3 perforations although, as shown in Figure 5.5, the measured values of *b** reached those corresponding to ripe fruits and were already decreasing.

As with firmness, the greatest changes occurred at the higher storage temperatures, and higher O_2 and lower CO_2 concentrations (more perforations or no packaging). Nonetheless, the combined effect of temperature and level of gases in the headspace was more apparent for L* and *a** than for *b**, with closer values for the latter by day 28 of storage. By day 21, the fruits packed at 17 °C with three perforations reached the color coordinates of the ripeness stage, as shown in Table 3. By day 28, the fruits at 12 and 17 °C reached the ripeness color coordinates, except the samples packed in bags with 1 perforation, while at 6 °C, only the packaging systems with 3 perforations were close to these values (L* = 60.97, *a** = 2.53 and *b** = 20.91). After 35 days of storage, only the fruits in bags without perforations at 6 °C had not reached the ripeness values. This evolution in color is caused, as with the other properties, by differences in temperature and concentration of gases in the headspace. A higher storage temperature results in a higher rate of degradation of chlorophylls by action of three Chl catabolic enzymes: chlorophyllase, phe+ophorbide*a* oxygenase (PAO) and red Chl catabolite reductase (RCCR), leading to higher values of *a** and *b**, and a greater rate of synthesis of carotenoids and anthocyanins, leading to lower L* values and higher values of *a** and *b**. The same occurs when fruits are exposed to

higher O_2 concentrations, which allows oxidation reactions, ending in color loss and flesh browning (Alam & Goyal, 2006; Hörtensteiner, 2006; Pathare, et al., 2013).

Table 5.5. Flesh color (L*, *a** and *b** coordinates) of the feijoa fruits during the storage time in the EMAP systems.

Parameter	EMAP	Day 0	Day 14	Day 21	Day 28	Day 35
Ligthness (L*)	6 °C, bag + no perf.	79.94 ± 1.99^{a}	72.81 ± 1.57^{b}	68.99 ± 2.45^{cde}	66.85 ± 1.95^{ghi}	63.17 ± 2.02^{lmn}
	6 °C, bag + 1 perf.	"	70.21 ± 1.18^{c}	66.77 ± 1.03^{ghi}	62.13 ± 1.35^{nop}	59.16 ± 1.82^{rs}
	6 °C, bag + 2 perf.	"	68.46 ± 1.84^{def}	65.31 ± 1.39^{ijk}	60.97 ± 1.17^{pq}	57.36 ± 1.94^{tuv}
	12 °C, bag + 1 perf.	"	70.39 ± 1.87^{c}	66.16 ± 1.49^{ghij}	62.70 ± 1.61^{mno}	..
	12 °C, bag + 2 perf.	"	67.60 ± 1.84^{efg}	62.07 ± 1.37^{nop}	58.73 ± 2.04^{rst}	..
	12 °C, bag + 3 perf.	"	65.82 ± 0.75^{hij}	61.59 ± 1.69^{nopq}	56.15 ± 1.64^{uv}	..
	17 °C, bag + 1 perf.	"	69.26 ± 0.89^{cd}	64.58 ± 2.25^{jkl}	60.06 ± 1.93^{qr}	..
	17 °C, bag + 2 perf.	"	67.31 ± 1.01^{fgh}	61.45 ± 3.7^{opq}	56.07 ± 2.61^{vw}	..
	17 °C, bag + 3 perf.	"	64.20 ± 1.90^{klm}	57.75 ± 1.67^{stu}	54.48 ± 2.15^{w}	..
	17 °C, No pack	"	55.87 ± 1.19^{vw}	..	..	..
Red/green (a*)	6 °C, bag + no perf.	-2.93 ± 0.11^{a}	-1.19 ± 0.51^{b}	-0.48 ± 0.31^{cd}	0.79 ± 0.40^{ij}	1.63 ± 0.41^{lm}
	6 °C, bag + 1 perf.	"	-0.42 ± 0.50^{cd}	0.62 ± 0.28^{ghi}	1.94 ± 0.23^{mn}	2.97 ± 0.32^{pq}
	6 °C, bag + 2 perf.	"	-0.28 ± 0.16^{de}	0.97 ± 0.58^{ij}	2.53 ± 0.62^{o}	3.69 ± 0.24^{r}
	12 °C, bag + 1 perf.	"	-0.55 ± 0.40^{c}	0.67 ± 0.26^{hi}	1.92 ± 0.35^{mn}	..
	12 °C, bag + 2 perf.	"	0.15 ± 0.41^{ef}	1.48 ± 0.40^{kl}	3.29 ± 0.39^{q}	..
	12 °C, bag + 3 perf.	"	0.27 ± 0.19^{fg}	2.11 ± 0.27^{n}	3.69 ± 0.22^{r}	..
	17 °C, bag + 1 perf.	"	-0.42 ± 0.12^{cd}	1.11 ± 0.42^{jk}	2.60 ± 0.34^{op}	..
	17 °C, bag + 2 perf.	"	0.30 ± 0.78^{fgh}	2.09 ± 0.63^{n}	3.98 ± 0.59^{rs}	..
	17 °C, bag + 3 perf.	"	0.71 ± 0.53^{i}	2.85 ± 0.49^{op}	4.67 ± 0.31^{t}	..
	17 °C, No pack	"	4.08 ± 0.49^{s}	..	..	..
Yellow/blue (b*)	6 °C, bag + no perf.	12.46 ± 1.30^{a}	15.38 ± 0.62^{b}	17.01 ± 0.63^{d}	18.95 ± 0.62^{ghi}	20.43 ± 1.10^{kl}
	6 °C, bag + 1 perf.	"	16.14 ± 0.47^{bc}	18.08 ± 1.20^{ef}	20.51 ± 1.03^{lm}	21.65 ± 0.86^{pqr}
	6 °C, bag + 2 perf.	"	16.71 ± 1.05^{cd}	18.43 ± 1.04^{fg}	21.33 ± 1.29^{nopq}	22.34 ± 1.05^{rst}
	12 °C, bag + 1 perf.	"	18.45 ± 0.96^{fg}	21.60 ± 0.90^{opqr}	22.90 ± 0.47^{t}	..
	12 °C, bag + 2 perf.	"	18.90 ± 0.37^{gh}	22.01 ± 0.69^{qrs}	22.10 ± 0.46^{qrs}	..
	12 °C, bag + 3 perf.	"	19.70 ± 0.94^{ijk}	22.50 ± 0.75st	21.68 ± 0.47^{pqr}	..
	17 °C, bag + 1 perf.	"	20.13 ± 1.14^{jk}	22.98 ± 0.66^{t}	20.91 ± 1.16^{lmnop}	..
	17 °C, bag + 2 perf.	"	20.82 ± 0.49^{lmno}	21.99 ± 0.51^{qrs}	19.38 ± 0.53^{hij}	..
	17 °C, bag + 3 perf.	"	21.11 ± 0.80^{mnop}	20.73 ± 0.96^{lmn}	18.60 ± 1.06^{fgh}	..
	17 °C, No pack	"	21.37 ± 1.21^{nopq}	..	..	..

Means with different letters across each column and row are significantly different at P≤ 0.05 by the Tukey's HSD test. SD included.

Table 5.6. Content of Oxalic, Citric and Malic acids in the feijoa fruits during the storage time in the EMAP systems.

Parameter	EMAP	Day 0	Day 14	Day 21	Day 28	Day 35
Oxalic acid (g kg^{-1})	6 °C, bag + no perf.	0.81 ± 0.18^{a}	0.57 ± 0.06^{b}	0.49 ± 0.06^{de}	0.42 ± 0.01^{ghi}	0.40 ± 0.03^{hijkl}
	6 °C, bag + 1 perf.	"	0.55 ± 0.01^{bc}	0.43 ± 0.07^{ghi}	0.35 ± 0.05^{jklmn}	0.34 ± 0.03^{mnno}
	6 °C, bag + 2 perf.	"	0.54 ± 0.07^{bc}	0.42 ± 0.04^{ghi}	0.34 ± 0.05^{lmno}	0.32 ± 0.02^{no}
	12 °C, bag + 1 perf.	"	0.50 ± 0.03^{cd}	0.43 ± 0.03^{fghi}	0.39 ± 0.01^{ijklm}	..
	12 °C, bag + 2 perf.	"	0.49 ± 0.03^{de}	0.41 ± 0.02^{ghi}	0.35 ± 0.02^{klmn}	..
	12 °C, bag + 3 perf.	"	0.48 ± 0.07^{de}	0.40 ± 0.07^{hij}	0.33 ± 0.04^{no}	..
	17 °C, bag + 1 perf.	"	0.51 ± 0.12^{cd}	0.45 ± 0.05^{efg}	0.40 ± 0.05^{hijk}	..
	17 °C, bag + 2 perf.	"	0.45 ± 0.08^{efgh}	0.41 ± 0.02^{ghi}	0.35 ± 0.05^{klmn}	..
	17 °C, bag + 3 perf.	"	0.41 ± 0.08^{ghi}	0.33 ± 0.07^{no}	0.30 ± 0.03^{o}	..
	17 °C, No pack	"	0.42 ± 0.10^{ghi}	..	..	..
Citric acid (g kg^{-1})	6 °C, bag + no perf.	39.80 ± 2.49^{a}	20.44 ± 1.72^{b}	19.60 ± 2.29^{bc}	15.33 ± 1.67^{fgh}	13.18 ± 1.91^{ij}
	6 °C, bag + 1 perf.	"	17.67 ± 2.15^{de}	16.59 ± 2.11^{ef}	13.07 ± 0.90^{ij}	11.78 ± 1.68^{jklmn}
	6 °C, bag + 2 perf.	"	18.41 ± 1.37^{cd}	15.11 ± 1.22^{gh}	12.02 ± 0.91^{jklmn}	10.12 ± 0.73^{op}
	12 °C, bag + 1 perf.	"	17.57 ± 0.49^{de}	15.18 ± 0.69^{fgh}	11.00 ± 1.00^{no}	..
	12 °C, bag + 2 perf.	"	15.18 ± 1.57^{fgh}	12.53 ± 2.03^{ijklm}	9.36 ± 0.71^{pq}	..
	12 °C, bag + 3 perf.	"	13.49 ± 1.84^{i}	11.23 ± 0.77^{mno}	8.22 ± 0.66^{q}	..
	17 °C, bag + 1 perf.	"	18.90 ± 1.98^{cd}	15.79 ± 1.56^{fg}	12.93 ± 2.01^{ijk}	..
	17 °C, bag + 2 perf.	"	17.72 ± 1.43^{de}	12.67 ± 2.24^{ijkl}	11.34 ± 2.65^{lmno}	..
	17 °C, bag + 3 perf.	"	13.95 ± 1.48^{hi}	11.53 ± 1.43^{klmno}	8.84 ± 0.66^{pq}	..
	17 °C, No pack	"	13.56 ± 1.67^{i}	..	..	..
Malic acid (g kg^{-1})	6 °C, bag + no perf.	1.55 ± 0.12^{a}	0.97 ± 0.06^{b}	0.78 ± 0.08^{d}	0.60 ± 0.03^{fg}	0.56 ± 0.09^{gh}
	6 °C, bag + 1 perf.	"	0.99 ± 0.10^{b}	0.73 ± 0.16^{de}	0.54 ± 0.03^{hij}	0.44 ± 0.04^{mn}
	6 °C, bag + 2 perf.	"	0.87 ± 0.04^{c}	0.62 ± 0.16^{f}	0.46 ± 0.02^{klm}	0.42 ± 0.05^{mn}
	12 °C, bag + 1 perf.	"	0.69 ± 0.06^{e}	0.56 ± 0.06^{ghi}	0.45 ± 0.05^{lmn}	..
	12 °C, bag + 2 perf.	"	0.53 ± 0.06^{hij}	0.40 ± 0.04^{no}	0.34 ± 0.02^{pqr}	..
	12 °C, bag + 3 perf.	"	0.53 ± 0.02^{hij}	0.35 ± 0.02^{opq}	0.28 ± 0.02^{s}	..
	17 °C, bag + 1 perf.	"	0.52 ± 0.07^{hijk}	0.40 ± 0.03^{nop}	0.32 ± 0.03^{qrs}	..
	17 °C, bag + 2 perf.	"	0.50 ± 0.04^{ijkl}	0.36 ± 0.03^{opq}	0.29 ± 0.02^{rs}	..
	17 °C, bag + 3 perf.	"	0.49 ± 0.05^{jkl}	0.34 ± 0.03^{pqr}	0.26 ± 0.03^{s}	..
	17 °C, No pack	"	0.42 ± 0.08^{mn}	..	..	..

Means with different letters across each column and row are significantly different at P≤ 0.05 by the Tukey's HSD test. SD included.

5.3.7 Organic acids

From the data obtained for the feijoa fruits, malic acid is the most abundant organic acid, followed by malic and oxalic, as reported in other studies (Galvis, 2003; Parra & Fischer, 2014). The concentration of organic acids measured for the different packed fruits decreased with storage time and, as with the other properties, was significantly different compared to the day zero values, as shown in Table 5.6. For the malic acid, the measured

values were lower and significantly different between the fruits without packaging and the packed fruits on day 14, while for citric and oxalic acids, the concentrations were lower for the samples without packaging, but only significantly different from the fruits stored at 12 and 6 °C. In this case, the storage temperature was also responsible for the greatest effect on decreasing the concentration of acids, followed by the gas levels. The smaller decrease in acid concentration was observed for the fruits stored at 6 °C without packaging and with one perforation, while the highest decrease, besides the fruits without packaging, was for samples packed at 17 °C with three perforations. In the fresh produce, organic acids accumulate during growth and are then used as substrates in respiration processes and energy production during ripening (Parra & Fischer, 2014; Selcuk & Erkan, 2015). By increasing the temperature and the O_2 concentration in the headspace, these oxidation reactions occur faster in the same way as reactions leading to changes in other properties of the fruits (Banda, et al., 2015; Selcuk & Erkan, 2015).

5.3.8 Most suitable EMAP system

According to the evolution of the evaluated properties and the rate of deterioration for the different EMAP systems, the bags with two perforations at 6 °C allowed the longest preservation time and greatest delay in the maturation process. For this EMAP, the ripeness stage was reached after 25 and 28 days of storage and the fruits could be kept for more than 35 days considering the evidence of deterioration. The fruits stored at 6 °C with three perforations were also kept for longer than 35 days, but there was a greater change in their properties with respect to the fruits packed with two perforations, and the coordinates L* and a* were significantly different between the two EMAP systems at day 35. In the bags without perforations, the fruits reached condition 3 of deterioration by day 35 due to the low O_2 concentration in the packaging headspace. As for the other temperatures, the fruits packed at 12 °C with two and three perforations were properly preserved after 31 days of storage although with greater changes in their properties with respect to the EMAP combinations mentioned above. The fruits packed at 6 °C with one perforation (at 11 % of O_2 and 7.8 % of CO_2) could be maintained for a period roughly two times longer with respect to the fruits stored at room conditions. Al-Harthy et al. (2009) and East et al. (2009) for their part, obtained a preservation approximately three times as long respecting the room conditions, storing the produce at 4-5 °C and 0-2 % of O_2 and 0-1 % of CO_2 for cultivars ‘Unique’ and ‘Opal Star’. However, these cultivars from New Zealand seem to have greater tolerance to chilling injury and very low concentrations of O_2 with respect to those used in

this study, which begin to experience deterioration at temperatures below 6 °C (Parra & Fischer, 2014) and as observed in the experiments at O_2 concentrations close to 1 %.

5.3.9 Modelling firmness and color

According to the experimental behavior, a first-order model with fractional conversion (Eq. 1.31) was used to represent the evolution in the fruit firmness, in similar way to that reported by Schouten et al. (2007) for tomato. As mentioned before, in the Eq. 1.31 the parameter k represents the rate of firmness loss due to the O_2 and CO_2 concentrations and temperature. The dependence of k, the rate of firmness loss, on the level of gases was represented using a Michaelis-Menten kinetics where the maximum rate of O_2 consumption by the fruit r_{O2}^{max} was included. By increasing the O_2 concentration available in the headspace, the rate of firmness loss was higher, as shown in Figure 5.2 at each test temperature. In addition, an increase in CO_2 concentration delays the firmness loss. The influence of the storage temperature was included in the parameters of Eq. 5.2 using Arrhenius' Law. The relationship between the temperature and firmness loss was direct, increasing the former by increasing the second, as can be seen by comparing the sub-plots in Figure 5.2 for the three storage temperatures. This behavior is similar to that reported by Castellanos & Algecira (2012) for banana, Hertog, et al. (2003) for avocado and Hertog, et al., (2004) for kiwi fruits. The parameters of the model of firmness are in Table 5.7 (top). The adjusted regression coefficient, R^2_{adj}, for the model of firmness was equal to 0.948, showing a good degree of fit with respect to the experimental behavior, as shown in Figure 5.2. For the bags without perforations at 6 °C, the values estimated by the model are far from those experimentally obtained because the low O_2 concentration in the headspace led to anaerobic degradation processes that were not considered in Eq. 5.2. In this case, to complement Eq. 5.2, a term corresponding to anaerobic respiration should be included (Hertog, et al., 2004) although it should be noted from which O_2 levels these processes begin to be relevant.

Decrease of lightness in the fruit flesh as a function of storage time was represented also by using a first-order model with fractional conversion (Eq. 5.4) according to the experimental behavior shown in Figure 5.3 for the several EMAP systems. This behavior is similar to that reported by Salinas-Hernández et al. (2015) for fresh-cut mango. The k parameter of lightness loss was linked to the O_2 and CO_2 concentrations through an equation of chemical kinetics (Eq. 5.7), while the temperature-influence was represented in the k_T parameter of lightness loss due to the storage temperature, using Arrhenius' Law.

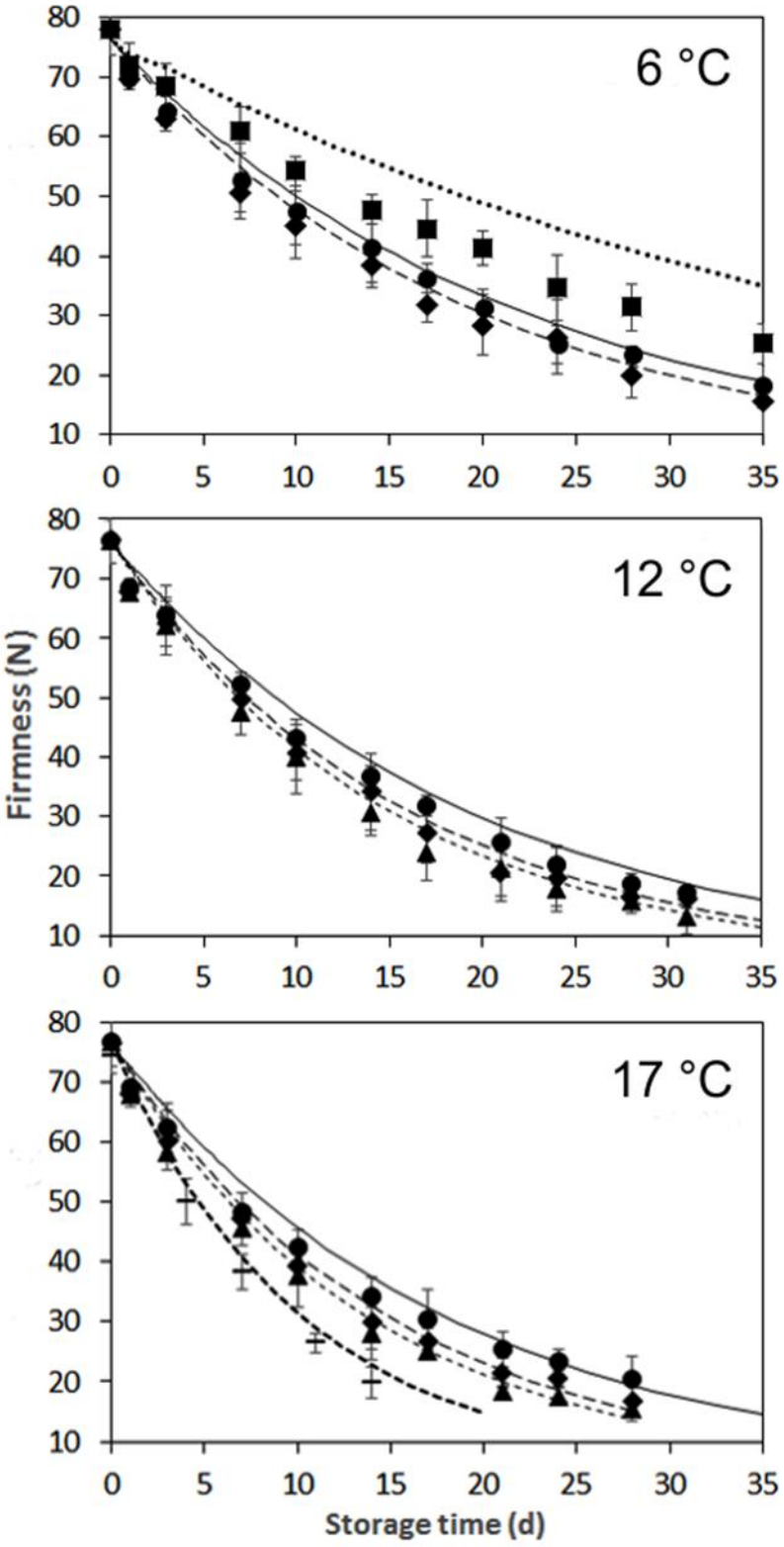

Figure 5.2. Evolution of the firmness in the feijoa fruits stored without packaging (-) and packed in PP bags without perforations (■) and with one (●), two (♦) or three (▲) 0.225 mm perforations at 6, 12 and 17 °C. Lines represent firmness values predicted by the model. Bars represent SD.

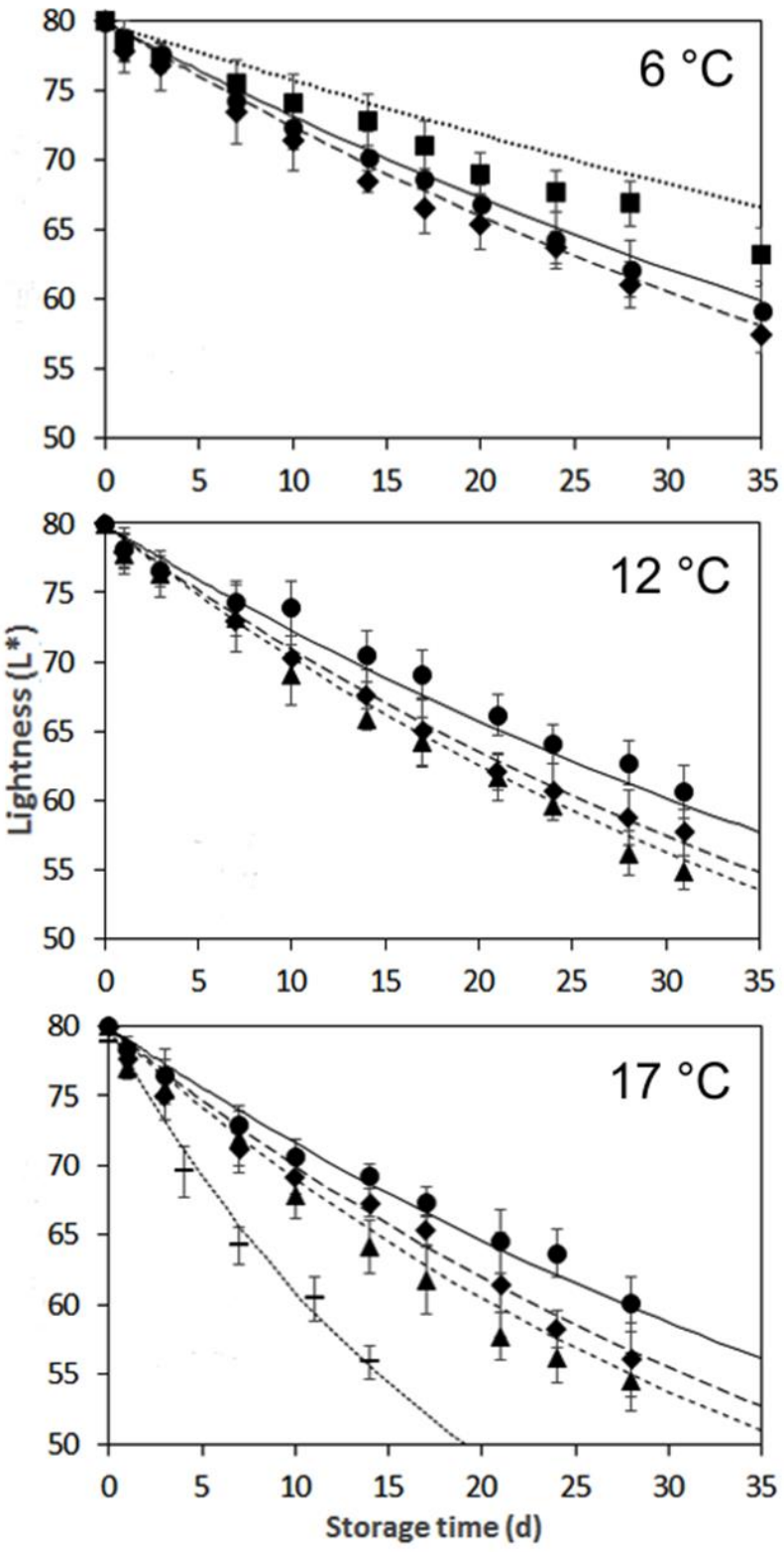

Figure 5.3. Evolution of the flesh lightness (L*) in the feijoa fruits stored without packaging (-) and packed in PP bags without perforations (■) and with one (●), two (♦) or three (▲) 0.225 mm perforations at 6, 12 and 17 °C. Lines represent L* values predicted by the model. Bars represent SD.

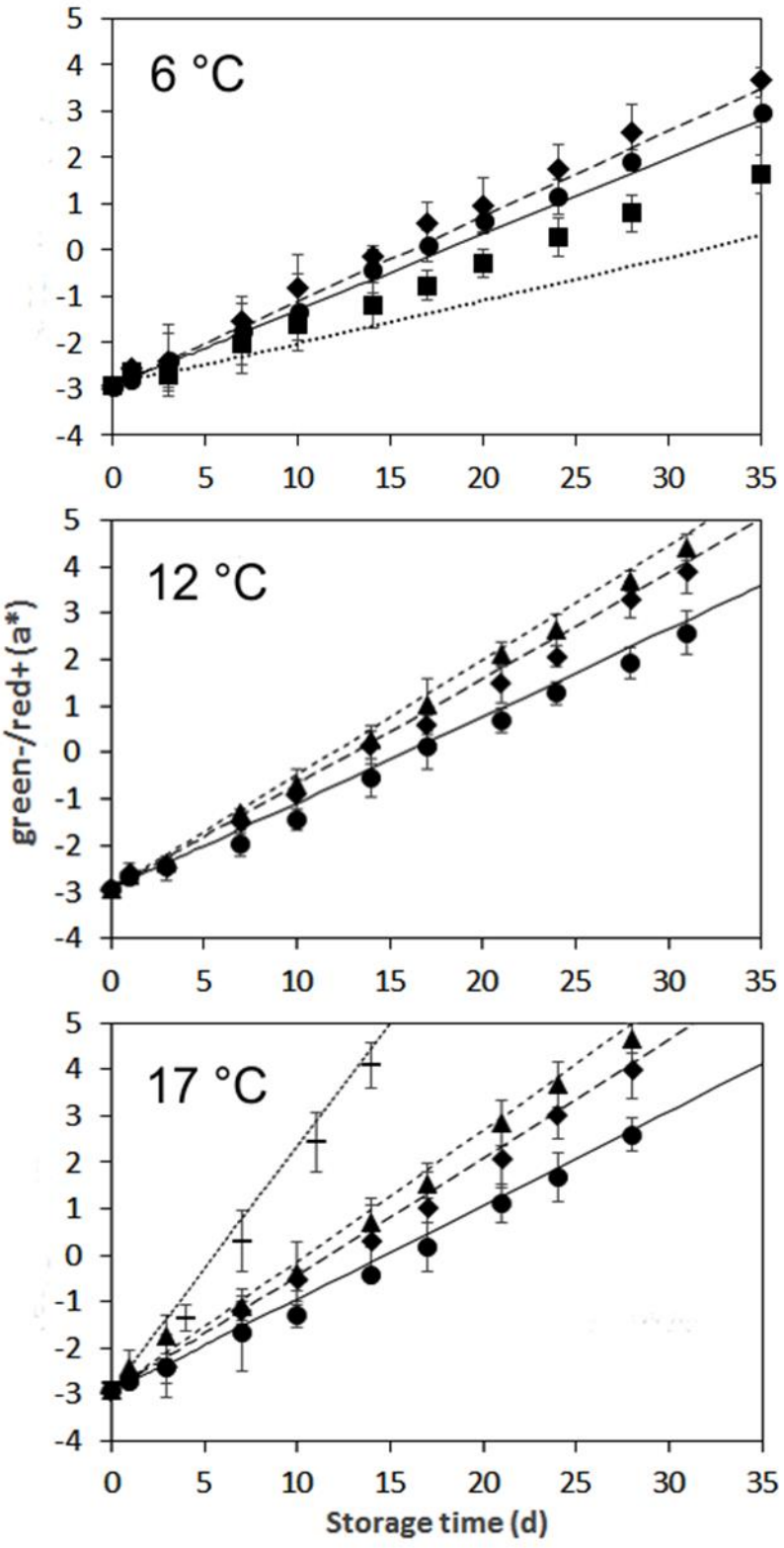

Figure 5.4. Evolution of flesh color (*a** coordinate) in the feijoa fruits stored without packaging (-) and packed in PP bags without perforations (■) and with one (●), two (♦) or three (▲) 0.225 mm perforations at 6, 12 and 17 °C. Lines represent *a** values predicted by the model. Bars represent SD.

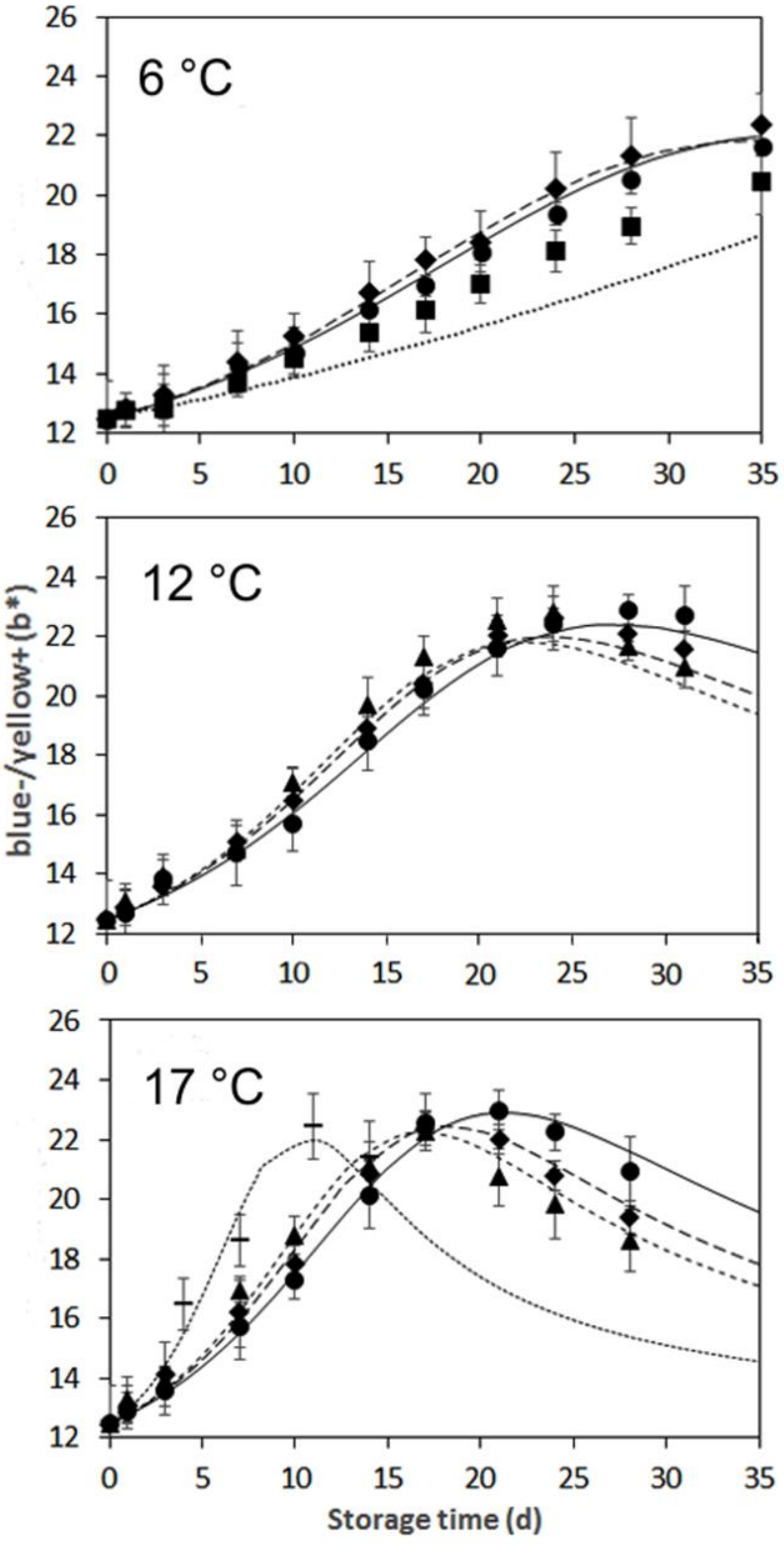

Figure 5.5. Evolution of flesh color (*b** coordinate) in the feijoa fruits stored without packaging (-) and packed in PP bags without perforations (■) and with one (●), two (♦) or three (▲) 0.225 mm perforations at 6, 12 and 17 °C. Lines represent *b** values predicted by the model. Bars represent SD.

The model parameters shown in Table 5.7, similar to those for firmness, by increasing the storage temperature and the O_2 concentration in the headspace, the rate of decrease in L*values became greater, as can be seen in Figure 5.3. As for the CO_2, the estimated apparent reaction order (-0.05) indicates that, by increasing the CO_2 concentration, the rate of lighness decreases although this effect is not so relevant. For L*, the R^2_{adj} was equal to 0.947, indicating a good degree of fit of the model with respect to the experimental results as can be seen in Figure 5.3. Similar to the firmness, at the lowest O_2 concentration, the behavior estimated by the model deviated from what was measured experimentally. This as explained above could be consequence of the low O_2 level and anaerobic processes, which were not considered in the lightness change (Eqs. 5.4 and 5.7).

Table 5.7. Parameters for the calculation of the evolution in firmness and flesh color of feijoa fruits as a function of O_2 and CO_2 concentrations, temperature and storage time in the EMAP system

Firmness (Eq. 1.31)					
F_o (N)	76.60 ± 3.93				
F_{fix} (N)	4.68 ± 1.11				
k parameters (Eqs. 5.2 and 5.3)	r_{O2}^{max} ($cm^3\ kg^{-1}\ d^{-1}$)[b]	k_O^{max} ($kg\ cm^{-3}$)	k_{mO2}	k_{muCO2}	
P_{ref} [a]	7.91 ± 0.35 x 10^3	1.50 ± 0.12 x 10^{-5}	3.17 ± 0.25 x 10^{-2}	0.19 ± 0.02	
E_a ($kJ\ mol^{-1}$)	68.51 ± 3.12	-80.62 ± 6.33	-90.94 ± 7.12	56.78 ± 4.45	
R^2_{adj}	0.948				
Color coordinates (CIELAB)	Lightness, L* (Eq. 5.4)	Red/green, *a** (Eq. 5.5)		Yellow/blue, *b** (Eq. 5.6)	
C_0	79.94 ± 1.99	-2.93 ± 0.11		12.46 ± 1.30	
C_{fix}	30.74 ± 2.69	…		…	
O_2 and CO_2 dependence (Eq. 5.7)	k (d^{-1})		k_1	k_2 (d^{-1})	k_3 (d^{-2})
a	0.56 ± 0.02	0.65 ± 0.09	-0.16 ± 0.02	0.34 ± 0.02	0.73 ± 0.06
b	-0.05 ± 0.01	-0.02 ± 0.00	0.06 ± 0.01	0.03 ± 0.00	0
Temperature dependence (Eq. 5.3)	k_T				
P_{ref} [a]	0.13 ± 0.01	1.93 ± 0.17	1.79 ± 0.08	-0.90 ± 0.04	0.13 ± 0.01
E_a ($kJ\ mol^{-1}$)	43.93 ± 1.87	45.77 ± 3.75	-38.81 ± 1.79	28.62 ± 1.32	79.28 ± 3.66
R^2_{adj}	0.947	0.942		0.949	

[a] Reference parameters (P_{ref}) at T = 23 °C (296.15 K).

[b] Taken from Castellanos et al. (2016). r_{O2}^{max} = 9.60 ± 0.42 x 10^{15} $cm^3\ kg^{-1}\ d^{-1}$ at T = ∞.

The standard deviation (SD) is included.

From the experimental evolution shown in Figure 5.4, it was observed that *a** followed a linear behavior, increasing with time for all of the EMAP combinations. For this reason, a

zero-order model depending storage time was adjusted to the experimental data. This model was used in other studies with banana where the k parameter is dependent on the concentration of gases and T (Castellanos & Algecira, 2012; Chen & Ramaswamy, 2002). As for L*, the k parameter of change in *a** was related to the O_2 and CO_2 concentrations through an equation of chemical kinetics (Eq. 5.7), while the influence of the temperature was represented in the k_T parameter using the Arrhenius equation. As discussed above, the rate of change of *a** is greater at higher T and O_2 levels and lower CO_2 levels in the headspace. The latter can be seen in the positive value of the reaction order in Eq. 5.7 for O_2 and the negative order for CO_2 (Table 5.7). In addition, the reaction order for CO_2 equal to -0.02 indicates that it had little effect on the total change of *a**. For this coordinate, the R^2_{adj} value was 0.942, indicating a satisfactory degree of fit of the model to the experimental results, as shown in Figure 5.4. For the fruits in unperforated bags at 6 °C, the model deviated again from the experimental behavior.

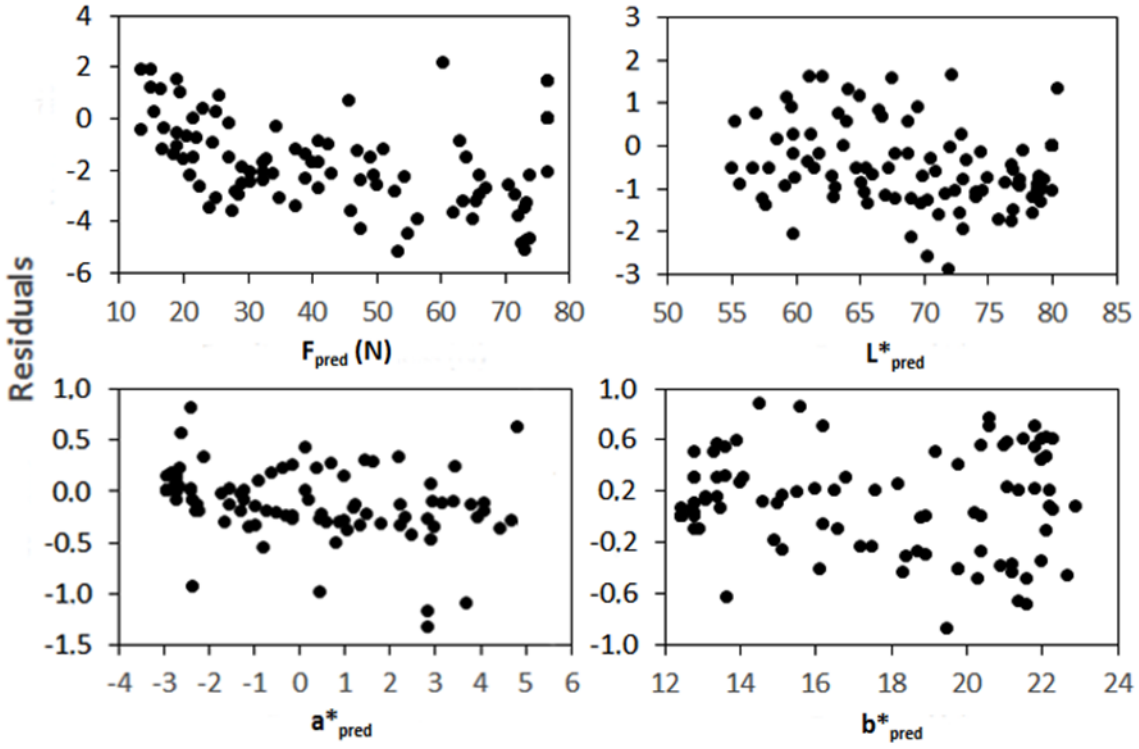

Figure 5.6. Residuals versus predicted values of firmness, L*, *a** and *b**.

The change of *b** did not fit a zero-order or first-order model, as shown in Figure 5.5. According to the experimental behavior, there was an increase of *b** to a maximum, close to the ripeness value and then a gradual decrease, so a modified enzyme kinetics were proposed to represent these changes (Eq. 5.6). This type of equation is similar to the

Michaelis-Menten kinetics except that, in this case, the term corresponding to the anti-competitive inhibition incorporates the square of the time, indicating that, after a certain storage period, the value of *b** begins to fall. The k_1, k_2 and k_3 parameters were adjusted in the same way as the L* and *a** parameters to chemical kinetics and then to the Arrhenius equation. The adjusted model satisfactorily represented the evolution of *b** except as the other properties, the behavior for the bags without perforations at 6 °C, as shown in Figure 5.5. For this coordinate, a R^2_{adj} value of 0.949 was obtained, indicating the goodness of the fit with respect to the experimental data for the O_2 levels greater than 1%. The proximity of R^2_{adj} to one indicates that, in general, the variables associated in the model (time, temperature, and level of O_2 and CO_2) explained the behavior of *b** in the fruit flesh in the same way as with firmness, L* and *a**.

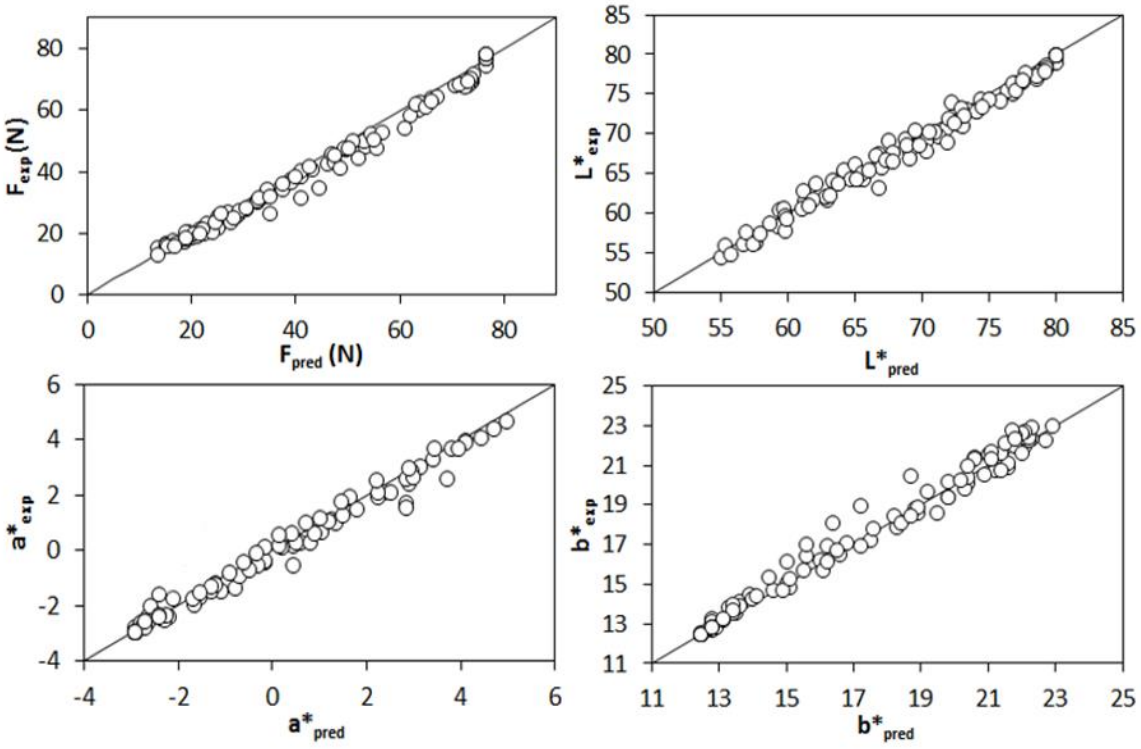

Figure 5.7. Experimental versus predicted values of firmness, L*, *a** and *b**.

The plot of residuals as a function of each predicted property shows the random patterns in all of the cases (Figure 5.6). In addition, the plot of experimental versus predicted values for each property (Figure 5.7) follows a linear behavior indicating the good fit obtained. Therefore, it is possible to confirm that the equations used and the estimated parameters are appropriate to adequately describe the evolution of firmness and color coordinates in packed fruits. The models can adequately describe the behavior of firmness and color coordinates at O_2 concentrations in the headspace of at least 4.1 kPa (PP bags with one

perforation at 6 °C), but when these levels decrease to values of about 1 kPa or less, the results estimated by the models deviated from the actual behavior. However, in practice, it is not expected to reach such a low O_2 level since it is not suitable for preserving fresh produce and, as can be seen for feijoa in this case, it ends up inducing deterioration as compared to higher equilibrium concentrations at the same temperature. Therefore, the models can be employed under aerobic storage conditions (>3-4 kPa of O_2).

The models developed for this study can be used to determine the shelf-life of a fresh produce stored at defined EMAP conditions. By knowing the values of firmness and color of the ripeness stage, it is possible to predict the time required to reach these values in the EMAP system. This will allow producers and distributors to improve their logistics, avoiding undesired losses by inadequate timing.

5.4 Conclusions

Storing the feijoa fruits in EMAP significantly delayed the rate of deterioration, as compared to the fruits stored without packaging. Among the evaluated EMAP systems, the fruits packed in perforated PP bags at 6 °C and with equilibrium gas levels in the headspace of 11 % kPa of O_2 and 7.8 % kPa of CO_2 showed the lowest deterioration and rate of change in their quality properties, with a total storage time of 38 days. The data obtained for the different EMAP configurations in this study enable a working range of temperature and gas concentrations for better preservation of these fruits in modified atmospheres.

It was possible to adequately represent the change in firmness and flesh color of the feijoa fruits stored in EMAP using suitable mathematical models for each property. The developed models can trace the evolution of firmness and color coordinates L*, *a** and *b** as a function of storage temperature and O_2 and CO_2 concentrations in the EMAP headspace at O_2 levels of at least 4 kPa (5.3 %). These models can be used in future research to estimate in advance the shelf-life of feijoa fruits under different conditions of temperature and packaging and can be used as a basis for estimating similar models for other fresh produce.

5.5 References

Alam, T. & Goyal, G.K. (2006), Colour and pigment changes during modified atmosphere packaging storage of fruits and vegetables. Steward Postharvest Review, 5:16.

Banda, K., Caleb, O., Jacobs, K. & Opara, U. 2015. Effect of active-modified atmosphere packaging on the respiration rate and quality of pomegranate arils (cv. Wonderful). *Postharvest Biology and Technology*, 109: 97-105.

Biswas, P., East, A., Hewett, E. & Heyes, J. 2014. Interpreting textural changes in low temperature stored tomatoes. *Postharvest Biology and Technology*, 87: 140-143.

Castellanos, D.A. & Algecira, N. 2012. Modelling change in color and firmness of baby banana (*Musa acuminata* AA) in modified atmosphere packaging. *Agronomía Colombiana*, 30(1): 84-94.

Castellanos, D.A., Mendoza, R., Gavara, R. & Herrera, A.O. 2016. Respiration and Ethylene Generation Modeling of 'Hass' Avocado and Feijoa Fruits and Modified Atmosphere Packaging Application. *International Journal of Food Properties*, doi: 10.1080/10942912.2016.1160921

Chen, C. & Ramaswamy, H. 2002. Color and texture change kinetics in ripening bananas. *LWT*, 35: 415–419.

Del-Valle, V., Hernández-Muñoz, P., Catalá, R. & Gavara, R. 2009. Optimization of an equilibrium modified atmosphere packaging (EMAP) for minimally processed mandarin segments. *Journal of Food Engineering*, 91: 474-481.

East, A.R., Trejo-Araya, X.I., Hertog, M.L.A.T.M., Nicholson, S.E. & Mawson, A.J. 2009. The effect of controlled atmospheres on respiration and rate of quality change in 'Unique' feijoa fruit. *Postharvest Biology and Technology*, 53: 66-71.

Galvis, J.A. 2003. Manejo de la cosecha y poscosecha de la feijoa. In: G. Fischer, D. Miranda, G. Cayón & M. Mazorra (Eds.), *Cultivo, poscosecha y exportación de la feijoa (Acca sellowiana Berg)*. Bogotá: Universidad Nacional de Colombia – Asohofrucol, pp. 111-124.

Gwanpua, S., Verlinden, B.E., Hertog, M.L.A.T.M., Bulens, I., Van de Poel, B., Van Impe, J., Nicolaï, B.M. & Geeraerd, A.H. 2012. Kinetic modeling of firmness breakdown in 'Braeburn' apples stored under different controlled atmosphere conditions. *Postharvest Biology and Technology*, 67: 68-74.

Hasbullah, R., Gardjito, Syarief, A.M. & Akinaga, T. 2000. Gas permeability characteristics of plastic films for packaging of fresh produce. *Journal of the Society of Agricultural Structures, Japan*, 31(2): 5-11.

Hertog, M.L.A.T.M., Nicholson, S.E. & Jeffery, P.B. 2004. The effect of modified atmospheres on the rate of firmness change of 'Hayward' kiwifruit. *Postharvest Biology and Technology*, 31: 251-261.

Hertog, M.L.A.T.M., Nicholson, S.E. & Whitmore, K. 2003. The effect of modified atmospheres on the rate of quality change in Hass avocado. *Postharvest Biology and Technology*, 29: 41-53.

Hörtensteiner, S. 2006. Chlorophyll degradation during senescence. *Annual Review of Plant Biology*, 57: 55-77.

Lana, M., Tijskens, L. & van Kooten, O. 2005. Effects of storage temperature and fruit ripening on firmness of fresh cut tomatoes. *Postharvest Biology and Technology*, 35(1): 87-95.

Mangaraj, S. & Goswami, T.K. 2011. Measurement and modeling of respiratio rate of guava (CV. Baruipur) for modified atmosphere packaging. *International journal of food properties*, 14: 609-628.

Mangaraj, S., Goswami, T. & Mahajan, P. 2009. Applications of plastic films for modified atmosphere packaging of fruits and vegetables: a review. *Food Engineering Reviews*, 1: 133-158.

Mistriotis, A., Briassoulis, D., Giannoulis, A. & D'Aquino, S. 2016. Design of biodegradable bio-based equilibrium modified atmosphere packaging (EMAP) for fresh fruits and vegetables by using micro-perforated poly-lactic acid (PLA). *Posthrvest Biology and Technology*, 111: 380-389.

Paliyath, G. & Murr, D. 2008. Biochemistry of fruits. In: G. Paliyath, D. Murr, A. Handa & S. Lurie, (Eds), *Postharvest biology and technology of fruits, vegetables and flowers*). Ames: Wiley-Blackwell, pp. 19-50.

Parra, A. & Fischer, G. 2014. Maduración y comportamiento poscosecha de la feijoa (Acca sellowiana (O. Berg) Burret). Una revisión. *Revista Colombiana de Ciencias Hortícolas*, 7(1): 98-110.

Pathare, P., Opara, U. & Al-Said, F. 2013. Colour Measurement and Analysis in Fresh and Processed Foods: A Review. *Food and Bioprocess Technology*, 6: 36–60.

Ren, K., Tu, K., Pan, L. & Chen, Y. 2006. Kinetics models of broccoli color changes during chilled storage. *Journal of Food Processing and Preservation*, 30: 180-193.

Salinas-Hernández, M., González-Aguilar, G. & Tiznado-Hernández, M. 2015. Utilization of physicochemical variables developed from changes in sensory attributes and consumer acceptability to predict the shelf life of fresh-cut mango fruit. *Journal of Food Science and Technology*, 52(1): 63-77.

Selcuk, N. & Erkan, M. 2015. The effects of modified and palliflex controlled atmosphere storage on postharvest quality and composition of 'Istanbul' medlar fruit. *Postharvest Biology and Technology*, 99: 9-19.

Sila, D.N., Smout, C., Vu, T. & Hendrickx, M. 2004. Effects of high-pressure pretreatment and calcium soaking on the texture degradation kinetics of carrots during thermal processing. *Journal of Food Science*, 69(5): E205–E211.

Sousa-Gallagher, M., Mahajan, P.V. & Mezdad, T. 2013. Engineering packaging design accounting for transpiration rate: Model development and validation with strawberries. *Journal of Food Engineering*, 119: 370-376.

Spiess, A. & Neumeyer, N. 2010. An evaluation of R^2 as an inadecuate measure for nonlinear models in pharmacological and biochemical research a Montecarlo Approach. *BMC Pharmacology*, 10(6): 1-11.

Techavises, N. & Hikida, Y. 2008. Development of a mathematical model for simulating gas and water vapor exchanges in modified atmosphere packaging with macroscopic perforations. *Journal of Food Engineering*, 85: 94-104.

Tijskens, L.M.M. & Schouten, E. 2009. Modeling Quality Attributes and Quality-related Product Properties. In: W. Florkowski & B. Bruckner (Eds.), *Postharvest Handling: A Systems Approach*. San Diego: Academic Press, pp. 483-512.

General conclusions and future research

This study was aimed to develop mathematical models to represent the change of three quality-indicative properties: weight, firmness and color, depending on the concentrations of O_2 and CO_2 and temperature in a MAP system for feijoa fruits, and by using these models, it was aimed to find MAP conditions suitable for the preservation of the fruits. In pursuit of this objective, a review of the state of the art about the available mathematical models to represent these properties as a function of storage conditions was done in first place, presenting the most relevant studies on this subject. From the literature review conducted for Chapter 1, helpful information was obtained about the representation of changes of firmness and color, as well as models to describe the processes of respiration and transpiration since the latter are closely related to the change of gas concentrations in the packing system and the change in weight of the packed product.

In the MAP system, the concentration of O_2 and CO_2 in the headspace depends on the interaction between the respiration of the packed product and the exchange of these gases through the packaging system, so it is first necessary to know the rate of development of these processes in order to determine the evolution of the system. For this reason in Chapter 2, the necessary equations were proposed to represent the processes inducing the change of the concentration of O_2 and CO_2 in the MAP system: product respiration, transfer of gases through the package and the perforations, volume change in the packaging headspace and temperature influence on all of these processes. During this first stage, tomato, a well-known fruit with a low rate of respiration was used for the experimental tests to verify that the MAP model was adequate, that all the necessary equations have been incorporated and that indeed it was possible to represent the evolution of gases in the packaging headspace with a fruit included. Furthermore, parameters of permeability for three packaging materials and of transmission of gases through the perforations were determined.

With the MAP model developed, in Chapter 3 were proposed the suitable equations and the required parameters were estimated to describe the rates of consumption O_2 and production of CO_2 for the feijoa fruits and then this information was incorporated into the

model after validation in a short storage test. With the MAP model ready to represent the evolution of O_2 and CO_2 in the packaging headspace, the equations necessary to represent the process of transpiration and weight loss of the fruit packed and the evolution of moisture in the packing system were also incorporated in Chapter 4. At this point, the weight of the fruit is no longer considered constant in the MAP system and the process of weight loss is considered as the sum of water transferred from the product due to the gain of energy from its respiration process and the difference in water activities between the product and the surrounding atmosphere. In this way, the MAP model can successfully describe the evolution in the concentration of O_2, CO_2 and water vapor in the packaging headspace, the weight loss of the packed fruit and the condensing water inside the packaging.

In Chapter 5, the MAP model was used to obtain through simulation, MAP systems with different equilibrium gas concentrations (EMAP) and thereafter it was used to determine which of these EMAP would best preserve the feijoa fruits. First, several quality-indicative properties of the fruits were measured in their physiological maturity stage and in their ripeness stage (commercial maturity). Then, the evolution in the deterioration index, weight, content of organic acids, firmness and color was measured for the different EMAP systems evaluating for which of these systems the change of the properties was lower. Afterwards, the models to represent the change in firmness and color of the packed fruits as a function of the concentrations of O_2 and CO_2 and the storage temperature were developed from experimental data and from the information obtained in the literature review literature in Chapter 1. Respecting color, a specific model for each of the three coordinates of the CIELAB space, L*, *a** and *b** was successfully obtained.

With the MAP model, it is possible to determine in advance the gas concentrations corresponding to a particular storage conditions for flexible packaging systems. This is very useful since it allows adjusting the most suitable packaging system for the fruit preservation through the combination of permeation and transmission of gases through the packaging film and the perforations, avoiding reach unfavorable concentrations of gases and excessive weight losses or product deterioration by excessive condensation inside the packaging.

With the firmness and color models for its part, it is possible to predict the behavior of these properties of the packed product in different MAP conditions and by knowing the values

corresponding to the ripeness stage, it is also possible to predict the storage-life of the product for a determined EMAP configuration.

Conclusions

An integrated mathematical model to describe the evolution of O_2 and CO_2 concentrations, and relative humidity in a MAP system with perforations and variable volume was successfully established and applied to feijoa fruits. In the model, the diffusive gas permeation through the packaging film and the perforations were taken into account using Fick's equations to describe these processes of gas exchange; the fruit respiration was represented using Michaelis-Menten enzyme kinetics and the fruit weight loss was described by considering the transfer of water from the packed product to the headspace and the water that is condensed in the packaging walls. The dependence on temperature was incorporated using the Arrhenius' Law in the permeation, respiration and weight loss parameters. The capacity of the model was verified with experimental data, achieving good prediction results for feijoa fruits packed in low-density polyethylene (LDPE), cast polypropylene (PP) and polylactic acid (PLA) bags at different storage temperatures.

The developed model was successfully used to set different equilibrium modified atmosphere packaging (EMAP) combinations with steady gas levels in the packaging headspace at different temperatures. By evaluating different EMAP configurations predicted by the model, it was possible to establish a packaging system with perforated PP bags that allowed the conservation of feijoa fruits for up to 38 days with equilibrium gas levels in the headspace of 8.21 kPa of O_2 and 5.82 kPa of CO_2 at 6 °C.

Once the evolution of gases in the MAP system was addressed, other models to represent the change in firmness and flesh color of the feijoa fruits stored in EMAP were successfully developed. First-order kinetics with fractional conversion were used to describe firmness and color lightness, a zero-order equation for color coordinate *a** and a modified enzyme kinetics for color coordinate *b**. The effect of the O_2 and CO_2 concentrations in the packaging headspace was considered using a Michaelis-Menten equation, incorporating a respiration term for firmness and using chemical kinetic equations for the color coordinates. The dependence on temperature was incorporated using Arrhenius' Law in the parameters of change of each property. These models can trace the evolution of firmness and color coordinates L*, *a** and *b** as a function of storage temperature and O_2 and CO_2 concentrations in the EMAP headspace at O_2 levels of at least 4kPa.

Future developments

The models developed in this study allows many additions to predict the behavior of complex packaging systems in a wider range of conditions.

Rigid packaging and temperature variations

In this study, the behavior of flexible packaging systems with variable volume was addressed; however, for many products, it is necessary to use rigid packaging to avoid mechanical damage or for easy carrying. In these rigid systems, the rate of gas exchange required to reach the EMAP concentrations occurs almost exclusively through perforations, but just as for flexible systems, it is possible to define in advance the amount and the number of perforations required to obtain the desired O_2 or CO_2 levels. Since the volume of the MAP system is constant, the change in the amount of gas in the headspace will lead to changes in the system pressure. This behavior can be incorporated into the model using Poiseulle's equation. If the package is large (capacity greater than 5-10 L), the concentration of gases cannot be considered uniform throughout the packaging headspace. In this case, Fick's equations of diffusion should be replaced or supplemented with equations to incorporate the change in gas concentration with respect to the position and to take into account the convection processes in the gas transfer through the headspace. Several models based on the Maxwell-Stefan equations have been proposed for this type of systems, where the numerical solution is achieved using finite element methods.

In the cold chain of storage, temperature often cannot be maintained at a constant throughout the period. By using the MAP model, it is possible to simulate a transport chain with storage intervals at different temperatures. For this, each storage interval at a given temperature is considered individually in the numerical solution of the entire problem. The initial conditions of the first interval (concentration of gases, P, T, interval duration, etc.) are defined in advance and the initial conditions of the subsequent intervals will be the final conditions of the previous ones, until a serial solution is reached for all of them. Here, it is necessary to experimentally check if changes in temperature have an effect on the metabolism of the product by changing the parameters of the equations of respiration and transpiration, which in principle are considered temperature-independent.

Active packaging

The storage life of a product packed in a MAP system can be extended using elements that contribute actively to this purpose. In fresh or minimally processed products, it is desirable to decrease the presence of O_2, ethylene or condensation inside the packaging to adequate levels and often, for practical or cost reasons, the permeation capacity of the packaging system is not enough to achieve this by itself. On the other hand, sometimes it is necessary to increase levels of substances needed for the best preservation of the product. The rate of removal or release of these compounds in the packaging headspace can be incorporated in the system of differential equations of the MAP model, adding the appropriate parameters. For example, in the case of ethylene, whose action should be reduced in the packed product, it is possible to incorporate a matrix, such as zeolite, silica gel or the packaging film, into the system to actively release 1-methylcyclopropene (1-MCP), which binds to the ethylene receptors in the cell membrane, decreasing its activity and delaying ripening. It is also possible to estimate the controlled release of other antioxidants or antimicrobials by incorporating the appropriate desorption kinetics into the model. In other studies have been proposed mathematical models to represent active packaging but none of these has been developed for use in MAP systems.

Predicting storage life

Regarding to the models of prediction of color and firmness, of course, it is necessary to find the parameters required for other fresh produce, which are important for producers and distributors. With this model, it is possible to predict the shelf-life of a packed product, in other words, to predict the time required for the produce properties to reach certain values, the values of ripeness, under established EMAP conditions. In this way, not only can the EMAP combination that results in a longer storage-life be estimated, but the preservation time in any type of storage conditions can also be defined beforehand. In practice, it is often not possible to have the desired EMAP system (type and surface area of packaging, perforation size or temperature), so it is useful to know what storage-life can be achieved with the attainable packaging conditions.

Annex A. Publications of the Thesis

Castellanos, D.A., Polanía, W. & Herrera, A.O. 2016. Development of an equilibrium modified atmosphere packaging for feijoa fruits and modeling color and firmness evolution, *Postharvest Biology and Technology*, 120: 193-203. http://dx.doi.org /10.1016/j.postharvbio.2016.06.012

Castellanos, D.A., Herrera, D.R. & Herrera, A.O. 2016. Modelling water vapour transport, transpiration and weight loss in a perforated modified atmosphere packaging for feijoa fruits, *Biosystems Engineering*, 151: 218-230. http://dx.doi.org/10.1016/j.biosystemseng.2016.08.015

Castellanos, D.A., Mendoza, R., Gavara, R. & Herrera, A.O. 2016. Respiration and ethylene generation modeling of 'Hass' avocado and feijoa fruits and application in modified atmosphere packaging, *International Journal of Food Properties*, http://dx.doi.org/10.1080/10942912.2016.1160921

Castellanos, D.A., Cerisuelo, J.P., Hernández-Muñoz, P., Herrera, A.O. & Gavara, R. 2016. Modelling the evolution of O_2 and CO_2 concentrations in MAP of a fresh product: application to tomato, *Journal of Food Engineering,* 168: 84-95. http://dx.doi.org/10.1016/j.jfoodeng.2015.07.019

Castellanos, D.A. & Herrera, A.O. 2015. Mathematical models for the representation of some physiological and quality changes during fruit storage. *Journal of Post-Harvest Technology,* 3(1): 18-35. http://dx.doi.org/10.5281/zenodo.47675

Castellanos, D.A., Herrera, D.R. & Herrera, A.O. 2014. Caracterización de algunas propiedades fisicoquímicas de feijoa (*Acca sellowiana* Berg) durante la poscosecha. *Revista Facultad Nacional De Agronomía*, 67(2), Supl. 2: 114-116. http://dx.doi.org/10.13140/RG.2.1.2098.1520

Additional publications in partnership with the 'Horticultura' research group

Mendoza R., Castellanos, D.A., Vargas, J.C. & Herrera, A.O. 2016. Simulation of an active packaging with catalytic oxidation of ethylene for 'Cavendish' banana. *Agronomía Colombiana*, Supl. 2016, 167-170.

Mendoza R., Castellanos, D.A., García, J.C., Vargas, J.C. & Herrera, A.O. 2016. Ethylene production, respiration, and gas exchange modelling in modified atmosphere packaging for banana fruits. *International Journal of Food Science and Technology*, 51: 777-788. http://dx.doi.org/10.1111/ijfs.13037

Castellanos, D.A. & Algecira, N. 2014. Modelado del cambio en la concentración de gases en el almacenamiento de 'baby banana' (*Musa acuminata* AA) en atmósferas modificadas. In: Zacarias L., Ballester, A.R., Marcos J.F. & Pérez-Gago, M.B. (Eds.), *Avances en la Poscosecha de Frutas y Hortalizas*. Fundación Universidad-Empresa ADEIT, Valencia, Spain, pp. 317-322. http://dx.doi.org/10.13140/RG.2.1.3721.0725/1

Annex B. Participation in academic and scientific events

Castellanos D.A., Herrera, A.O. 2015. Modelado del transporte de agua, transpiración y pérdida de peso en el almacenamiento en atmósferas modificadas de frutos de feijoa (*Acca sellowiana* Berg). Oral and poster presentations in the *Segundo Coloquio Doctoral de la Facultad de Ingeniería, Universidad Nacional de Colombia*. Bogotá, Colombia. November 27, 2015. http://dx.doi.org/10.13140/RG.2.1.3122.7921

Mendoza, R., Castellanos, D.A. & Herrera, A.O. 2015. Simulation of change in gas concentrations for modified atmosphere packaging systems of variable volume: application to fruits. Oral presentation in the *10th European Congress of Chemical Engineering*. Nice, France. September 29, 2015.
http://dx.doi.org/10.13140/RG.2.1.2143.4003

Castellanos, D.A., Cerisuelo, J.P., Hernández-Muñoz, P., Herrera, A.O. & Gavara, R. 2015. Modelling MAP evolution of fresh tomato. Poster presentation in the *27th IAPRI Symposium on Packaging*. Valencia, Spain. June 11, 2015.
http://dx.doi.org/10.13140/RG.2.1.2114.9848

Castellanos, D.A., Herrera, D.R. & Herrera, A.O. 2014. Caracterización de algunas propiedades fisicoquímicas de feijoa (*Acca sellowiana* Berg) durante la poscosecha. Poster presentation in the *II Congreso Internacional de Investigación e Innovación en Ingeniería, Ciencia y Tecnología de Alimentos*. Medellín, Colombia. May 28, 2014. http://dx.doi.org/10.13140/RG.2.1.2713.2561

Additional events in partnership with the 'Horticultura' research group

Castellanos, D.A. & Algecira, N.A. 2014. Modelado del cambio en la concentración de gases en el almacenamiento de 'baby banana' (*Musa acuminata* AA) en atmósferas modificadas. Poster presentation in the *XI Simposio Nacional y VIII Ibérico Sobre Maduración y Postcosecha*. Valencia, Spain. October 22, 2014.
http://dx.doi.org/10.13140/RG.2.1.1664.6806

Annex C. Funded projects

“Modelado de la cinética de respiración y de generación de etileno en frutos de feijoa (*Acca sellowiana* Berg) y Aguacate (*Persea americana* Mill)”. Funded by the *Research and Extension Vice-presidency of the Universidad Nacional de Colombia*. Convocation of the National Program of Projects to Strengthen Research, Creation and Innovation in Graduate Studies at the National University of Colombia 2013-2015. Grant number: 20228. Amount of funding: 30 million COP. Project developed between May 2014 and July 2015.

Diego Alberto Castellanos Espinosa
Universidad Nacional de Colombia. Bogotá, Colombia

Modelado del cambio de propiedades indicativas de calidad en el almacenamiento de feijoa (*Acca Sellowiana Berg*) utilizando atmósferas modificadas

Modelling change of quality-indicative properties of feijoa (*Acca sellowiana* Berg) in modified atmosphere packaging

Tesis presentada como requisito parcial para optar al título de **Doctor en Ingeniería, Área de Ingeniería Química**

A thesis presented in partial fulfilment of the requirements for the Degree of Doctor of Engineering – Field of Chemical Engineering

Campo de estudio: Envases y empaques en alimentos
Research field: Food Packaging

Páginas del documento: 200 Manuscript pages: 200

FIRMA DE APROBACIÓN DEL DIRECTOR DE TESIS:_____